Linchpin empowers promiscuous electrophile to enable site-selective modification of histidine and aspartic acid in proteins

Dattatraya Gautam Rawale,[a] Kalyani Thakur,[a] Pranav Sreekumar,[a] Sajeev T. K.,[b] Ramesh A.,[a] Srinivasa Rao Adusumalli,[a] Ram Kumar Mishra,[b] and Vishal Rai*[a]

[a] Department of Chemistry and [b] Department of Biological Sciences

Indian Institute of Science Education and Research Bhopal

Contents

1. General information

The reagents, proteins, and enzymes were purchased from Sigma-Aldrich, Alfa Aeser, Spectrochem, and Merck. The organic solvents used were reagent grade. Aqueous buffers were prepared freshly using Millipore Grade I water (Resistivity > 5 MΩ cm, Conductivity < 0.2 µS/cm, TOC <30 ppb). Mettler Toledo (FE20) pH meter was used to adjust the final pH. The reaction mixture for the small molecules was stirred (Heidolph, 500-600 rpm). Proteins were either vortexed or incubated in Thermo Scientific MaxQ 8000 incubator shaker (350 rpm, 25-37 ^{o}C). Cellulose membrane (MWCO, 6-8 kD) from Spectrum labs was used for dialysis. Amicon® Ultra-0.5 mL 3-10 kDa MWCO centrifugal filters from Merck Millipore was used to remove small molecules from protein mixture, desalting, and buffer exchange. Organic solvents were removed by BUCHI rotavapor R-210/215 whereas aqueous samples were lyophilized by CHRiST ALPHA 2-4 LD plus lyophilizer. Circular Dichroism (CD) measurements were recorded on JASCO J-815 CD spectropolarimeter equipped with peltier temperature controller. All the spectra were measured with a scan speed of 50 nm/min, spectral band width 1 nm using 1 cm path length cuvette at 25 ^{o}C. Steady-state fluorescence spectra was carried out in HORIBA JOBIN YVON, FLUOROLOG 3-111. The fluorescence spectra were measured with a quartz cuvette of 1 cm path length.

Chromatography: Thin-layer chromatography (TLC) was performed on silica gel coated aluminium TLC plates (Merck, TLC Silica gel 60 F254). The compounds were visualized using a UV lamp (254 nm) and stains such as iodine, ninhydrin, 2,4-dinitrophenylhydrazine. Wherever compounds were purified by chromatography, flash column chromatography was carried out on Combiflash Rf 200, Combiflash NextGen 300+, or gravity columns using silica gel (230-400 or 100-200 mesh) from Merck.

Nuclear magnetic resonance spectra: ^{1}H, ^{13}C, ^{19}F NMR spectra were recorded on Bruker Avance III 400 and 500 MHz NMR spectrometer. ^{1}H, ^{13}C, and ^{19}F spectra NMR spectra were referenced to TMS (0 ppm), $CDCl_3$ (77.16 ppm), and trifluoroacetic acid (-75.76 ppm) respectively. Peak multiplicities are designated by the following abbreviations: s, singlet; bs, broad singlet; d, doublet; t, triplet; q, quartet; m, multiplet; dd, doublet of doublets; ddd, doublet of doublet of doublets. Spectra were recorded at 298 K.

Mass spectrometry: SCIEX X500B QTOF coupled with ExionLC AD UHPLC and Agilent 6130 single quad coupled with Agilent 1200 series HPLC (ESI/APCI) were used for LC-MS and protein sequencing. Poroshell 300 SB-C18 HPLC column (2.1 × 75 mm × 5 µm, flow rate 0.4 ml/min) and XB-C18 UHPLC column (2.5 x 150 mm, 1.7 µm, 100 Å, flow rate 0.3 ml/min) were used for small molecules and protein-derived samples respectively. HRMS data were recorded on Bruker Daltonics MicroTOF-Q-II with electron spray ionization (ESI). Matrix assisted laser desorption/ionisation time of flight mass spectrometry was performed with Bruker Daltonics UltrafleXtreme Software-Flex control version 3.4, using sinapic acid and

α-cyano-4-hydroxycinnamic acid (HCCA) matrix. Data analysis was performed using SCIEX Bio-pharma view Flex, Flex analysis, and Bruker data analysis software. Peptide mass and fragment ion calculator (http://db.systemsbiology.net:8080/proteomicsToolkit/FragIonServlet.html) were used for peptide mapping and sequencing.

Acetonitrile and H_2O were buffered with 0.01% formic acid and used as the mobile phase. Method A was used to record the LC-ESI-MS data for proteins and method B used for peptide mapping and MS/MS.

Table S1.

Method A (Column: Agilent, Poroshell 300 Å, SB-C18 5 µm 2.1 × 75 mm, flow rate 0.4 ml/minutes)

Time (minutes)	**H_2O (%)**	**Acetonitrile (%)**
0	90	10
1	90	10
8	40	60
12	10	90
15	10	90

Table S2.

Method B (Column: Phenomenex, Poroshell 100 Å, 2.5 x 150 mm, 1.7 µm, flow rate 0.3 ml/min)

Time (minutes)	**H_2O (%)**	**Acetonitrile (%)**
0	95	5
2	95	5
25	50	50
26	20	80
28	95	5
30	95	5

Reaction conversion determination for protein labeling

ESI-MS: Conversion for protein labeling was calculated based on the relative peak intensity of native protein and labeled protein in the deconvoluted mass spectrum.

% Conversion = $I_{\text{desired product}}$ /$I_{\text{all relevant species}}$, where $I_{\text{desired product}}$ is the peak intensity of labeled protein, and $I_{\text{all relevant species}}$ is the sum of the peak intensities of native protein and labeled protein in the deconvoluted mass spectra.

MALDI-ToF-MS: Conversion for protein labeling was calculated based on the relative peak intensity of native protein and labeled protein in the mass spectrum.

2. General procedures

2a. Protein labeling

Site-selective modification of native proteins

Protein **1** (10 nmol) in phosphate buffer (140 µl, 0.1 M, pH 7.8) was taken in a 2 ml microcentrifuge tube. Reagent **2** (1.25 mM) in DMSO (60 µl) from a freshly prepared stock solution was added to it followed by vortexing (350 rpm) at 37 °C. After 4-72 h, the reaction mixture was diluted with acetonitrile:buffer (10:90, 3600 µl). Unreacted reagent and salts were removed by using Amicon® Ultra-4 mL 3-kDa or 10-kDa MWCO centrifugal filters spin concentrator. The sample was further washed with buffer (2 × 4 ml) and concentrated to 190 µl. To this solution, hydroxylamine **4** (5 µmol) in water (10 µl) from a freshly prepared stock solution was added. The reaction mixture was vortexed at 25 °C for 15 minutes to form oxime derivative. The excess of hydroxylamine and salts were removed by using spin concentrator and the sample was collected in water. The modification of protein was analyzed by ESI-MS and MALDI-ToF-MS. The concentrated sample was subjected to digestion, peptide mapping, and sequencing by MS-MS.

Late-stage tagging of labeled ubiquitin

The labeled protein **3a/3b** was prepared according to the procedure given above. The labeled protein **3a/3b** was concentrated to 160 µl of phosphate buffer (0.1 M, pH 7.0). The O-hydroxylamine derivative **6a**/**6b**/**6c** (1 µmol) in DMSO (40 µl) was added to convert the mono-labeled ubiquitin **3a/3b** into its oxime derivatives (**7a/7b/7c**). The excess of O-hydroxylamine derivative and salts were removed by the spin concentrator (4 ml, 3-kDa MWCO). The tagged protein (**7a**-**7c**) was analyzed by ESI-MS.

Purification of the labeled ubiquitin from reaction mixture

Hydrazide beads **9** (200 µl, hydrazide resin loading: 16 µmol/ml) were taken in a 5 ml fritted polypropylene chromatography column with end tip closures. The beads were re-suspended in phosphate buffer (100 µl) after washing with phosphate buffer (1 M, pH 7.0, 6 x 1 ml). Protein mixture (**1a** and labeled protein **3a/3b**, 200 µM) in phosphate buffer (200 µl, 1 M, pH 7.0) and *p*-phenylenediamine (*p*-PDA, 100 mM) in phosphate buffer (100 µl, 1 M, pH 7.0) were added to the beads followed by end-to-end rotation (30 rpm, rotary mixer) at 25 °C for 4 h. The immobilization of the labeled protein on hydrazide resin was monitored by UV-absorbance of the supernatant (complete loading of labeled protein was also confirmed by ESI-MS of supernatant). After collecting the supernatant, the beads were washed with phosphate buffer (0.3 M, pH 7.3, 5 x 1 ml) and KCl (1 M, 4 x 1 ml) to remove the adsorbed protein from resin. The beads were further washed with buffer (0.3 M, pH 7.0, 5 x 1 ml) and re-suspended in phosphate buffer (200 µl, 0.3 M, pH 7.0).

The labeled protein from its immobilized derivative was released by adding O-hydroxylamine hydrochloride (50 µl, 1 M in buffer, 0.3 M, pH 7.0) (end-to-end rotation at 25 °C for 2 h). The supernatant was collected and then the salts, p-PDA and O-hydroxylamine were removed using the spin concentrator (3 kDa or 10-kDa MWCO). The purity of the labeled protein **5a** was confirmed by ESI-MS.

2b. Protein digestion

All solutions were made freshly prior to use.[1]

Procedure for in-solution digestion of insulin and α-lactalbumin

In a 1.5 ml microcentrifuge tube, protein (0.1 mg) in 100 mM tris (10 µl, pH 7.8) with urea (6 M) was incubated for 30 minutes at 37 °C. To this solution, reducing agent (1 µl, 0.2 M DTT in 0.1 M tris) was added and sample was incubated for 1 h at 37 °C. Alkylating agent (4 µl, 0.2 M iodoacetamide in 0.1 M tris) was added to the solution and incubated (in dark) for 1 h at 25 °C for blocking the free sulfhydryl groups. The unreacted iodoacetamide was quenched with reducing agent (4 µl, 0.2 M DTT in 0.1 M tris) for 1 h at 25 °C. The sample was desalted using using Amicon® Ultra-1.5 mL 3-kDa spin concentrator. The sample was collected in 100 µl grade I water. To this solution, 5 µl of enzyme (α-chymotrypsin/trypsin) solution [5 µg, enzyme/protein (1:20); enzyme was dissolved in grade I water] was added and the mixture was incubated at 37 °C for 12 h. Subsequently, the sample was used for peptide mapping by MS and sequencing by MS-MS.

Procedure for in-solution digestion of ubiquitin and myoglobin

Protein (0.1 mg) in 100 mM tris (10 µl, pH 7.8) with urea (6 M) was taken in a 1.5 ml microcentrifuge tube. To this solution, tert-butanol (10 µl) was added and incubated for 3 h at 37 °C. The sample was desalted using using Amicon® Ultra-1.5 mL 3-kDa spin concentrator. The sample was collected in 100 µl grade I water. To this solution, 5 µl of enzyme (α-chymotrypsin/trypsin) solution [5 µg, enzyme/protein (1:20); enzyme was dissolved in grade I water] was added and the mixture was incubated at 37 °C for 12 h. Subsequently, the sample was used for peptide mapping by MS and sequencing by MS-MS.

2c. Insulin bioactivity assay

Immunofluorescence

HEK293T cells were grown on coverslips in a six-well plate format in Dulbecco's modified Eagle's medium (DMEM) and serum-starved for 24 h in 1% serum-containing DMEM medium. Subsequently, cells were treated with 50 µM LY294002 for 30 min. After LY294002 treatment, cells were washed twice

with PBS and treated with either native insulin or purified insulin (3 µg each) in 1 ml of 1% FBS containing DMEM media for 30 min. Post-treatment, cells were again washed twice with PBS and fixed using 100% chilled methanol for 15 min at 4 °C. The cells were then rehydrated and permeabilized with rehydration buffer (10 mM Tris, 150 mM NaCl, 0.1% Triton X-100) for 10 min. Cells were blocked with 5% Normal Goat Serum (NGS) for 1 h at 4 °C after rehydration. The cells were stained for 2 h with pAkt antibodies (1:600, anti-pAKT-S473, CST #4060) at 4 °C. After primary antibody incubation, cells were washed three times with PBS-T (5 min each) and incubated with Alexa Fluor-568 conjugated goat anti-rabbit IgG (1:1000, Life Technologies) for 1 h. Cells were washed thrice with PBS-T and mounted on slides using DAPI containing mounting medium (SIGMA F6057). Fluorescence signals were captured on Zeiss LSM 780 confocal microscope, and images were analyzed using Image J software.

Western blotting

Cells were cultured and treated as mentioned in the immunofluorescence section. Post-treatment, cells were washed twice with PBS and lysed directly in the 1X Laemmli buffer (containing 1 mM Sodium orthovanadate and 1 mM PMSF) by boiling at 100 °C for 10 min. The cleared lysates were obtained by centrifugation and analyzed on 8% SDS-PAGE. Following wet transfer protocols, proteins were transferred onto the methanol-activated 0.2 µm PVDF membrane (MERCK, Cat #ISEQ85R) using 1X transfer buffer (2.5 mM Tris-HCl pH 7.5, 19.2 mM Glycine). The membrane was blocked for 1 h in 5% BSA. Further, the membrane was incubated overnight with anti-pAkt-S473 (1:2000, CST #4060) and anti-Actin (1:8000, BD #612656) antibodies. The membrane was later washed three times for 10 min each with TBS-T buffer (20 mM Tris HCl pH 7.5, 150 mM NaCl, 0.1% Tween-20). The membrane was incubated with Alexa fluor Plus 680 secondary antibodies (Invitrogen #A32734) for 1 h. Later, it was washed with TBS-T buffer (three times for 10 min each). Images were taken using LI-COR IR system. Anti-Actin (1:8000, BD #612656) antibodies were used for loading control detection.

2d. Docking investigations

Coordinate Preparation: Docking of reagent **2c** to ubiquitin's surface was performed by using AutoDock suite version 4.2. The coordinates were obtained from protein data bank (www.rcsb.org) with PDB ID: 1UBQ. The ligand coordinate file was prepared after structural optimization with semi-empirical calculations. For the PDB file, we deleted the water molecules and added hydrogen atoms. The protonation state and valency of heteroatoms in both the protein and ligand PDB files were verified. Using AutoDockTools (ADT) GUI, the coordinates were read, the Gasteiger-Marsili charges of the molecules were computed, non-polar hydrogen atoms were merged, and atom types were assigned. The edited protein

molecule was saved as a PDBQT file. After customizing the torsional degrees of freedom of the ligand (12 rotatable bonds and 17 non-rotatable bonds), an output file in the PDBQT format was generated.

AutoGrid: The PDBQT files for both protein and ligand were read by ADT. The searching space for docking was defined by generating a grid box that covers the entire protein surface. The map types were determined by running AutoGrid.

AutoDock: The ligand and macromolecule for docking simulation were specified by selecting the corresponding PDBQT files. The Genetic Algorithm (GA) search method was employed with 1000 GA runs. The docking parameter file for GA was taken as a DPF output file. Docking simulation was performed using this file, and the results were analyzed using ADT. The optimum energy conformation was written as a PDB file and visualized in PyMOL along with the protein. The image files were rendered using PyMOL.

3. Synthesis and characterization data of reagents

3a. Alkylating reagents 2a-2f

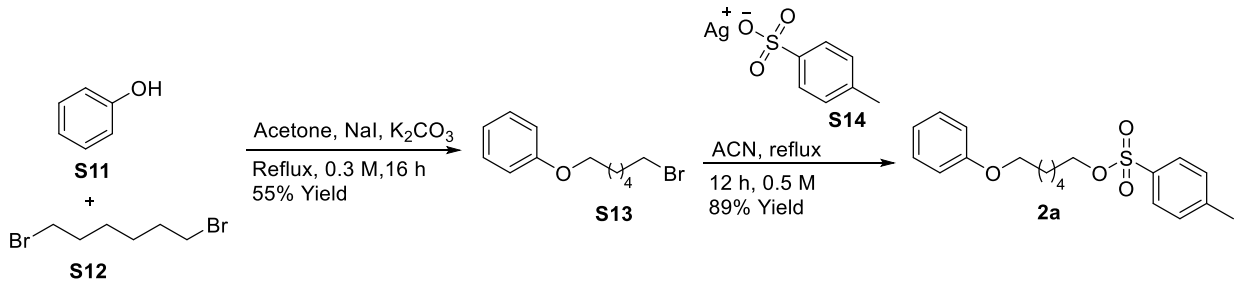

Scheme S1. Synthesis of 6-phenoxyhexyl 4-methylbenzenesulfonate (**2a**)

Synthesis of ((6-bromohexyl)oxy)benzene (S13)

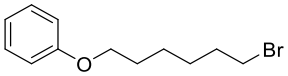

S13

In a 25 ml round bottom flask, phenol **S11** (188 mg, 2 mmol), potassium carbonate (276 mg, 2 mmol), sodium iodide (298 mg, 2 mmol), and 1,6-dibromohexane **S12** (303 µl, 2 mmol) were dissolved in 10 ml acetone. The reaction mixture was refluxed and the progress of reaction was monitored by TLC. After 16 h, reaction mixture was filtered, concentrated, and purified by silica gel flash column chromatography using n-hexane to isolate **S13** (382 mg, 55% yield; R_f 0.69, ethyl acetate:n-hexane 10:90; colorless liquid). **^{1}H NMR** (500 MHz, $CDCl_3$) δ 7.33-7.23 (m, 2H), 6.96-6.91 (m, 1H), 6.96-6.86 (m, 2H), 3.96 (t, *J* = 6.4 Hz, 2H), 3.42 (t, *J* = 6.8 Hz, 2H), 1.94-1.86 (m, 2H), 1.85-1.76 (m, 2H), 1.56-1.46 (m, 4H) ppm. **^{13}C NMR** (126 MHz, $CDCl_3$) δ 159.1, 129.5, 120.6, 114.6, 67.7, 33.9, 32.8, 29.2, 28.0, 25.4 ppm. **LRMS** (ESI) $[M+H]^+$ calcd. $C_{12}H_{18}BrO$ 257.1, found 257.1.

Synthesis of 6-phenoxyhexyl 4-methylbenzenesulfonate (**2a**)

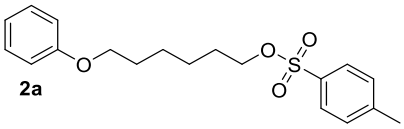

2a

In a 10 ml round bottom flask, ((6-bromohexyl)oxy) benzene **S13** (280 mg, 1.1 mmol), silver tosylate **S14** (337 mg, 1.21 mmol) were taken and dissolved in 5 ml acetone to reflux. The progress of reaction was monitored by TLC. After 12 h, the reaction mixture was filtered, concentrated, and purified by silica gel flash column chromatography (ethyl acetate:n-hexane, 6:94) to isolate **2a** (340 mg, 89% yield; R_f 0.25, ethyl acetate:n-hexane 10:90; White solid). **^{1}H NMR** (500 MHz, $CDCl_3$) δ 7.79 (d, *J* = 8.3 Hz, 2H), 7.33

(d, *J* = 8.3 Hz, 2H), 7.30-7.24 (m, 2H), 6.96-6.90 (m, 1H), 6.90-6.84 (m, 2H), 4.04 (t, *J* = 6.5 Hz, 2H), 3.91 (t, *J* = 6.4 Hz, 2H), 2.44 (s, 3H), 1.78-1.62 (m, 4H), 1.47-1.33 (m, 4H) ppm. **^{13}C NMR** (126 MHz, $CDCl_3$) δ 159.1, 144.8, 133.3, 129.9, 129.6, 128.1, 120.7, 114.6, 70.6, 67.6, 29.2, 28.9, 25.6, 25.3, 21.7 ppm. **HRMS** (ESI) $[M+Na]^+$ calcd. $C_{19}H_{24}O_4SNa$ 371.1293, found 371.1301.

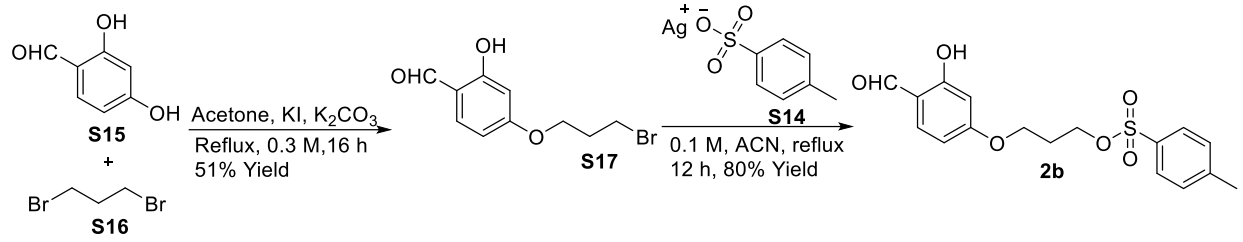

Scheme S2. 3-(4-formyl-3-hydroxyphenoxy)propyl 4-methylbenzenesulfonate (**2b**)

Synthesis of 4-(3-bromopropoxy)-2-hydroxybenzaldehyde (**S17**)

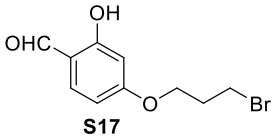

In a 25 ml round bottom flask, 2, 4 dihydroxy phenol **S15** (500 mg, 3.6 mmol), potassium carbonate (500 mg, 3.6 mmol), sodium iodide (536 mg, 3.6 mmol), and 1,3-dibromohexane **S16** (377 µl, 3.6 mmol) were dissolved in 16 ml acetone. The reaction mixture was refluxed and the progress of reaction was monitored by TLC. After 16 h, reaction mixture was filtered, concentrated, and purified by silica gel flash column chromatography using n-hexane ethyl acetate to isolate **S17** (472 mg, 51% yield; R_f 0.53, ethyl acetate:n-hexane 12:88; white solid). **^{1}H NMR** (400 MHz, $CDCl_3$) δ 11.46 (s, 1H), 9.72 (s, 1H), 7.44 (d, *J* = 8.7 Hz, 1H), 6.54 (dd, *J* = 8.7, 2.3 Hz, 1H), 6.44 (d, *J* = 2.3 Hz, 1H), 4.17 (t, *J* = 5.8 Hz, 2H), 3.59 (t, *J* = 6.4 Hz, 2H), 2.40-2.27 (m, 2H) ppm. **^{13}C NMR** (101 MHz, $CDCl_3$) δ 194.5, 165.9, 164.6, 135.4, 115.4, 108.6, 101.4, 65.9, 32.0, 29.5 ppm. **LRMS** (ESI) $[M+H]^+$ calcd. $C_{10}H_{11}BrO_3$ 258.9, found 258.3.

Synthesis of 3-(4-formyl-3-hydroxyphenoxy)propyl 4-methylbenzenesulfonate (2b)

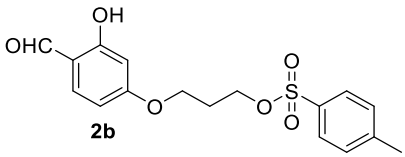

In a 25 ml round bottom flask, 4-(3-bromopropoxy)-2-hydroxybenzaldehyde **S17** (283 mg, 1.1 mmol), silver tosylate **S14** (337 mg, 1.21 mmol) were taken and dissolved in 11 ml acetonitrile to reflux. The progress of reaction was monitored by TLC. After 12 h, the reaction mixture was filtered, concentrated,

and purified by silica gel flash column chromatography (ethyl acetate:n-hexane, 6:94) to isolate **2b** (309 mg, 80% yield; R_f 0.35, ethyl acetate:n-hexane 15:85; White solid). **^{1}H NMR** (400 MHz, $CDCl_3$) δ 11.44 (s, 1H), 9.72 (s, 1H), 7.76 (d, *J* = 8.2 Hz, 2H), 7.41 (d, *J* = 8.6 Hz, 1H), 7.27 (d, *J* = 8.2 Hz, 2H), 6.42 (dd, *J* = 8.6, 2.2 Hz, 1H), 6.27 (d, *J* = 2.2 Hz, 1H), 4.24 (t, *J* = 5.9 Hz, 2H), 3.99 (t, *J* = 5.8 Hz, 2H), 2.38 (s, 3H), 2.20-2.07 (m, 2H) ppm. **^{13}C NMR** (101 MHz, $CDCl_3$) δ 194.5, 165.7, 164.4, 145.0, 135.3, 132.8, 129.9, 127.9, 115.4, 108.4, 101.4, 66.6, 63.7, 28.6, 21.7 ppm. **HRMS** (ESI) $[M+Na]^+$ calcd. $C_{17}H_{18}O_6SNa$ 373.0722, found 373.0739.

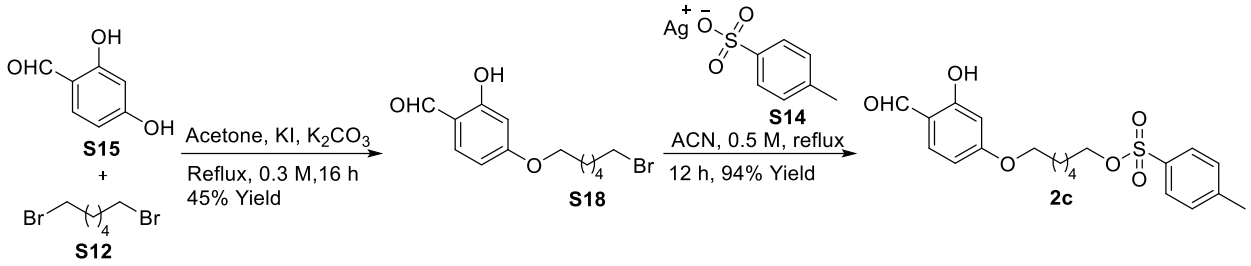

Scheme S3. Synthesis of 6-(4-formyl-3-hydroxyphenoxy)hexyl 4-methylbenzenesulfonate (**2c**)

4-((6-bromohexyl)oxy)-2-hydroxybenzaldehyde (S18)

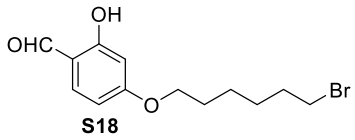

In a 25 ml round bottom flask, 2,4-dihyroxybenzaldehyde **S15** (276 mg, 2 mmol), potassium carbonate (276 mg, 2 mmol), sodium iodide (298 mg, 2 mmol), and 1,6-dibromohexane **S12** (606 µl, 4 mmol) were dissolved in 10 ml acetone to reflux. The progress of reaction was monitored by TLC. After 16 h, the reaction mixture was filtered, concentrated and purified by silica gel flash column chromatography (ethyl acetate:n-hexane, 2:98) to isolate **S18** (270 mg, 45% yield; R_f 0.51, white solid). **^{1}H NMR** (500 MHz, $CDCl_3$) δ 11.48 (s, 1H), 9.70 (s, 1H), 7.42 (d, *J* = 8.7 Hz, 1H), 6.52 (dd, *J* = 8.5, 2.3 Hz, 1H), 6.40 (d, *J* = 2.3 Hz, 1H), 4.01 (t, *J* = 6.4 Hz, 2H), 3.42 (t, *J* = 6.8 Hz, 2H), 1.96-1.86 (m, 2H), 1.85-1.77 (m, 2H), 1.58-1.43 (m, 4H) ppm. **^{13}C NMR** (126 MHz, $CDCl_3$) δ 194.4, 166.4, 164.6, 135.3, 115.2, 108.8, 101.2, 68.4, 33.8, 32.7, 28.9, 27.9, 25.3 ppm. **HRMS** (ESI) $[M+H]^+$ calcd. $C_{13}H_{18}BrO_3$ 301.0439, found 301.0453.

6-(4-formyl-3-hydroxyphenoxy)hexyl 4-methylbenzenesulfonate (2c)

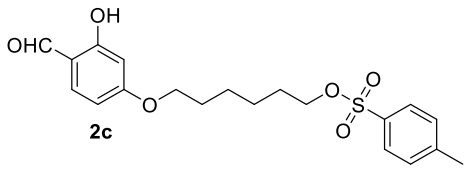

In a 5 ml round bottom flask of 4-((6-bromohexyl)oxy)-2-hydroxybenzaldehyde **S18** (360 mg, 1.2 mmol) and silver tosylate **S14** (363 mg, 1.3 mmol) were dissolved in 5 ml acetone. The reaction mixture was refluxed and the progress of reaction was monitored by TLC. After 12 h, the reaction mixture was filtered, concentrated, and purified by silica gel flash column chromatography (ethyl acetate:n-hexane, 15:85) to isolate **2c** (442 mg, 94% yield; R_f 0.57, white solid). **^{1}H NMR** (500 MHz, $CDCl_3$) δ 11.47 (s, 1H), 9.71 (s, 1H), 7.78 (d, *J* = 8.3 Hz, 2H), 7.42 (d, *J* = 8.7 Hz, 1H), 7.34 (d, *J* = 8.0 Hz, 2H), 6.50 (dd, *J* = 8.7, 2.3 Hz, 1H), 6.38 (d, *J* = 2.3 Hz, 1H), 4.04 (t, *J* = 6.4 Hz, 2H), 3.96 (t, *J* = 6.4 Hz, 2H), 2.44 (s, 3H), 1.79-1.71 (m, 2H), 1.71-1.64 (m, 2H), 1.49-1.32 (m, 4H) ppm. **^{13}C NMR** (126 MHz, $CDCl_3$) δ 194.4, 166.3, 164.4, 144.8, 135.3, 133.1, 129.9, 127.8, 115.0, 108.6, 101.1, 70.5, 68.3, 28.7, 28.7, 25.3, 25.1, 21.6 ppm. **HRMS** (ESI) $[M+H]^+$ calcd. $C_{20}H_{25}O_6S$ 393.1372, found 393.1390.

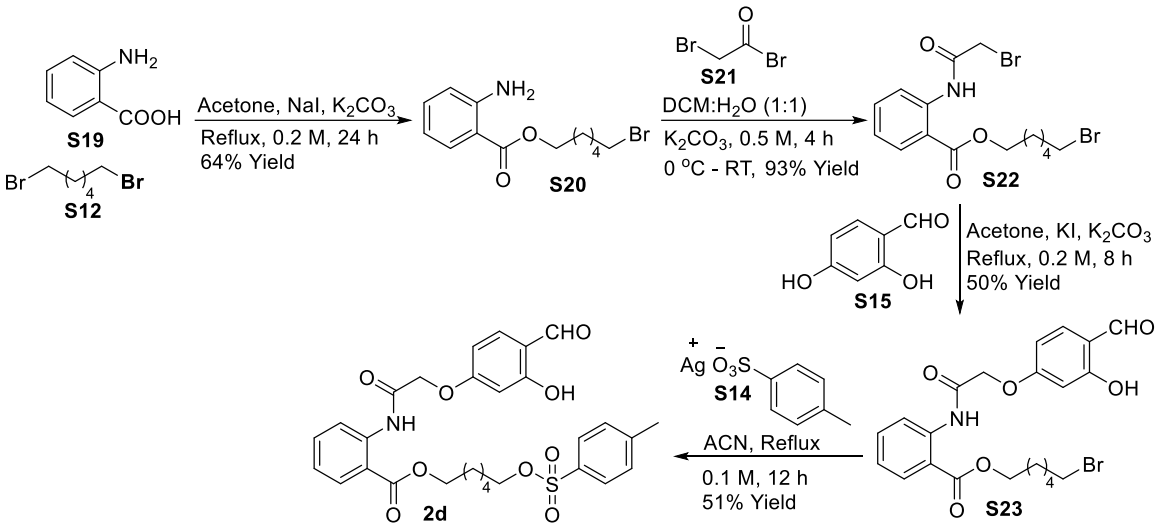

Scheme S4. Synthesis of 6-(tosyloxy)hexyl 2-(2-(4-formyl-3-hydroxyphenoxy)acetamido)benzoate (**2d**)

Synthesis of 6-bromohexyl 2-aminobenzoate (S20)

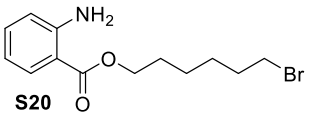

In a 50 ml round bottom flask, anthranilic acid **S19** (411 mg, 3 mmol) was dissolved in acetone (15 ml) at room temperature followed by addition of 1,6-dibromohexane **S12** (686 µl, 4.5 mmol), sodium iodide (89 mg, 0.6 mmol), and potassium carbonate (828 mg, 6 mmol). The reaction mixture was heated to reflux for 24 h. The progress of reaction was monitored by TLC. Finally, the reaction mixture was cooled to room temperature, subjected to aqueous workup, and purification by silica gel column chromatography (ethyl acetate:n-hexane, 2:98) to isolate **S20** (585 mg, 64% yield; R_f 0.62, off-white solid). **^{1}H NMR** (500 MHz,

$CDCl_3$) δ 7.92 – 7.85 (m, 1H), 7.34 – 7.24 (m, 1H), 6.71 – 6.62 (m, 2H), 5.73 (s, 2H), 4.29 (t, *J* = 6.6 Hz, 2H), 3.43 (t, *J* = 6.8 Hz, 2H), 1.95 – 1.87 (m, 2H), 1.84 – 1.75 (m, 2H), 1.63 – 1.42 (m, 4H) ppm. **^{13}C NMR** (126 MHz, $CDCl_3$) δ 168.2, 150.6, 134.1, 131.2, 116.8, 116.3, 111.0, 64.2, 33.8, 32.7, 28.7, 27.9, 25.4 ppm. **HRMS** (ESI) $[M+Na]^+$ calcd. $C_{13}H_{18}BrNO_2$ 322.0419, found 322.0393.

Synthesis of 6-bromohexyl 2-(2-bromoacetamido)benzoate (S22)

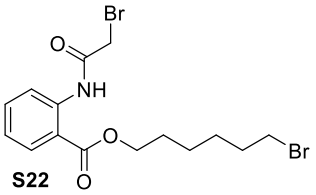

In a 10 ml round bottom flask, a stirred solution of 6-bromohexyl 2-aminobenzoate **S20** (585 mg, 1.9 mmol) and potassium carbonate (538 mg, 3.9 mmol) in DCM:H_2O (4 ml) bromoacetyl bromide **S21** (341 µl) were added slowly by pressure equalizer funnel at 0 °C and stirred for 2 h. The reaction mixture was brought to room temperature and stirred for another 2 h. The progress of reaction was monitored by TLC. Later, a saturated Na_2CO_3 solution was added to the reaction mixture followed by extraction by dichloromethane (50 ml, 3 times). Next, the organic layer was washed with brine solution and dried with Na_2SO_4. Subsequently, it was concentrated on a rotary evaporator and purified by silica gel flash column chromatography (ethyl acetate:hexane, 1:99) to render white solid product **22** (750 mg, 93%). **^{1}H NMR** (500 MHz, $CDCl_3$) δ 11.74 (s, 1H), 8.71 – 8.63 (m, 1H), 8.10 – 8.01 (m, 1H), 7.60 – 7.52 (m, 1H), 7.19 – 7.09 (m, 1H), 4.35 (t, *J* = 6.6 Hz, 2H), 4.01 (s, 2H), 3.41 (t, *J* = 6.7 Hz, 2H), 1.93 – 1.85 (m, 2H), 1.84 – 1.77 (m, 2H), 1.60 – 1.43 (m, 4H) ppm. **^{13}C NMR** (126 MHz, $CDCl_3$) δ 168.0, 164.9, 140.7, 134.6, 130.9, 123.4, 120.4, 116.0, 65.5, 33.7, 32.6, 29.7, 28.4, 27.8, 25.3 ppm. **HRMS** (ESI) $[M+H]^+$ calcd. $C_{15}H_{19}Br_2NO_3$ 419.9810, found 419.9812.

Synthesis of 6-bromohexyl 2-(2-(4-formyl-3-hydroxyphenoxy)acetamido)benzoate (S23)

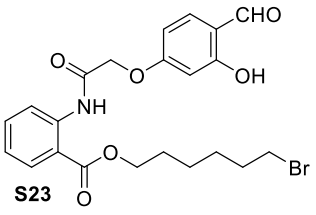

In a 25 ml round bottom flask, 6-bromohexyl 2-(2-bromoacetamido) benzoate **S22** (750 mg, 1.7 mmol), 2,4-dihydroxybenzaldehyde **S15** (234 mg, 1.7 mmol), and potassium carbonate (234 mg, 1.7 mmol) were dissolved in acetone (8.5 ml) and heated to reflux for 8 h. The progress of reaction was monitored by TLC. The reaction mixture was concentrated on a rotary evaporator and purified by silica gel flash column chromatography (ethyl acetate:hexane, 4:96) to give compound **S23** (410 mg, 50%). **^{1}H NMR** (500 MHz,

$CDCl_3$) δ 12.11 (s, 1H), 11.42 (s, 1H), 9.73 (s, 1H), 8.81 – 8.70 (m, 1H), 8.10 – 7.97 (m, 1H), 7.57 – 7.52 (m, 1H), 7.49 (d, *J* = 8.6 Hz, 1H), 7.16 – 7.09 (m, 1H), 6.74 (dd, *J* = 8.6, 2.3 Hz, 1H), 6.57 (d, *J* = 2.3 Hz, 1H), 4.65 (s, 2H), 4.34 (t, *J* = 6.6 Hz, 2H), 3.41 (t, *J* = 6.7 Hz, 2H), 1.95 – 1.84 (m, 2H), 1.84 – 1.72 (m, 2H), 1.58 – 1.41 (m, 4H) ppm. **^{13}C NMR** (126 MHz, $CDCl_3$) δ 194.7, 167.8, 165.9, 164.2, 164.0, 140.3, 135.7, 134.5, 130.8, 123.3, 120.4, 116.1, 115.9, 108.2, 102.4, 67.5, 65.3, 33.7, 32.6, 28.4, 27.8, 25.3 ppm. **HRMS** (ESI) $[M+Na]^+$ calcd. $C_{22}H_{24}BrNO_6$ 500.0685, found 500.0706.

Synthesis of 6-(tosyloxy)hexyl 2-(2-(4-formyl-3-hydroxyphenoxy)acetamido)benzoate (2d)

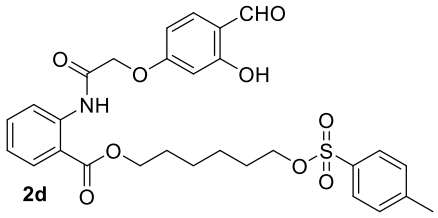

In a 10 ml round bottom flask, 6-bromohexyl 2-(2-(4-formyl-3-hydroxyphenoxy)acetamido) benzoate **S23** (239 mg, 0.5 mmol) and silver tosylate **S14** (167 mg, 0.6 mmol) were added in acetonitrile (5 ml). The resultant solution was heated for reflux for 12 h. After completion, the reaction mixture was concentrated on a rotary evaporator followed by aqueous workup and extraction with dichloromethane. The organic fraction was dried and the crude reaction mixture was purified by flash column chromatography (ethyl acetate: n-hexane, 30:70) to give **2d** (145 mg, 51%).**^{1}H NMR** (500 MHz, $CDCl_3$) δ 12.12 (s, 1H), 11.43 (s, 1H), 9.75 (s, 1H), 8.76 (d, *J* = 8.5 Hz, 1H), 8.08 – 7.99 (m, 1H), 7.77 (d, *J* = 8.2 Hz, 2H), 7.59 – 7.54 (m, 1H), 7.52 (d, *J* = 8.6 Hz, 1H), 7.33 (d, *J* = 8.3 Hz, 2H), 7.18 – 7.10 (m, 1H), 6.75 (dd, *J* = 8.6, 2.3 Hz, 1H), 6.58 (d, *J* = 2.2 Hz, 1H), 4.67 (s, 2H), 4.31 (t, *J* = 6.6 Hz, 2H), 4.03 (t, *J* = 6.4 Hz, 2H), 2.43 (s, 3H), 1.80 – 1.62 (m, 4H), 1.46 – 1.37 (m, 4H) ppm. **^{13}C NMR** (126 MHz, $CDCl_3$) δ 194.8, 167.9, 166.0, 164.3, 164.1, 144.8, 140.3, 135.8, 134.6, 133.2, 130.9, 129.9, 127.9, 123.4, 120.5, 116.2, 116.0, 108.3, 102.4, 70.4, 67.6, 65.3, 28.8, 28.4, 25.5, 25.2, 21.7 ppm. **HRMS** (ESI) $[M+Na]^+$ calcd. $C_{29}H_{31}NO_9SNa$ 592.1617, found 592.1628.

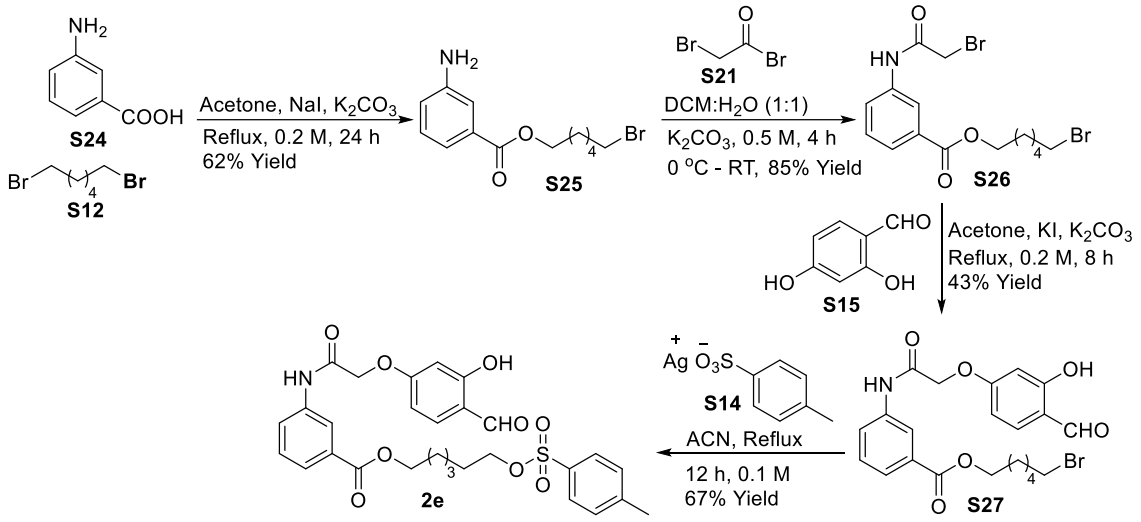

Scheme S5. Synthesis of 6-(tosyloxy)hexyl 3-(2-(4-formyl-3-hydroxyphenoxy)acetamido)benzoate (**2e**)

The procedure for synthesis of LDM reagent **2e** is similar to the LDM reagent **2d.**

Synthesis of 6-bromohexyl 3-aminobenzoate (S25)

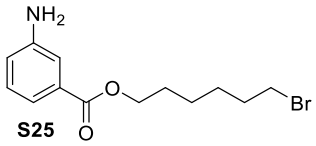

Yield 62%; R_f 0.48, white solid. **^{1}H NMR** (500 MHz, $CDCl_3$) δ 7.42 (d, *J* = 7.7 Hz, 1H), 7.37 – 7.31 (m, 1H), 7.24 – 7.18 (m, 1H), 6.90 – 6.82 (m, 1H), 4.29 (t, *J* = 6.6 Hz, 2H), 3.59 (s, *J* = 12.9 Hz, 2H), 3.41 (t, *J* = 6.8 Hz, 2H), 1.95 – 1.82 (m, 2H), 1.81 – 1.68 (m, 2H), 1.59 – 1.37 (m, 4H) ppm. **^{13}C NMR** (126 MHz, $CDCl_3$) δ 168.5, 150.3, 134.5, 131.9, 116.5, 116.5, 111.3, 64.1, 33.6, 32.8, 28.4, 27.4, 25.2 ppm. **HRMS** (ESI) $[M+H]^+$ calcd. $C_{13}HNO_2$ 300.0599, found 300.0575.

Synthesis of 6-bromohexyl 3-(2-bromoacetamido)benzoate (S26)

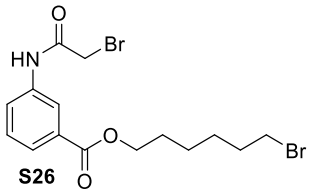

Yield 85%; R_f 0.57, off-white solid. **^{1}H NMR** (500 MHz, $CDCl_3$) δ 8.34 (s, 1H), 8.07 – 8.01 (m, 1H), 7.96 – 7.87 (m, 1H), 7.87 – 7.80 (m, 1H), 7.49 – 7.40 (m, 1H), 4.33 (t, *J* = 6.6 Hz, 2H), 4.05 (s, 2H), 3.42 (t, *J* = 6.8 Hz, 2H), 1.94 – 1.83 (m, 2H), 1.83 – 1.73 (m, 2H), 1.62 – 1.39 (m, 4H) ppm. **^{13}C NMR** (126 MHz, $CDCl_3$) δ 166.2, 164.1, 137.2, 131.4, 129.4, 126.3, 124.7, 121.1, 65.3, 33.8, 32.7, 29.4, 28.6, 27.9, 25.3 ppm. **HRMS** (ESI) $[M+H]^+$ calcd. $C_{15}H_{19}Br_2NO_3$ 419.9810, found 419.9813.

Synthesis of 6-bromohexyl 3-(2-(4-formyl-3-hydroxyphenoxy)acetamido)benzoate (S27)

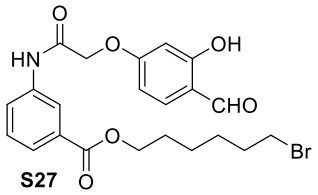

Yield 43%, off-white solid. **^{1}H NMR** (500 MHz, $CDCl_3$) δ 11.44 (s, 1H), 9.78 (s, 1H), 8.26 (s, 1H), 8.09 – 8.03 (m, 1H), 8.03 – 7.96 (m, 1H), 7.87 – 7.81 (m, 1H), 7.54 (d, *J* = 8.6 Hz, 1H), 7.49 – 7.41 (m, 1H), 6.67 (dd, *J* = 8.6, 2.4 Hz, 1H), 6.54 (d, *J* = 2.4 Hz, 1H), 4.68 (s, 2H), 4.33 (t, *J* = 6.6 Hz, 2H), 3.42 (t, *J* = 6.8 Hz, 2H), 1.95 – 1.86 (m, 2H), 1.84 – 1.74 (m, 2H), 1.58 – 1.42 (m, 4H) ppm. **^{13}C NMR** (126 MHz, $CDCl_3$) δ 194.6, 166.0, 165.1, 164.3, 163.4, 136.8, 135.8, 131.3, 129.3, 126.1, 124.6, 121.0, 116.4, 107.9, 102.3, 67.3, 65.1, 33.7, 32.6, 28.5, 27.8, 25.2 ppm. **HRMS** (ESI) $[M+H]^+$ calcd. $C_{22}H_{24}BrNO_6$ 478.0865, found 478.0849.

Synthesis of 6-(tosyloxy)hexyl 3-(2-(4-formyl-3-hydroxyphenoxy)acetamido)benzoate (2e)

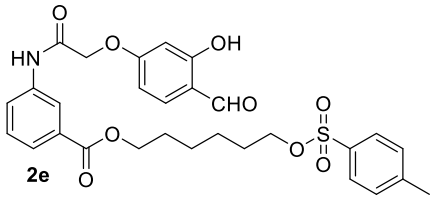

Yield 67%; R_f 0.32, off-white solid. **^{1}H NMR** (500 MHz, $CDCl_3$) δ 11.42 (s, 1H), 9.77 (s, 1H), 8.35 (s, 1H), 8.07 – 8.00 (m, 2H), 7.86 – 7.81 (m, 1H), 7.76 (d, *J* = 8.3 Hz, 2H), 7.52 (d, *J* = 8.6 Hz, 1H), 7.48 – 7.42 (m, 1H), 7.32 (d, *J* = 8.0 Hz, 2H), 6.66 (dd, *J* = 8.6, 2.4 Hz, 1H), 6.51 (d, *J* = 2.3 Hz, 1H), 4.66 (s, 2H), 4.29 (t, *J* = 6.5 Hz, 2H), 4.04 (t, *J* = 6.3 Hz, 2H), 2.43 (s, 3H), 1.80 – 1.62 (m, 4H), 1.49 – 1.35 (m, 4H) ppm. **^{13}C NMR** (126 MHz, $CDCl_3$) δ 194.8, 166.1, 165.3, 164.4, 163.6, 144.9, 137.0, 135.9, 133.1, 131.4, 129.9, 129.4, 127.9, 126.2, 124.9, 121.1, 116.4, 108.1, 102.4, 70.5, 67.4, 65.1, 28.7, 28.5, 25.5, 25.2, 21.7 ppm. **HRMS** (ESI) $[M+Na]^+$ calcd. $C_{29}H_{31}NO_9SNa$ 592.1617, found 592.1633.

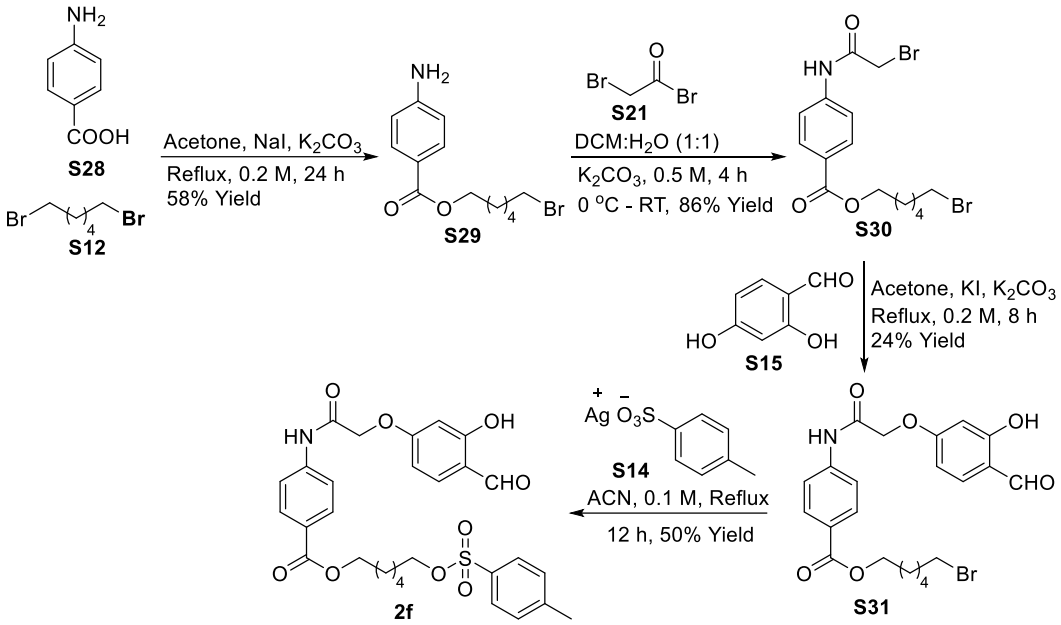

Scheme S6. Synthesis of 6-bromohexyl 4-(2-(4-formyl-3-hydroxyphenoxy)acetamido)benzoate (**2f**)

The procedure for synthesis of LDM reagent **2f** is similar to the LDM reagent **2d**.

Synthesis of 6-bromohexyl 4-aminobenzoate (S29)

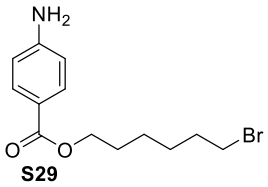

Yield 58%; R_f 0.45, white solid. **^{1}H NMR** (500 MHz, $CDCl_3$) δ 7.84 (d, *J* = 8.6 Hz, 2H), 6.63 (d, *J* = 8.6 Hz, 2H), 4.25 (t, *J* = 6.6 Hz, 2H), 4.09 (s, 2H), 3.40 (t, *J* = 6.8 Hz, 2H), 1.93 – 1.82 (m, 2H), 1.80 – 1.71 (m, 2H), 1.56 – 1.40 (m, 4H). **^{13}C NMR** (176 MHz, $CDCl_3$) δ 166.8, 150.9, 131.7, 120.2, 113.9, 64.4, 33.9, 32.8, 28.8, 28.0, 25.5. **HRMS** (ESI) $[M+H]^+$ calcd. $C_{13}H_{18}BrNO_2$ 300.0599, found 300.0587.

Synthesis of 6-bromohexyl 4-(2-bromoacetamido) benzoate (S30)

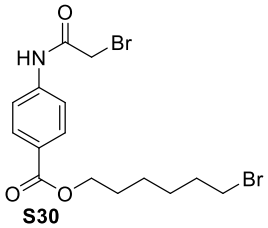

Yield 86%; R_f 0.49, white solid. **^{1}H NMR** (500 MHz, $CDCl_3$) δ 8.26 (s, 1H), 8.09 – 8.00 (m, 2H), 7.70 – 7.58 (m, 2H), 4.31 (t, *J* = 6.6 Hz, 2H), 4.04 (s, 2H), 3.42 (t, *J* = 6.8 Hz, 2H), 1.96 – 1.84 (m, 2H), 1.84 –

1.70 (m, 2H), 1.61 – 1.40 (m, 4H) ppm. **^{13}C NMR** (126 MHz, $CDCl_3$) δ 166.1, 163.6, 141.0, 130.9, 127.0, 119.2, 65.0, 33.8, 32.7, 29.4, 28.7, 27.9, 25.4 ppm. **HRMS** (ESI) $[M+Na]^+$ calcd. $C_{15}H_{19}Br_2NO_3$ 441.9629, found 441.9641.

Synthesis of 6-bromohexyl 4-(2-(4-formyl-3-hydroxyphenoxy)acetamido)benzoate (S31)

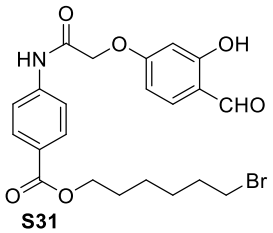

S31

Yield 24%; R_f 0.37, white solid. **^{1}H NMR** (500 MHz, $CDCl_3$) δ 11.43 (s, 1H), 9.79 (s, 1H), 8.28 (s, 1H), 8.11 – 7.98 (m, 2H), 7.73 – 7.64 (m, 2H), 7.55 (d, *J* = 8.6 Hz, 1H), 6.67 (dd, *J* = 8.6, 2.4 Hz, 1H), 6.54 (d, *J* = 2.4 Hz, 1H), 4.68 (s, 2H), 4.31 (t, *J* = 6.6 Hz, 2H), 3.42 (t, *J* = 6.8 Hz, 2H), 1.97 – 1.83 (m, 2H), 1.84 – 1.74 (m, 2H), 1.58 – 1.43 (m, 4H) ppm. **^{13}C NMR** (126 MHz, $CDCl_3$) δ 194.8, 166.0, 165.2, 164.4, 163.4, 140.7, 136.0, 131.0, 126.9, 119.4, 116.6, 107.9, 102.5, 67.5, 65.0, 33.8, 32.7, 28.7, 28.2, 25.4 ppm. **HRMS** (ESI) $[M+H]^+$ calcd. $C_{22}H_{24}BrNO_6$ 478.0865 found 478.0848.

Synthesis of 6-bromohexyl 4-(2-(4-formyl-3-hydroxyphenoxy)acetamido)benzoate (2f)

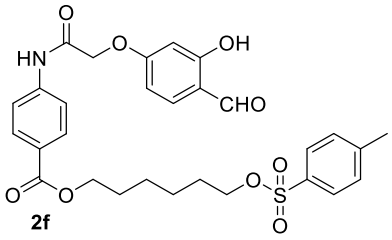

2f

Yield 50%; R_f 0.34, white solid. **^{1}H NMR** (500 MHz, $CDCl_3$) δ 11.43 (s, 1H), 9.78 (s, *J* = 13.5 Hz, 1H), 8.31 (s, 1H), 8.03 (d, *J* = 8.7 Hz, 2H), 7.78 (d, *J* = 8.2 Hz, 2H), 7.68 (d, *J* = 8.7 Hz, 2H), 7.54 (d, *J* = 8.6 Hz, 1H), 7.33 (d, *J* = 8.0 Hz, 2H), 6.66 (dd, *J* = 8.6, 2.4 Hz, 1H), 6.54 (d, *J* = 2.3 Hz, 1H), 4.67 (s, 2H), 4.26 (t, *J* = 6.6 Hz, 2H), 4.03 (t, *J* = 6.4 Hz, 2H), 2.44 (s, 3H), 1.76 – 1.64 (m, 4H), 1.47 – 1.34 (m, 4H) ppm. **^{13}C NMR** (126 MHz, $CDCl_3$) δ 194.8, 166.0, 165.2, 164.4, 163.4, 144.8, 140.7, 136.0, 133.2, 131.0, 129.9, 128.0, 126.8, 119.4, 116.5, 107.9, 102.5, 70.5, 67.4, 64.9, 28.8, 28.6, 25.5, 25.2, 21.7 ppm. **HRMS** (ESI) $[M+Na]^+$ calcd. $C_{29}H_{31}NO_9SNa$ 592.1617, found 592.1618.

3b. Derivatives of O-hydroxylamine

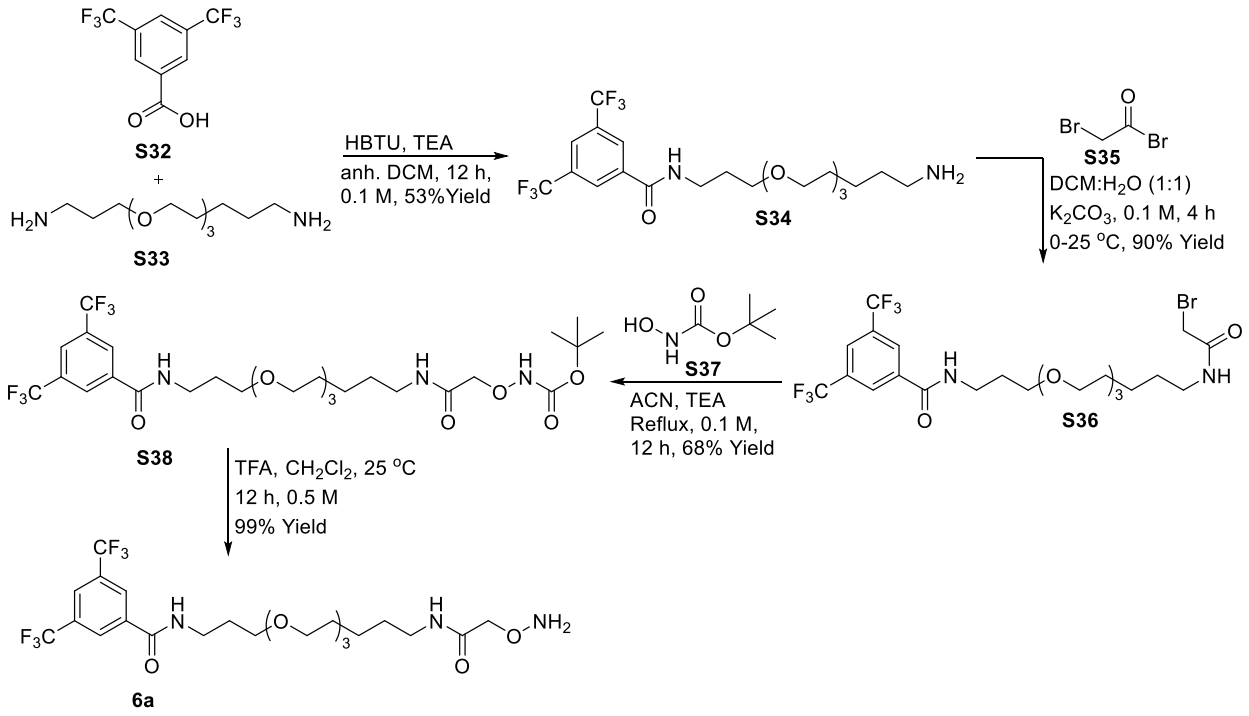

Scheme S7. N-(1-(aminooxy)-2-oxo-7,10,13-trioxa-3-azahexadecan-16-yl)-3,5-bis(trifluoromethyl)benzamide (**6a**)

Synthesis of N-(1-bromo-2-oxo-7,10,13-trioxa-3-azahexadecan-16-yl)-3,5-bis(trifluoromethyl) benzamide (S36)

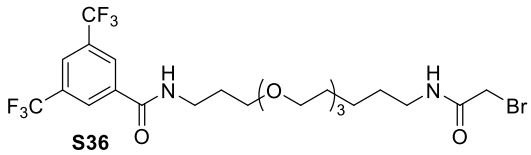

In a 10 ml round bottom flask, N-(3-(2-(2-(3-aminopropoxy)ethoxy)ethoxy)propyl)-3,5-bis(trifluoromethyl)benzamide **S34** (200 mg, 0.43 mmol) and potassium carbonate (237 mg, 1.72 mmol) in DCM:H_2O (1:1, 4.3 ml) were stirred at 0 °C for 5 minutes. To this solution, 2- bromoacetyl bromide **S35** (162 µl, 1.29 mmol) was added slowly over a period of 1 hour. The reaction mixture was brought to room temperature and stirred for another 3 h. The progress of the reaction was monitored by TLC. The reaction mixture was concentrated using rotary evaporator. The purification of crude reaction mixture was performed by silica gel flash column chromatography using ethyl acetate:n-hexane (70:30) to isolate **S36** (225 mg, 90% yield; viscous liquid). **^{1}H NMR** (500 MHz, CD_3OD) δ 8.45 (s, 2H), 8.17 (s, 1H), 3.84 (s, 2H), 3.69 – 3.51 (m, 14H), 3.35 – 3.32 (m, 2H), 1.98 – 1.89 (m, 2H), 1.83 – 1.74 (m, 2H). **^{13}C NMR** (126

MHz, CD_3OD) δ 169.3, 166.5, 138.2, 132.9, 128.9, 125.8, 123.5, 71.5, 71.2, 70.0, 69.8, 38.9, 38.8, 38.5, 30.3, 30.0, 28.8. **HRMS** (ESI) $[M+Na]^+$ calcd. $C_{21}H_{28}BrF_6N_2O_5Na$ 603.0905, found 603.0911.

Synthesis of tert-butyl ((1-(3,5-bis(trifluoromethyl)phenyl)-1,17-dioxo-6,9,12-trioxa-2,16-diazaoctadecan-18-yl)oxy)carbamate (S38)

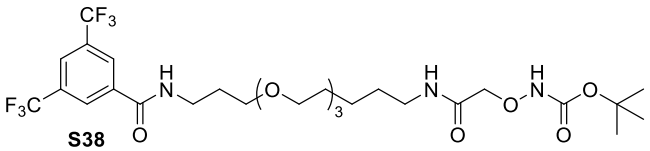

S38

In a 5 ml round bottom flask, N-(1-bromo-2-oxo-7,10,13-trioxa-3-azahexadecan-16-yl)-3,5-bis(trifluoromethyl)benzamide **S36** (200 mg, 0.34 mmol), tert-butyl hydroxycarbamate **S37** (91 mg, 0.69 mmol), and triethyl amine (103 µl, 1.0 mmol) were dissolved in acetonitrile (3.4 ml) and heated to reflux for 12 h. The progress of reaction was monitored by TLC. The reaction mixture was concentrated on a rotary evaporator and purified by silica gel flash column chromatography (ethyl acetate:hexane, 60:40) to give compound **S38** (146 mg, 68%). **^{1}H NMR** (500 MHz, CD_3OD) δ 8.43 (s, 2H), 8.16 (s, 1H), 4.23 (s, 2H), 3.68 – 3.50 (m, 14H), 3.34 (t, *J* = 6.8 Hz, 2H), 1.95 – 1.88 (m, 2H), 1.82 – 1.75 (m, 2H), 1.47 (s, 9H). **^{13}C NMR** (126 MHz, CD_3OD) δ 171.3, 166.5, 159.7, 138.2, 132.9, 128.9, 125.6, 123.5, 82.9, 76.4, 71.5, 71.2, 71.2, 70.0, 69.8, 38.9, 37.4, 30.32, 30.2 (2C), 28.4 (3C). **HRMS** (ESI) $[M+Na]^+$ calcd. $C_{26}H_{38}F_6N_3O_8Na$ 656.2383, found 656.2400.

N-(1-(aminooxy)-2-oxo-7,10,13-trioxa-3-azahexadecan-16-yl)-3,5-bis(trifluoromethyl) benzamide (6a)

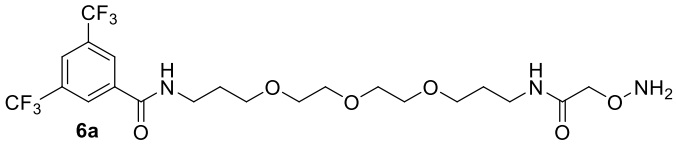

6a

In a 5 ml round bottom flask, tert-butyl ((1-(3,5-bis(trifluoromethyl)phenyl)-1,17-dioxo-6,9,12-trioxa-2,16-diazaoctadecan-18-yl)oxy)carbamate **S38** (130 mg, 0.20 mmol), was dissolved in ACN:H_2O (2 ml). To this solution, trifluoroacetic acid (92 µl, 0.8 mmol) was added slowly over 15 minutes and stirred at 25 °C for 12 h. The reaction mixture was concentrate and dried on rotary evaporator, and triturate in diethyl ether, concentrated in vacuo to give **6a** (105 mg, yield 99%; pale yellow liquid. **^{1}H NMR** (700 MHz, CD_3OD) δ 8.44 (s, 2H), 8.16 (s, 1H), 4.56 (s, 2H), 3.72 – 3.46 (m, 14H), 3.35 – 3.32 (m, 2H), 1.97 – 1.86 (m, 2H), 1.83 – 1.73 (m, 2H). **^{13}C NMR** (176 MHz, CD_3OD) δ 168.3, 165.2, 136.8, 127.6, 124.5, 123.9, 122.4, 70.9, 70.1, 69.8, 68.5, 38.9, 37.5, 36.4, 33.1, 28.9, 28.8 (2). **HRMS** (ESI) $[M+H]^+$ calcd. $C_{21}H_{30}F_6N_3O_6$ 534.2039, found 534.2006.

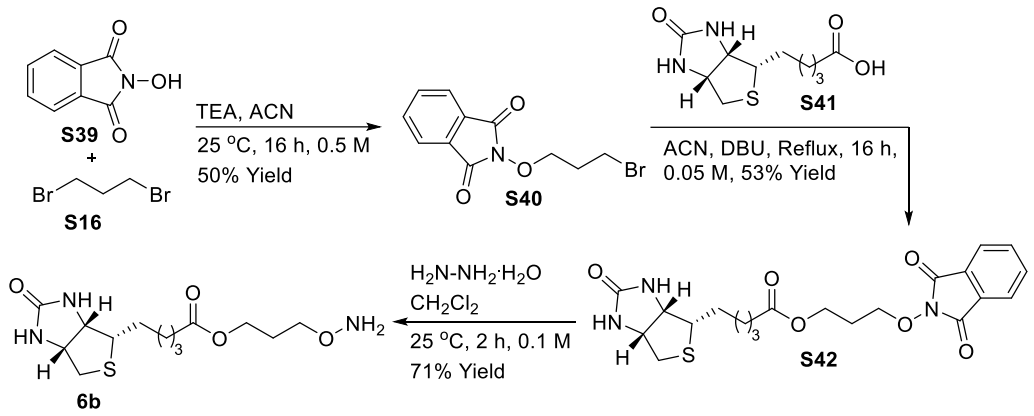

Scheme S8. Synthesis of 3-(aminooxy)propyl 5-(2-oxohexahydro-1H-thieno[3,4-d]imidazol-4-yl) pentanoate (**6b**)

Synthesis of 2-(3-bromopropoxy)isoindoline-1,3-dione (S40)[2]

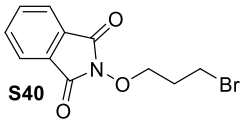

In a 250 ml round bottom flask, N-hydroxyphthalimide **S39** (4.894 g, 30 mmol) and triethyl amine (6.09 ml, 60 mmol) were dissolved in acetonitrile (60 ml). To this solution, 1,3-dibromopropane **S16** (8.34 ml, 60 mmol) was added and stirred at 25 °C for 16 h. The reaction mixture was concentrated in vacuo followed by addition of 1 N NaOH solution and ethyl acetate. The organic layer was separated, dried over anh. sodium sulfate, filtered, and concentrated in vacuo. The purification of the crude reaction mixture was performed by silica gel flash column chromatography using ethyl acetate:hexane (3:97) to isolate **S40** (4.259 g, 50% yield; R_f 0.57, ethyl acetate:n-hexane 30:70; white solid). **^{1}H NMR** (400 MHz, $CDCl_3$) δ 7.89-7.81 (m, 2H), 7.80-7.73 (m, 2H), 4.37 (t, *J* = 5.8 Hz, 2H), 3.71 (t, *J* = 6.5 Hz, 2H), 2.36-2.26 (m, 2H) ppm. **^{13}C NMR** (101 MHz, $CDCl_3$) δ 163.7, 134.7, 129.0, 123.7, 76.2, 31.6, 29.4 ppm. **HRMS** (ESI) $[M+Na]^+$ calcd. $C_{11}H_{11}{}^{79}BrNO_3Na$ 305.9742 found 305.9739.

Synthesis of 3-((1,3-dioxoisoindolin-2-yl)oxy)propyl 5-(2-oxohexahydro-1H-thieno[3,4-d]imidazol-4-yl)pentanoate (S42)

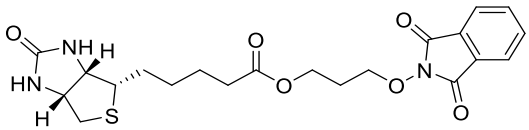

S42

In a 5 ml round bottom flask, biotin **S41** (244 mg, 1 mmol), 2-(3-bromopropoxy)isoindoline-1,3-dione **S40** (568 mg, 2 mmol), and DBU (304 µl, 2 mmol) were dissolved in acetonitrile (20 ml). The reaction mixture was refluxed and the progress of the reaction was monitored by TLC. After 16 h, the reaction mixture was concentrated in vacuum. This was followed by solvent-solvent extraction using ethyl acetate and water. The organic fractions were combined, dried on anh. sodium sulfate, filtered, and concentrated on rotary evaporator. The purification of crude reaction mixture was performed by silica gel flash column chromatography (MeOH:DCM, 0.5-5%) to isolate 3-((1,3-dioxoisoindolin-2-yl)oxy)propyl 5-(2-oxohexahydro-1H-thieno[3,4-d]imidazol-4-yl)pentanoate **S42** (224 mg, 50% yield; R_f 0.33, MeOH:DCM 05:95; white solid). **^{1}H NMR** (500 MHz, $CDCl_3$) δ 7.89-7.82 (m, 2H), 7.80-7.73 (m, 2H), 5.96 (s, 1H), 5.48 (s, 1H), 4.56-4.47 (m, 1H), 4.38-4.26 (m, 5H), 3.23-3.13 (m, 1H), 2.92 (dd, *J* = 12.8, 5.0 Hz, 1H), 2.74 (d, *J* = 12.8 Hz, 1H), 2.36 (t, *J* = 7.4 Hz, 2H), 2.16-2.09 (m, 2H), 1.80-1.60 (m, 4H), 1.54-1.39 (m, 2H) ppm. **^{13}C NMR** (126 MHz, $CDCl_3$) δ 173.7, 163.8, 163.7, 134.7, 129.0, 123.7, 75.1, 62.0, 60.7, 60.2, 55.5, 40.7, 34.0, 28.4, 28.3, 27.8, 24.9 ppm. **HRMS** (ESI) $[M+H]^+$ calcd. $C_{21}H_{26}N_3O_6S$ 448.1542, found 448.1548.

Synthesis of 3-(aminooxy)propyl 5-(2-oxohexahydro-1H-thieno[3,4-d]imidazol-4-yl)pentanoate (6b)

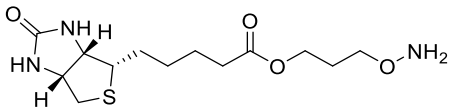

6b

In a 5 ml round bottom flask, 3-((1,3-dioxoisoindolin-2-yl)oxy)propyl 5-(2-oxohexahydro-1H-thieno[3,4-d]imidazol-4-yl)pentanoate **S42** (134 mg, 0.3 mmol) in DCM (3 ml) and hydrazine monohydrate (80%, 37 µl, 0.75 mmol) were stirred at room temperature. The progress of the reaction was followed by TLC. After 2 h, the reaction mixture was filtered and concentration of the filtrate in vacuo led to the isolation of 3-(aminooxy)propyl 5-(2-oxohexahydro-1H-thieno[3,4-d]imidazol-4-yl)pentanoate **6b** (67 mg, 71% yield; R_f 0.21, MeOH:DCM 05:95; white solid. **^{1}H NMR** (500 MHz, D_2O) δ 4.63 (dd, *J* = 7.9, 4.9 Hz, 1H), 4.45 (dd, *J* = 7.9, 4.5 Hz, 1H), 4.21 (t, *J* = 6.3 Hz, 2H), 3.90 (t, *J* = 6.2 Hz, 2H), 3.45-3.27 (m, 1H), 3.02 (dd, *J* = 13.1, 5.0 Hz, 1H), 2.80 (d, *J* = 13.0 Hz, 1H), 2.44 (t, *J* = 7.3 Hz, 2H), 2.08-1.94 (m, 2H), 1.84-1.55 (m, 4H), 1.53-1.37 (m, 2H) ppm. **^{13}C NMR** (126 MHz, D_2O) δ 176.9, 165.3, 72.4, 62.1, 62.0, 60.3, 55.3, 39.7, 33.6, 27.9, 27.6, 26.7, 24.1 ppm. **HRMS** (ESI) $[M+H]^+$ calcd. $C_{13}H_{24}N_3O_4S$ 318.1488, found 318.1467.

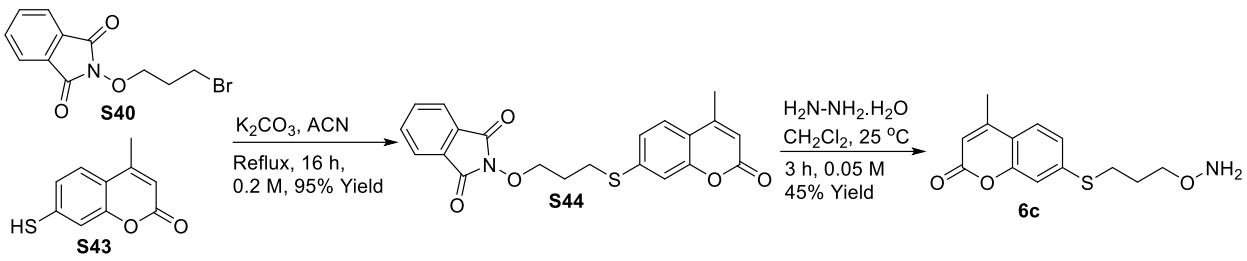

Scheme S9. Synthesis of 7-((3-(aminooxy)propyl)thio)-4-methyl-2H-chromen-2-one (**6c**)

Synthesis of 2-(3-((4-methyl-2-oxo-2H-chromen-7-yl)thio)propoxy)isoindoline-1,3-dione (S44)

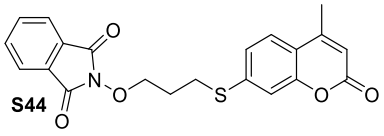

In a 25 ml round bottom flask, 7-mercapto-4-methylcoumarin **S43** (192 mg, 1 mmol), K_2CO_3 (276 mg, 2 mmol), and 2-(3-bromopropoxy)isoindoline-1,3-dione **S40** (568 mg, 2 mmol) were dissolved in degassed acetonitrile (5 ml) and refluxed for 16 h. The reaction mixture was concentrated in vacuo and purified by silica gel flash column chromatography using ethyl acetate:hexane (7:3) to give **S44** (375 mg, 95% yield; R_f 0.37, ethyl acetate:n-hexane 50:50; white solid). **^{1}H NMR** (400 MHz, $CDCl_3$) δ 7.90-7.81 (m, 2H), 7.80-7.73 (m, 2H), 7.48 (d, *J* = 8.2 Hz, 1H), 7.26-7.20 (m, 2H), 6.22 (d, *J* = 0.8 Hz, 1H), 4.36 (t, *J* = 5.8 Hz, 2H), 3.35 (t, *J* = 7.1 Hz, 2H), 2.41 (d, *J* = 0.9 Hz, 3H), 2.23-2.08 (m, 2H) ppm. **^{13}C NMR** (101 MHz, $CDCl_3$) δ 163.8, 160.7, 154.0, 152.3, 142.6, 134.7, 129.0, 124.9, 123.8, 123.4, 117.5, 114.8, 114.1, 76.6, 28.7, 27.8, 18.7 ppm. **HRMS** (ESI) $[M+H]^+$ calcd. $C_{21}H_{18}NO_5S$ 396.0906, found 396.0925.

Synthesis of 7-((3-(aminooxy)propyl)thio)-4-methyl-2H-chromen-2-one (6c)

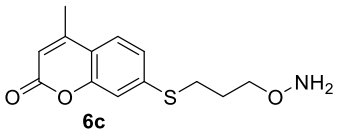

2-(3-((4-methyl-2-oxo-2H-chromen-7-yl)thio)propoxy)isoindoline-1,3-dione **S44** (237 mg, 0.6 mmol) was dissolved in CH_2Cl_2 (12 ml) in a 50 ml round bottom flask. To this solution, hydrazine monohydrate (80%, 29 µl, 0.6 mmol) was added and stirred at 25 °C for 3 h. The reaction mixture was filtered and the filtrate was concentrated. The purification of crude reaction mixture was performed by reverse phase preparative HPLC to isolate **6c** (76 mg, 45% yield; R_f 0.6, ethyl acetate:n-hexane 50:50; pale green viscous liquid). **^{1}H NMR** (400 MHz, $CDCl_3$) δ 7.46 (d, *J* = 8.3 Hz, 1H), 7.23-7.13 (m, 2H), 6.18 (d, *J* = 0.9 Hz, 1H), 3.79 (t, *J* = 5.9 Hz, 2H), 3.07 (t, *J* = 7.3 Hz, 2H), 2.40 (d, *J* = 0.8 Hz, 3H), 2.02-1.90 (m, 2H) ppm. **^{13}C NMR** (101

MHz, $CDCl_3$) δ 160.7, 154.0, 152.3, 143.3, 124.7, 123.1, 117.2, 114.1, 113.9, 73.9, 29.0, 27.8, 18.6 ppm. **HRMS** (ESI) $[M+H]^+$ calcd. $C_{13}H_{16}NO_3S$ 266.0851, found 266.0841.

4. Protein labeling data

4a. Table S3 Control reaction of reagent (2a) with native ubiquitin

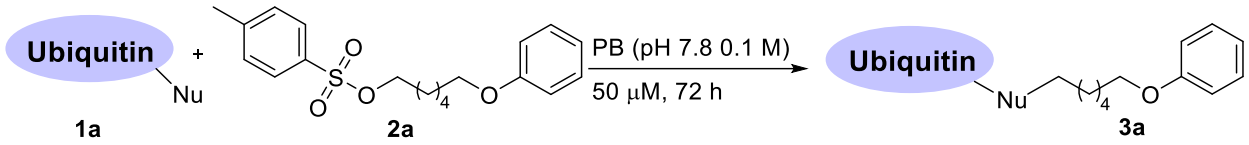

Sr. No.	Equivalent (2a)	Temp (°C)	% Conversion[a]
1	25	25	0
2	25	37	0
3	50	25	0
4	50	37	0
5	100	25	0
6	100	37	0

[a] % Conversion was determined by ESI-MS.

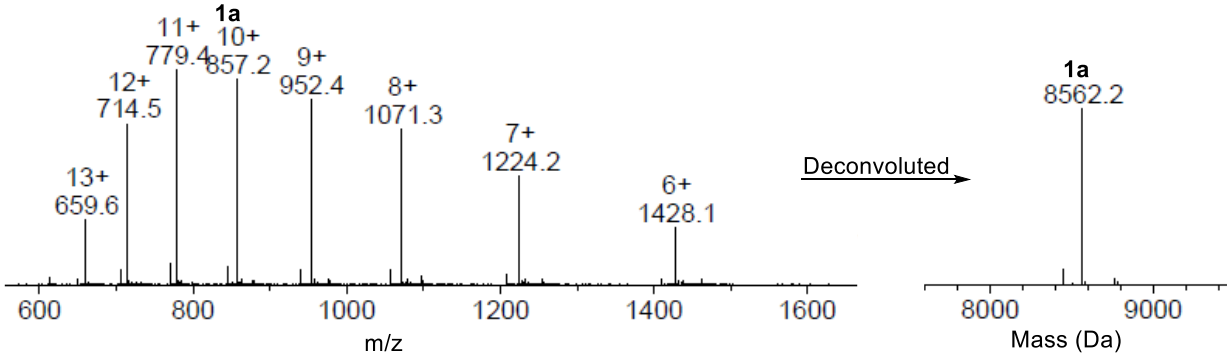

Figure S1. ESI-MS spectrum for labeled ubiquitin (**3a**)

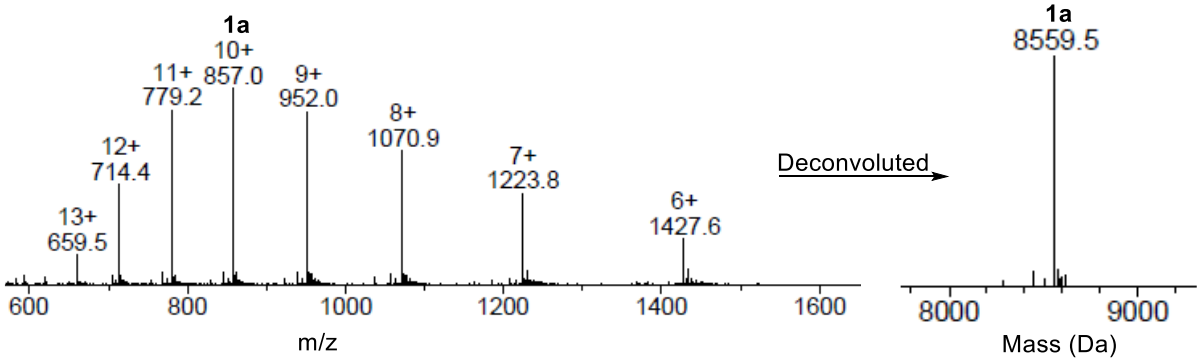

Figure S2. ESI-MS spectrum for labeled ubiquitin (**3a**)

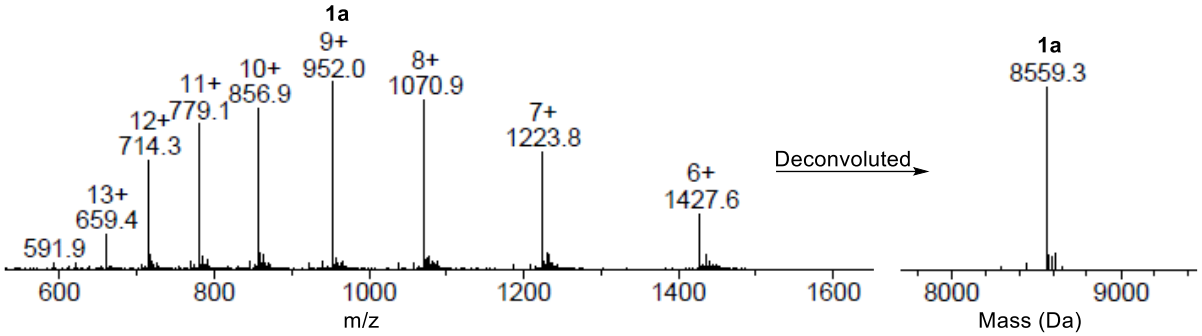

Figure S3. ESI-MS spectrum for labeled ubiquitin (**3a**)

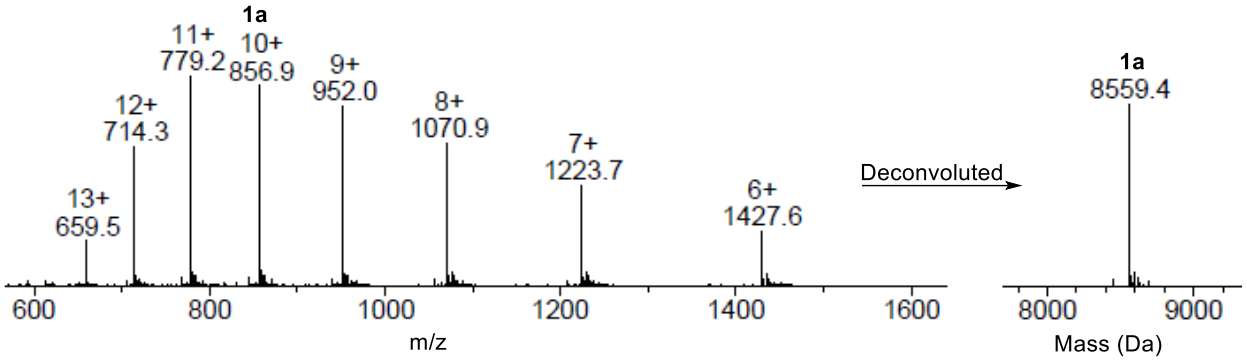

Figure S4. ESI-MS spectrum for labeled ubiquitin (**3a**)

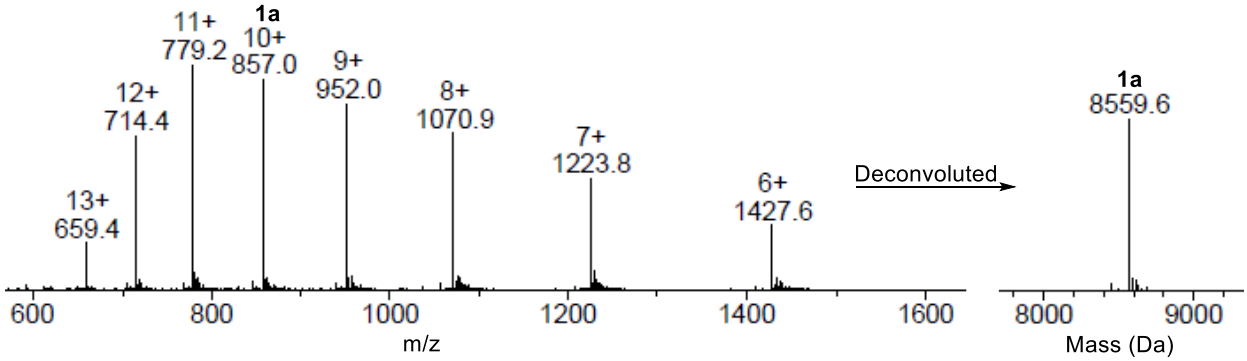

Figure S5. ESI-MS spectrum for labeled ubiquitin (**3a**)

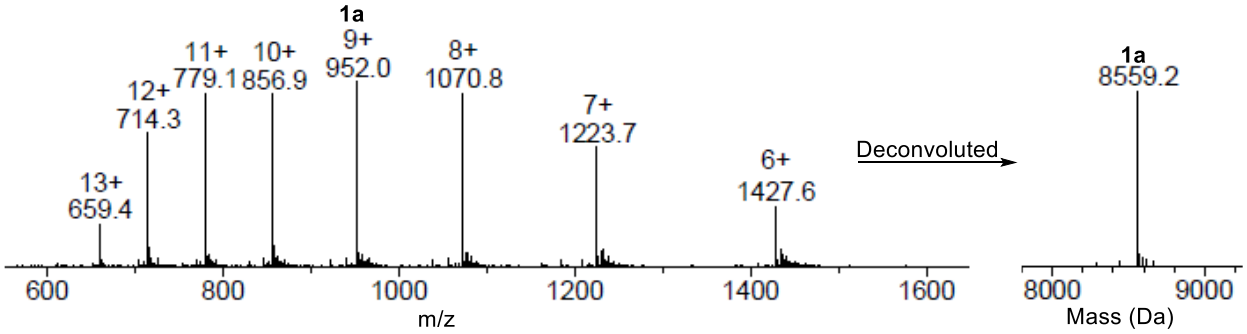

Figure S6. ESI-MS spectrum for labeled ubiquitin (**3a**)

4b. Table S4 Control reaction of reagent (2a) with native proteins

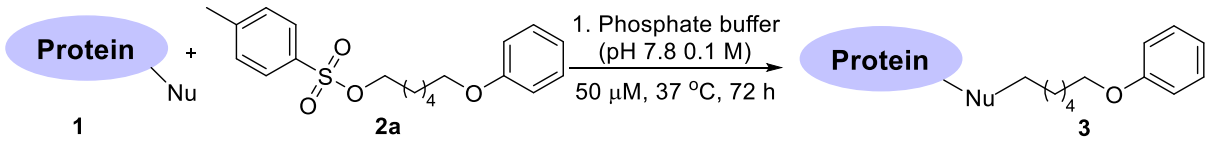

Entry	Proteins	% Conversion[a] (3)
1	Insulin (**1b**)	0
2	α-Lactalbumin (**1c**)	4
3	Myoglobin (**1d**)	5

[a] % Conversion was determined by ESI-MS.

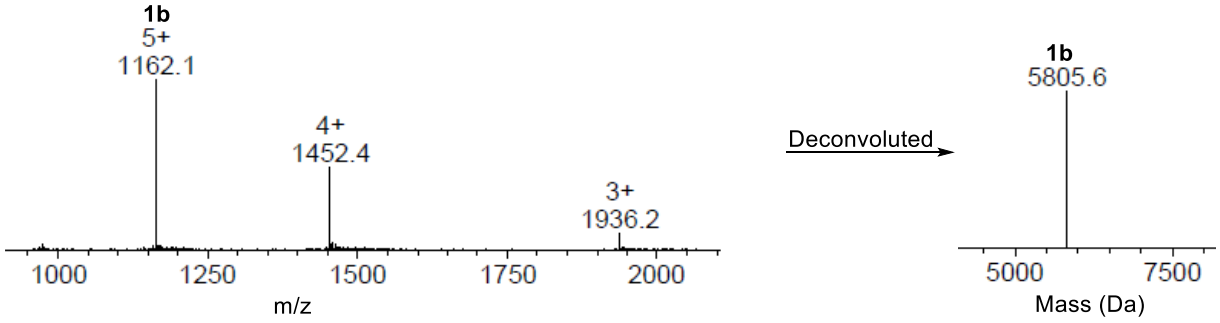

Figure S7. ESI-MS spectrum for labeled insulin (**3b**)

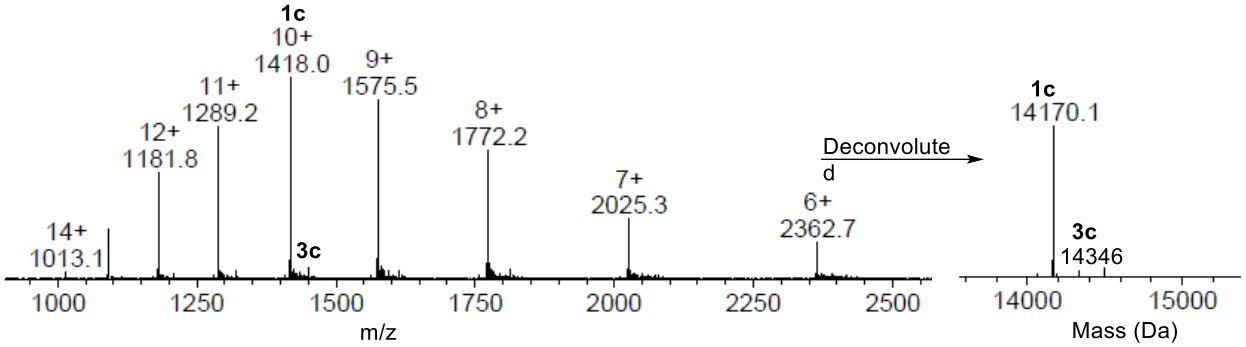

Figure S8. ESI-MS spectrum for labeled α-lactalbumin (**3c**)

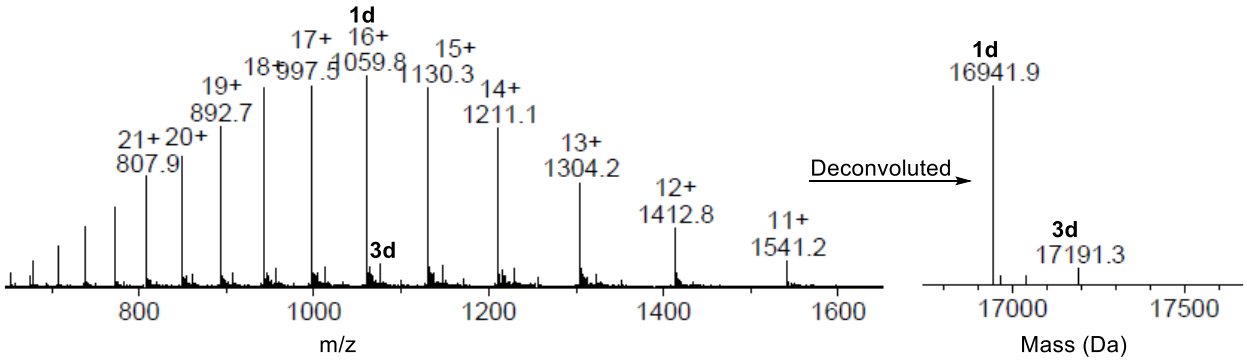

Figure S9. ESI-MS spectrum for labeled myoglobin (**3d**)

4c. Single-site labeling of native proteins

a)

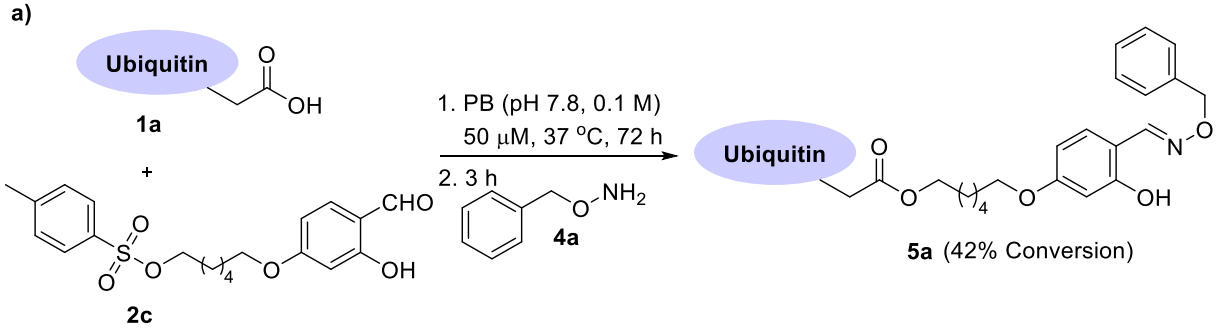
Ubiquitin
1a
+
2c
1. PB (pH 7.8, 0.1 M)
50 μM, 37 °C, 72 h
2. 3 h
4a
Ubiquitin
5a (42% Conversion)

b)

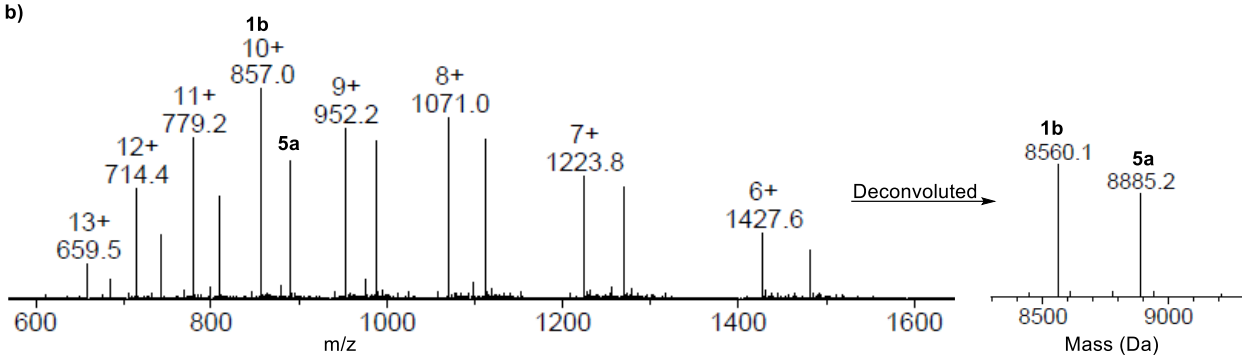
1b
10+
857.0
11+
779.2
12+
714.4
13+
659.5
5a
9+
952.2
8+
1071.0
7+
1223.8
6+
1427.6
600
800
1000
1200
1400
1600
m/z
Deconvoluted
1b
8560.1
5a
8885.2
8500
9000
Mass (Da)

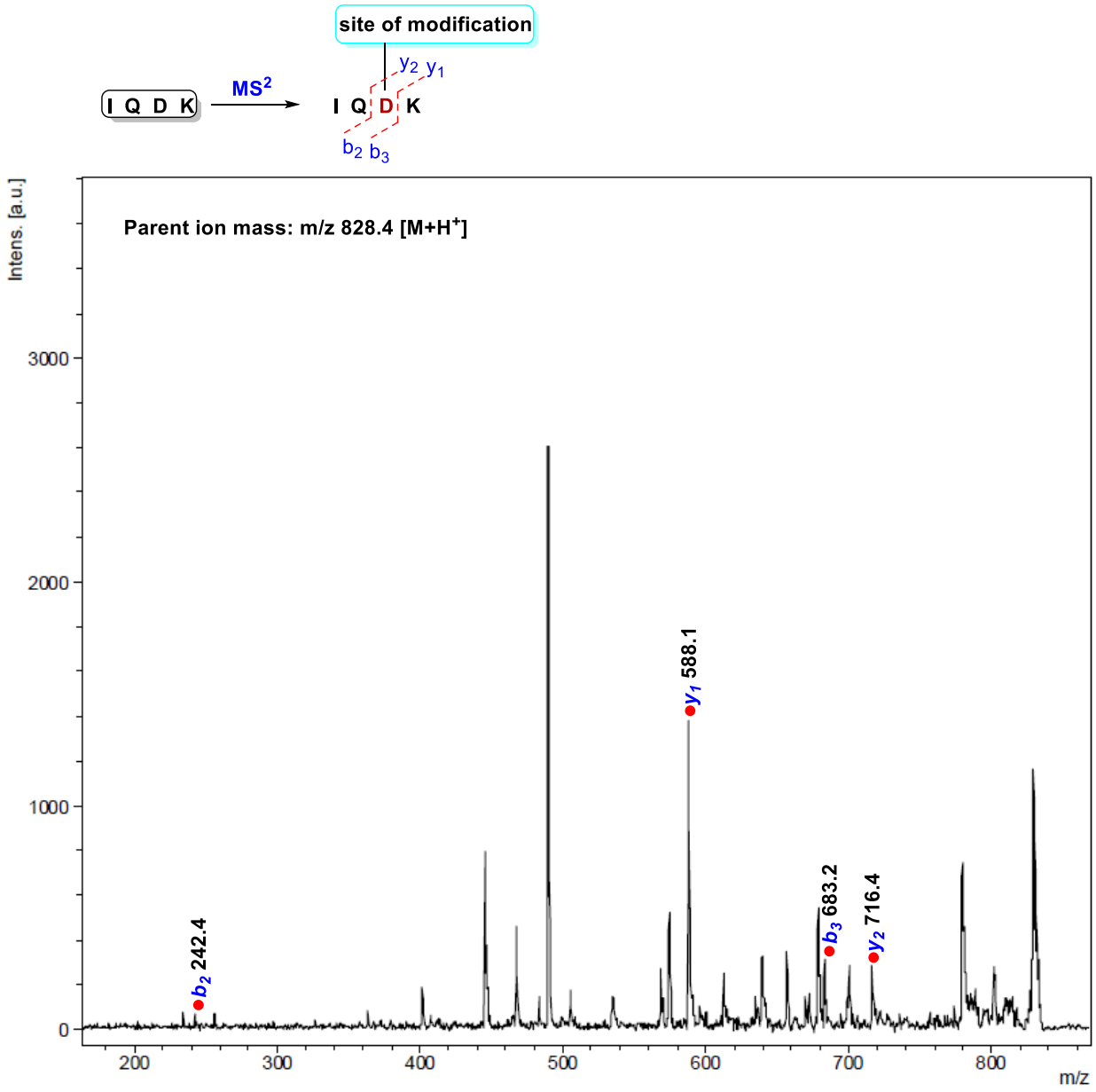

Figure S10. (a) Site-selective labeling of ubiquitin **1a** enabled by LDM reagent **2c** (25 equiv.). (b) ESI-MS spectrum for mono-labeled ubiquitin (**5a**) after oxime formation. (c) MS-MS spectrum of labeled ubiquitin after the digestion of **5a** with trypsin. The site of modification is D32.

a)

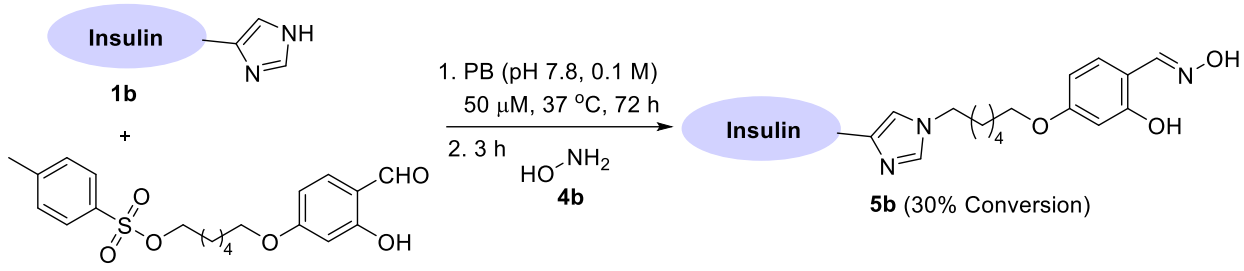
Insulin
NH
N
1b
+
CHO
OH
O
S
O
O
4
O
1. PB (pH 7.8, 0.1 M)
50 μM, 37 °C, 72 h
2. 3 h
HO
NH2
4b
Insulin
N
N
4
O
OH
N
OH
5b (30% Conversion)

b)

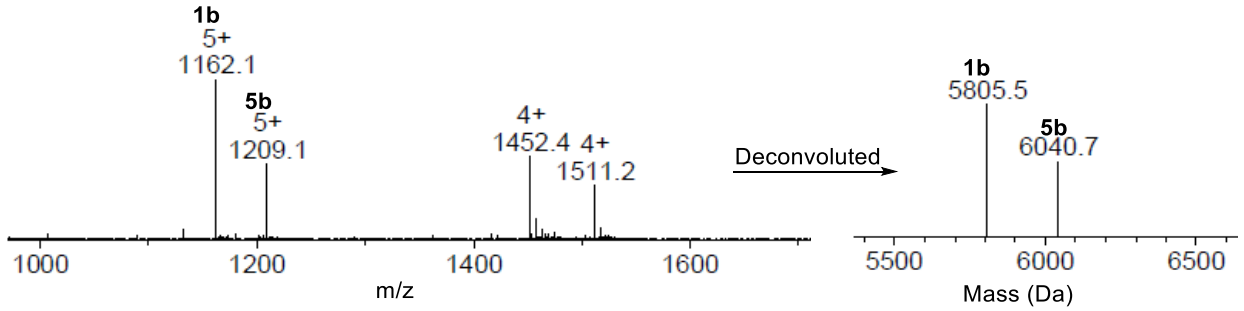
1b
5+
1162.1
5b
5+
1209.1
4+
1452.4
4+
1511.2
1000
1200
1400
1600
m/z
Deconvoluted
1b
5805.5
5b
6040.7
5500
6000
6500
Mass (Da)

c)

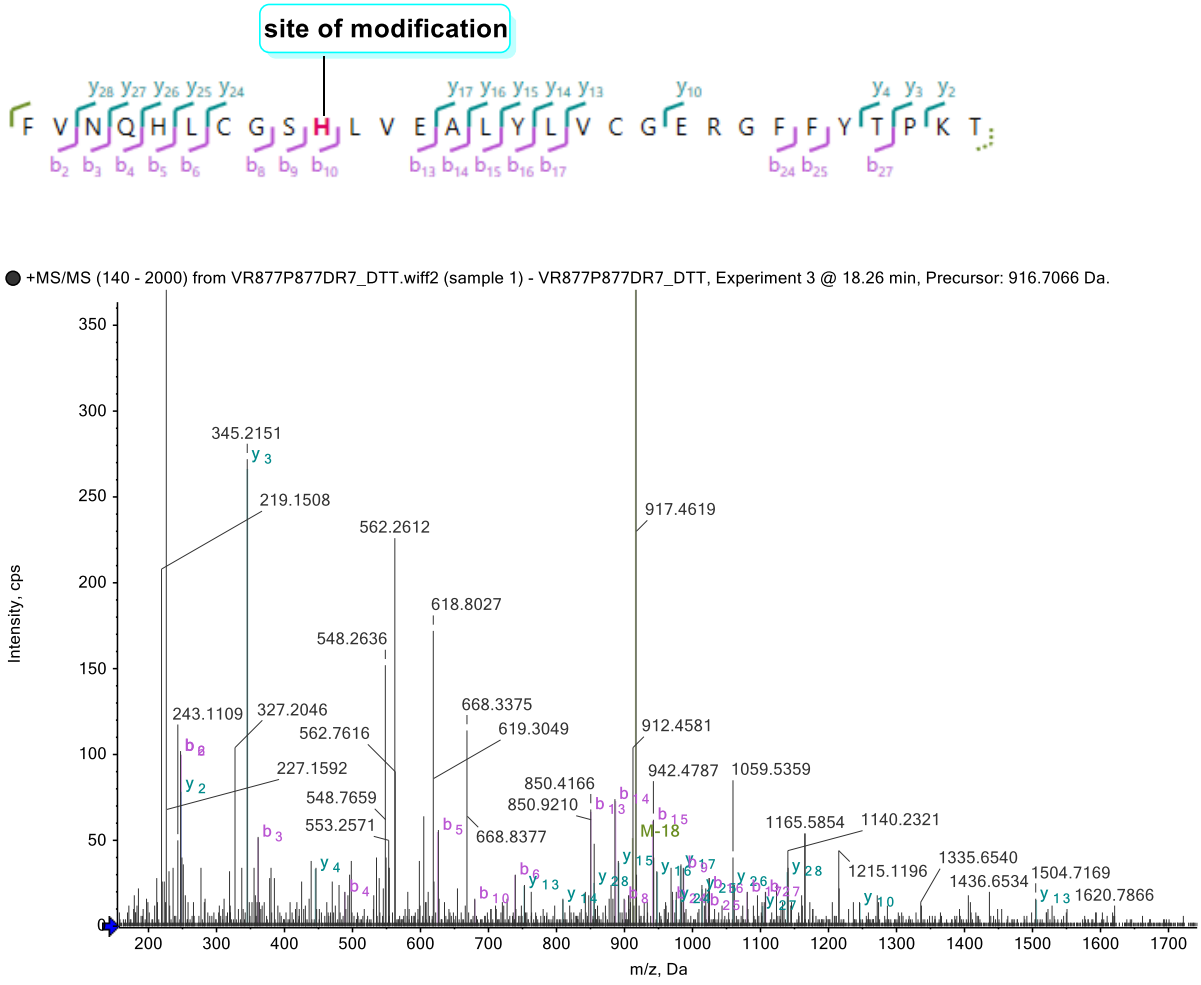

Figure S11. (a) Site-selective labeling of insulin **1b** enabled by LDM reagent **2c** (25 equiv.). (b) ESI-MS spectrum for mono-labeled insulin (**5b**) after oxime formation. (c) MS-MS spectrum of labeled insulin after the reduced the **5b** with DTT. The site of modification is H10.

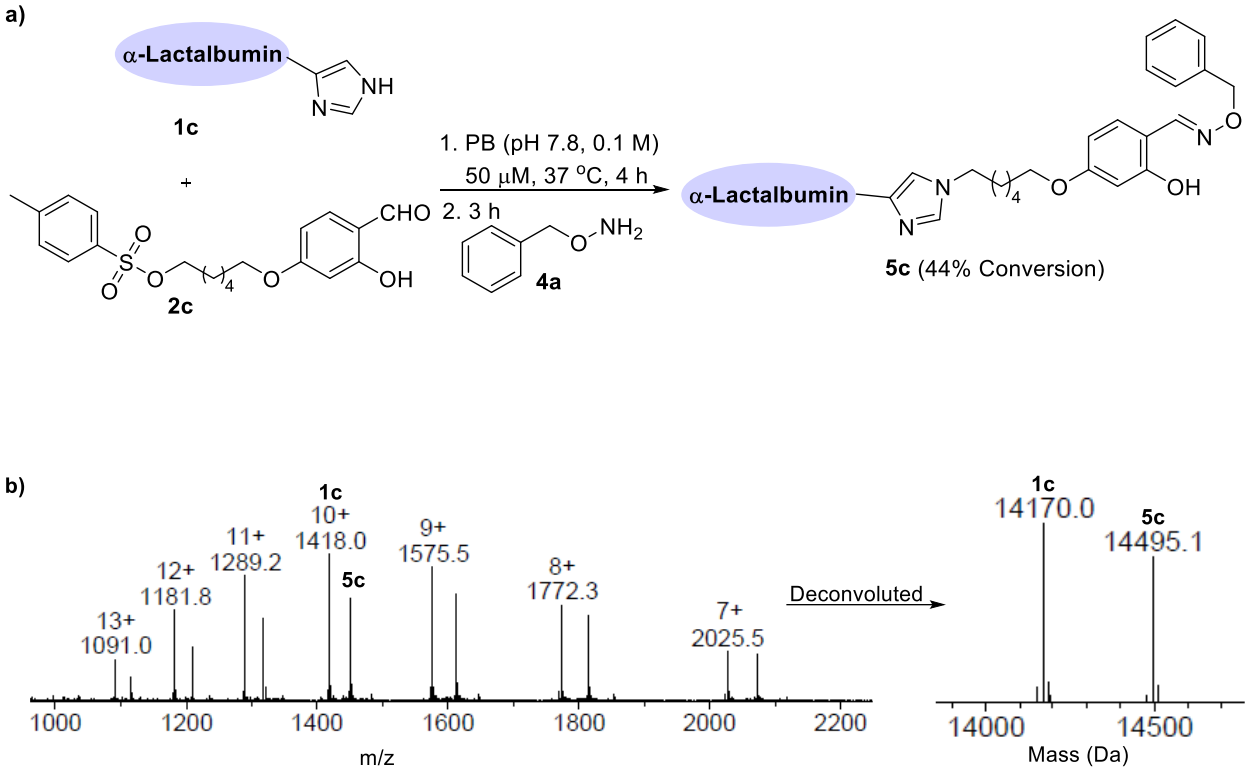
a)
α-Lactalbumin
NH
N
1c
+
CHO
OH
O
S
O
O
4
O
2c
1. PB (pH 7.8, 0.1 M)
50 μM, 37 °C, 4 h
2. 3 h
NH2
O
4a
α-Lactalbumin
N
N
4
O
N
O
OH
5c (44% Conversion)
b)
1c
10+
1418.0
11+
1289.2
12+
1181.8
13+
1091.0
5c
9+
1575.5
8+
1772.3
7+
2025.5
1000
1200
1400
1600
1800
2000
2200
m/z
Deconvoluted
1c
14170.0
5c
14495.1
14000
14500
Mass (Da)

c)

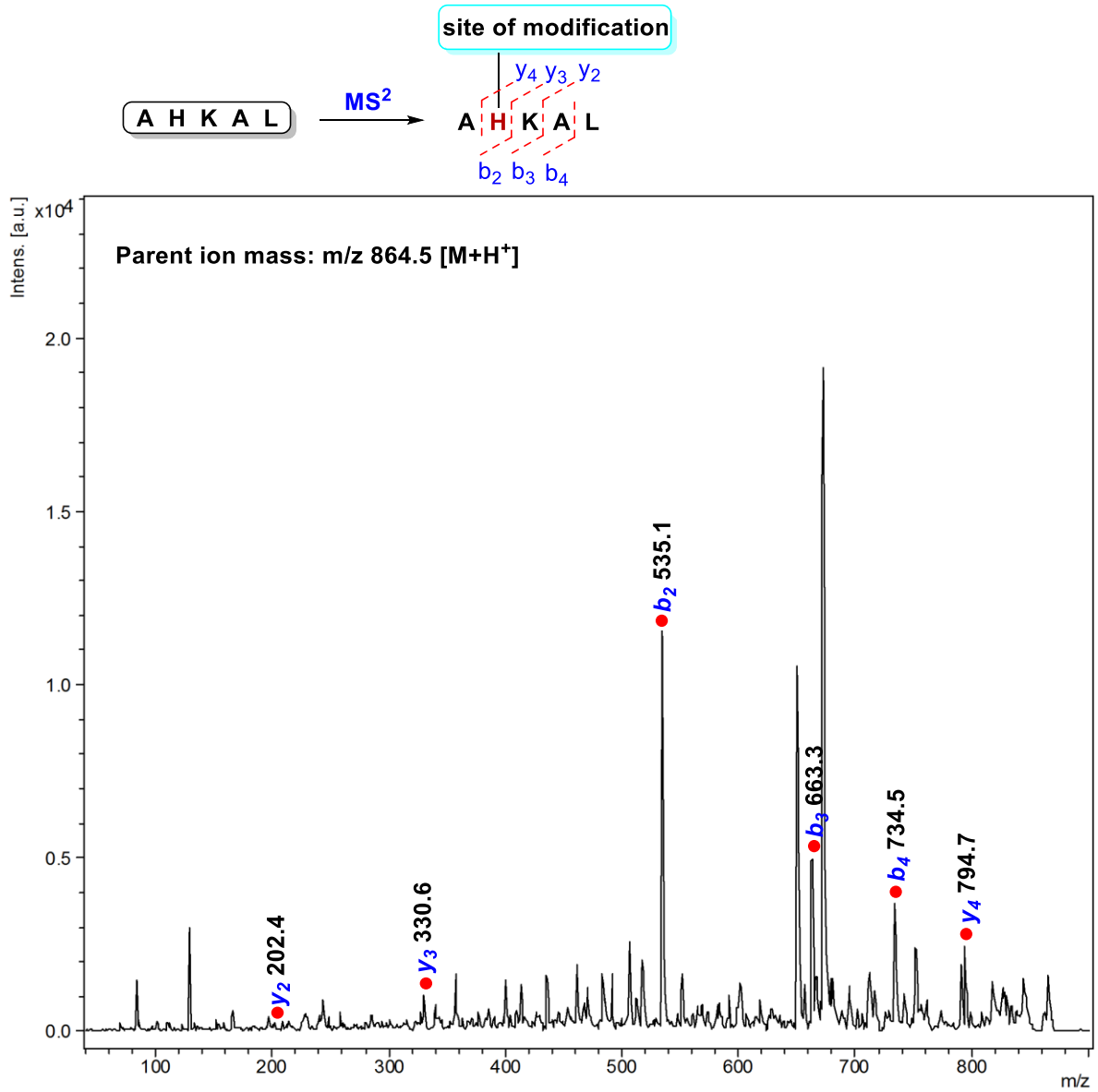

Figure S12. (a) Site-selective labeling of α-lactalbumin **1c** enabled by LDM reagent **2c** (25 equiv.). (b) ESI-MS spectrum for mono-labeled α-lactalbumin (**5c**) after oxime formation. (c) MS-MS spectrum of labeled α-lactalbumin after the digestion of **5c** with α-chymotrypsin. The site of modification is H107.

a)

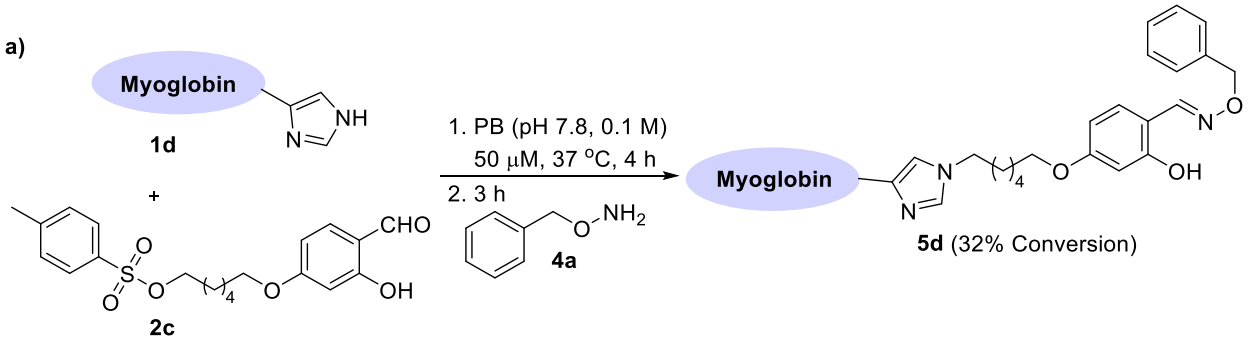
Myoglobin
1d
+
2c
1. PB (pH 7.8, 0.1 M)
50 μM, 37 °C, 4 h
2. 3 h
4a
Myoglobin
5d (32% Conversion)

b)

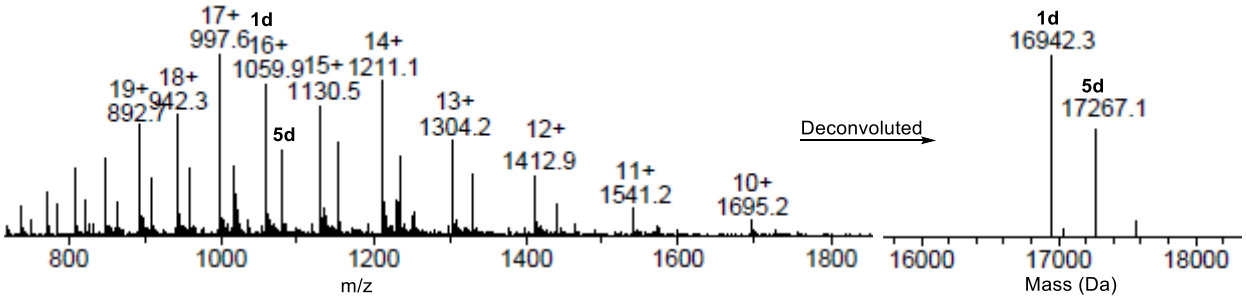
17+
997.6
1d
16+
1059.9
15+
1130.5
14+
1211.1
13+
1304.2
12+
1412.9
11+
1541.2
10+
1695.2
19+
892.7
18+
942.3
5d
800
1000
1200
1400
1600
1800
m/z
Deconvoluted
1d
16942.3
5d
17267.1
16000
17000
18000
Mass (Da)

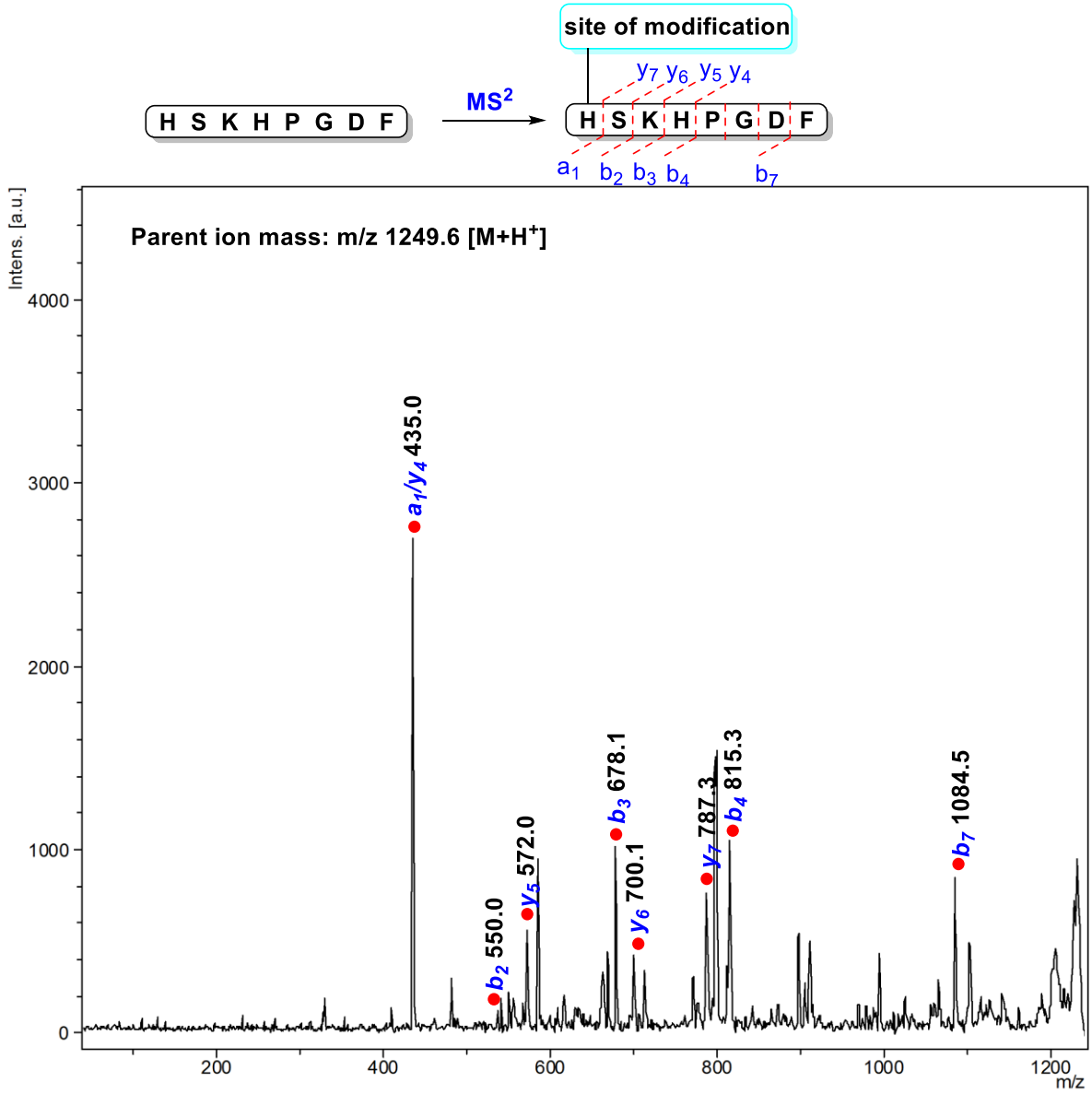

Figure S13. (a) Site-selective labeling of myoglobin **1d** enabled by LDM reagent **2c** (25 equiv.). (b) ESI-MS spectrum for mono-labeled myoglobin (**5d**) after oxime formation. (c) MS-MS spectrum of labeled myoglobin after the digestion of **5d** with α-chymotrypsin. The site of modification is H116.

4d. Tagging of labeled ubiquitin

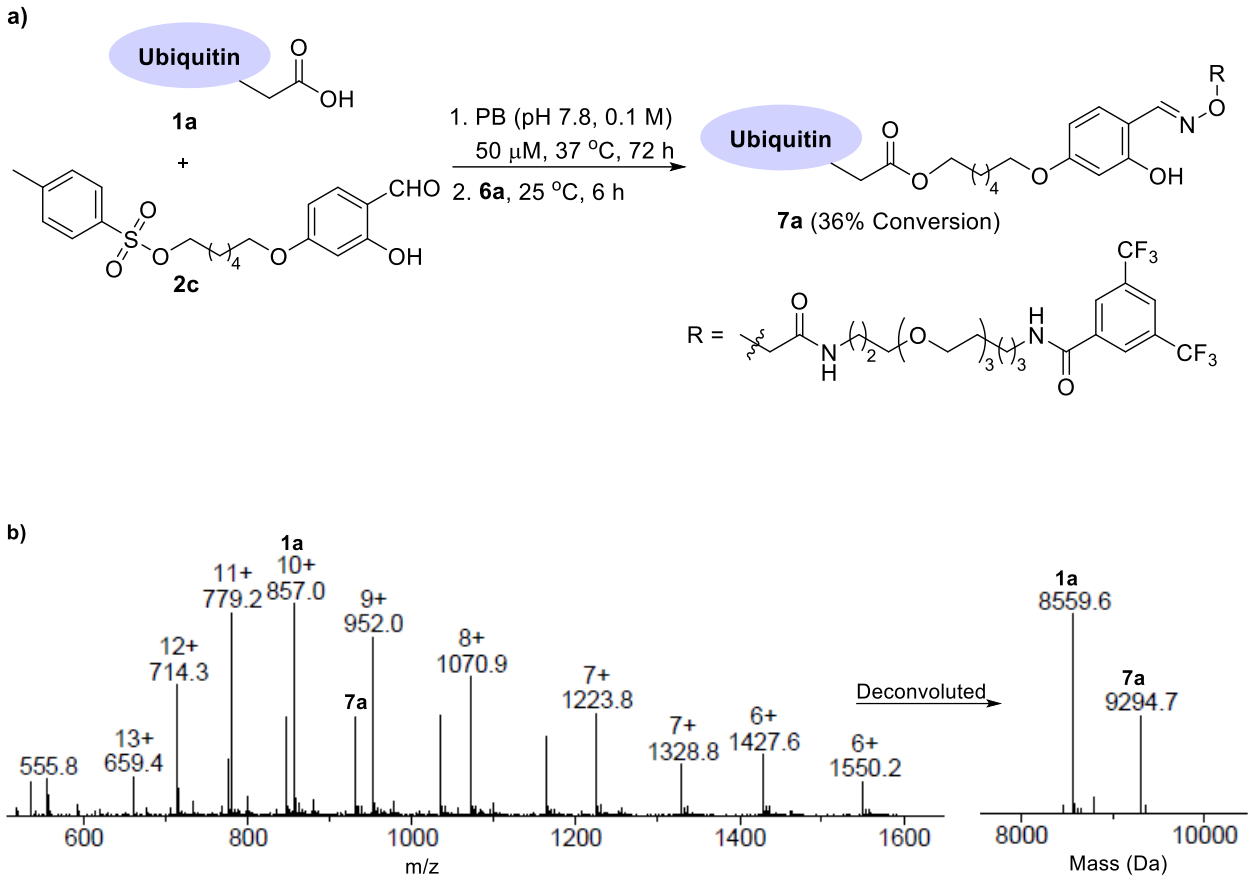

Figure S14. (a) Site-selective labeling of ubiquitin **1a** enabled by LDM reagent **2c** (25 equiv.). (b) ESI-MS spectrum of ^{19}F NMR probe tagged ubiquitin (**7a**).

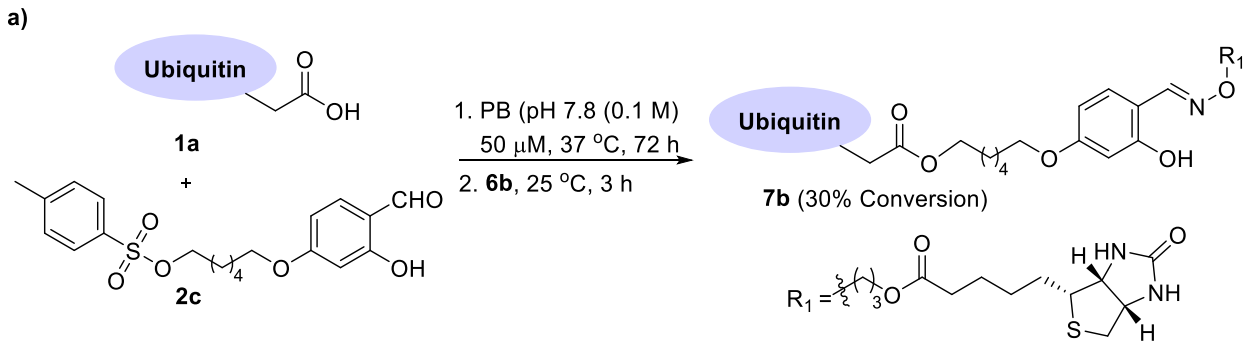

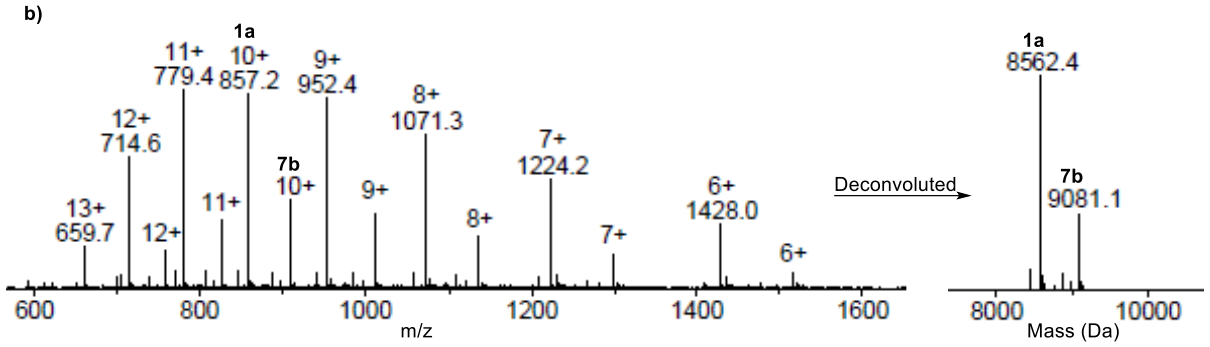

Figure S15. (a) Site-selective labeling of ubiquitin **1a** enabled by LDM reagent **2c** (25 equiv.). (b) ESI-MS spectrum of biotin probe tagged ubiquitin (**7b**).

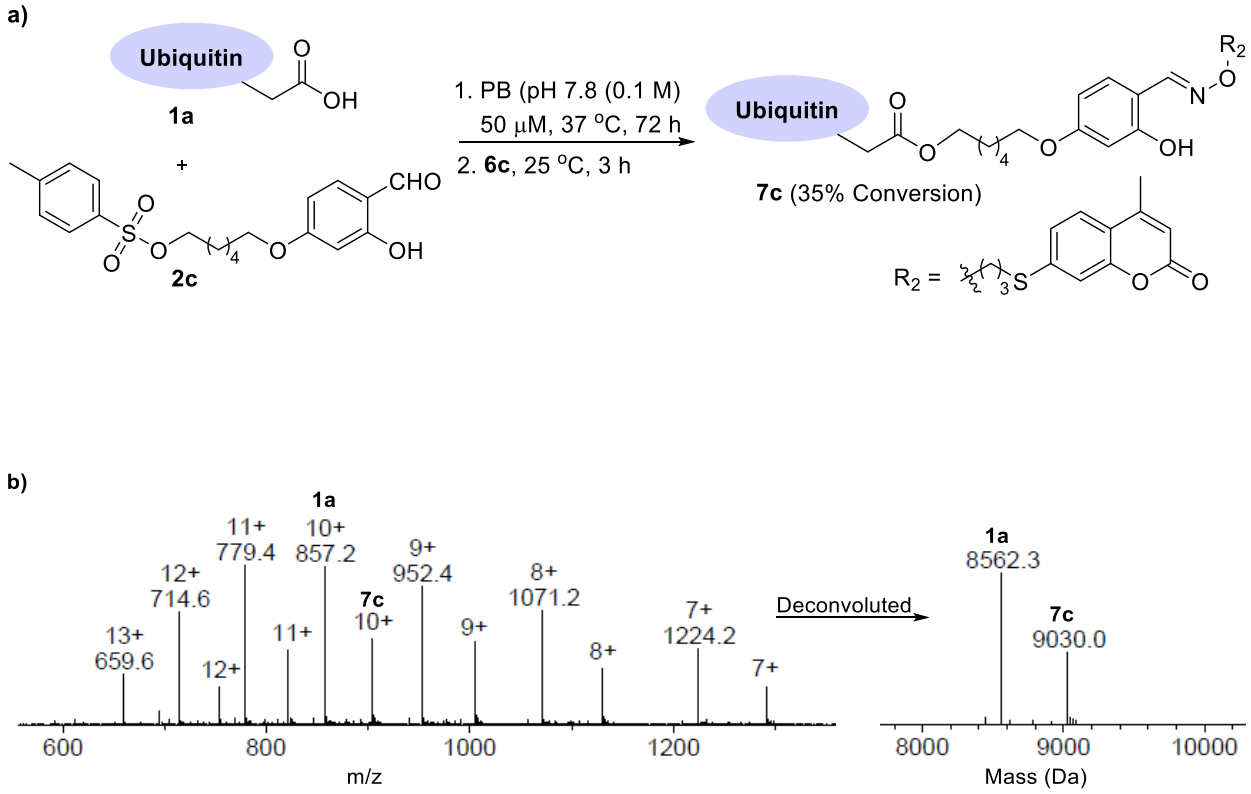

Figure S16. (a) Site-selective labeling of ubiquitin **1a** enabled by LDM reagent **2c** (25 equiv.). (b) ESI-MS spectrum of coumarin probe tagged ubiquitin (**7c**).

4e. Purification of labeled ubiquitin

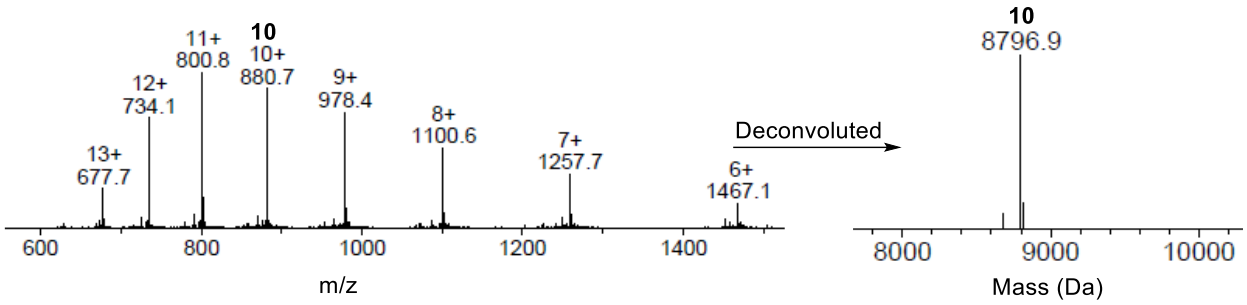

Figure S17. ESI-MS spectrum of purified mono-labeled ubiquitin (**10**).

5. Additional data

5a. Protein labeling

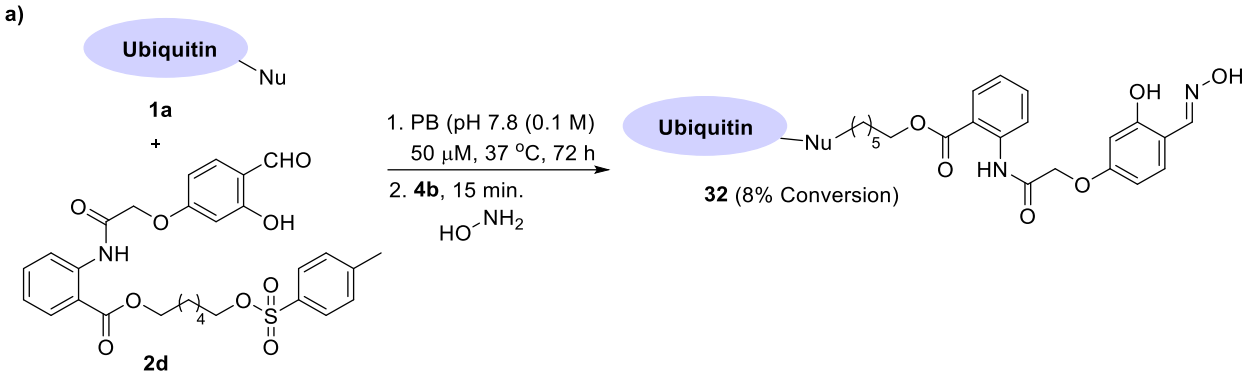

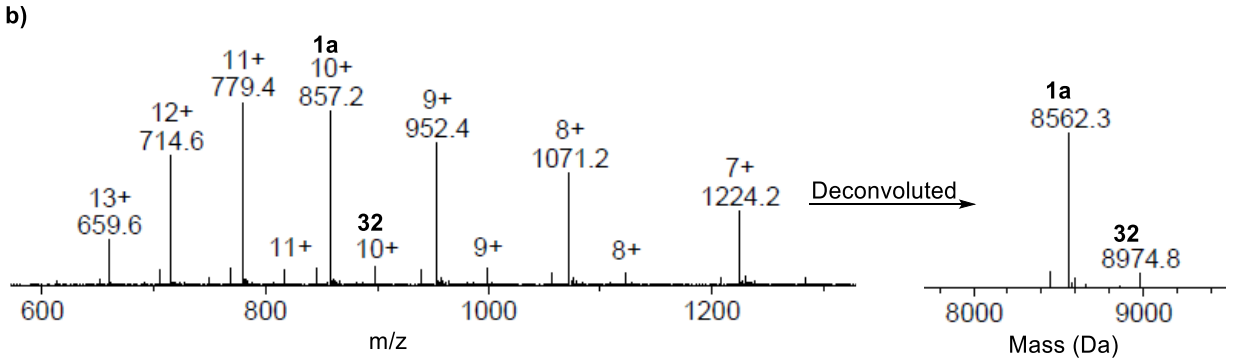

Figure S18. (a) Site-selective labeling of ubiquitin **1a** enabled by LDM reagent **2c** (25 equiv.). (b) ESI-MS spectrum of labeled ubiquitin (**32**).

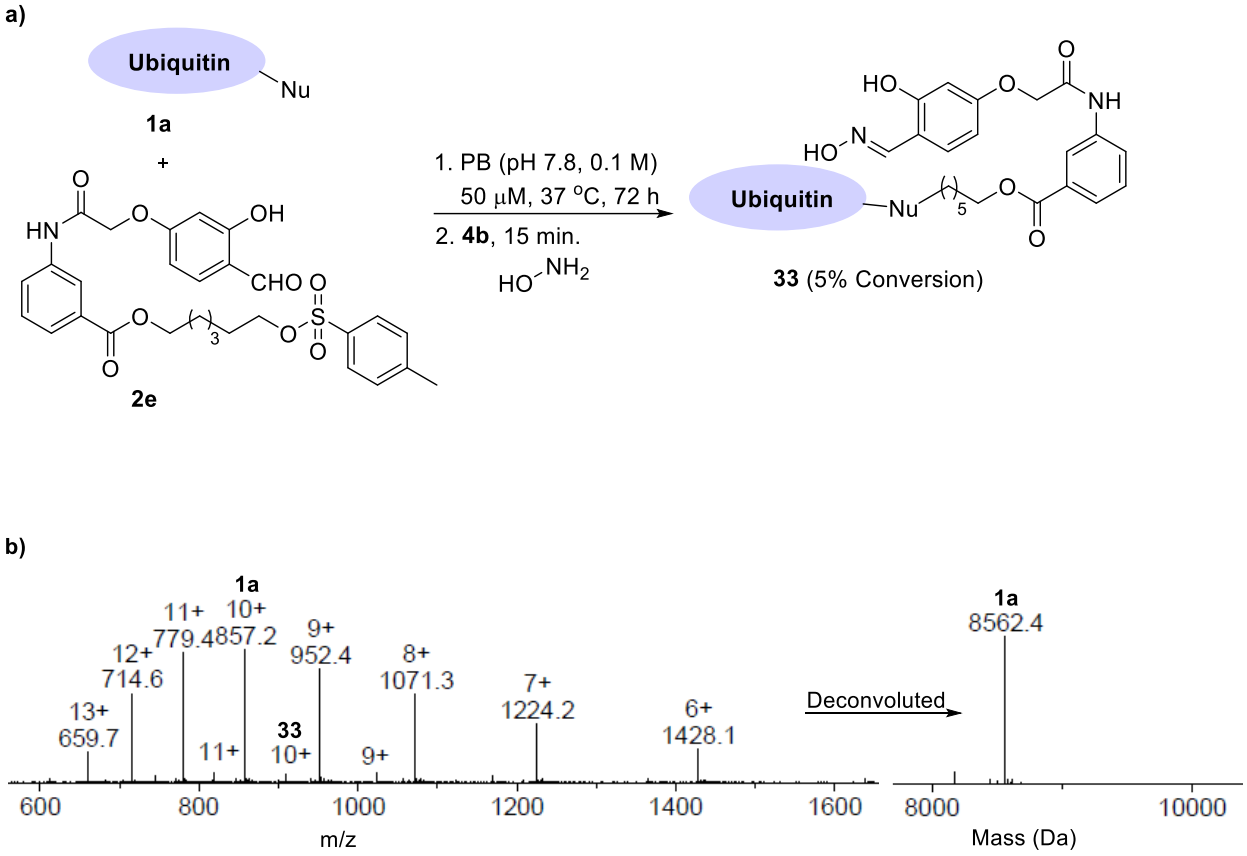

Figure S19. (a) Site-selective labeling of ubiquitin **1a** (1 equiv.) enabled by LDM reagent **2c** (25 equiv.). (b) ESI-MS spectrum of labeled ubiquitin (**33**).

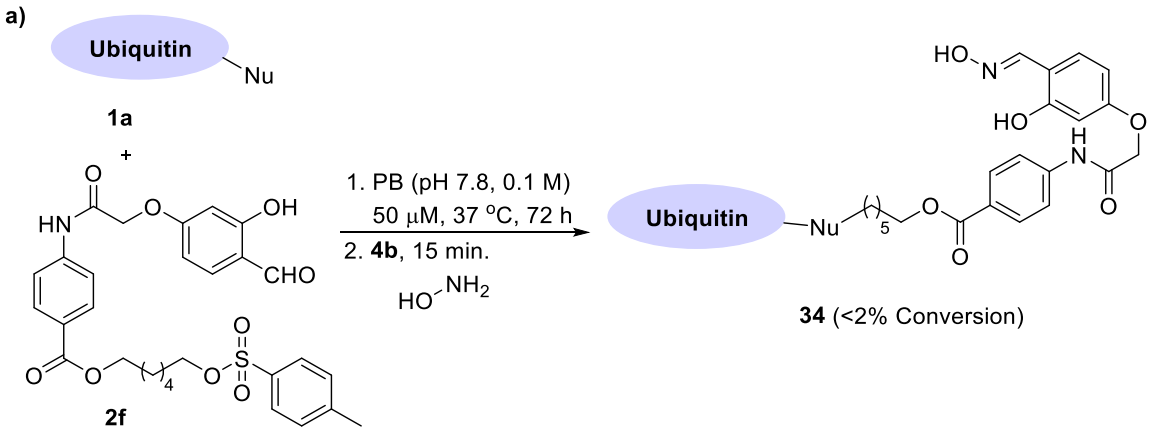

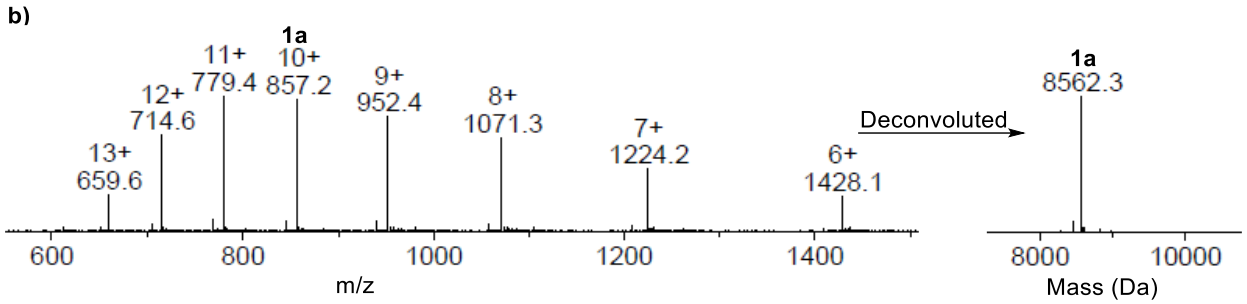

Figure S20. (a) Site-selective labeling of ubiquitin **1a** enabled by LDM reagent **2f** (25 equiv.). (b) ESI-MS spectrum labeled ubiquitin (**34**).

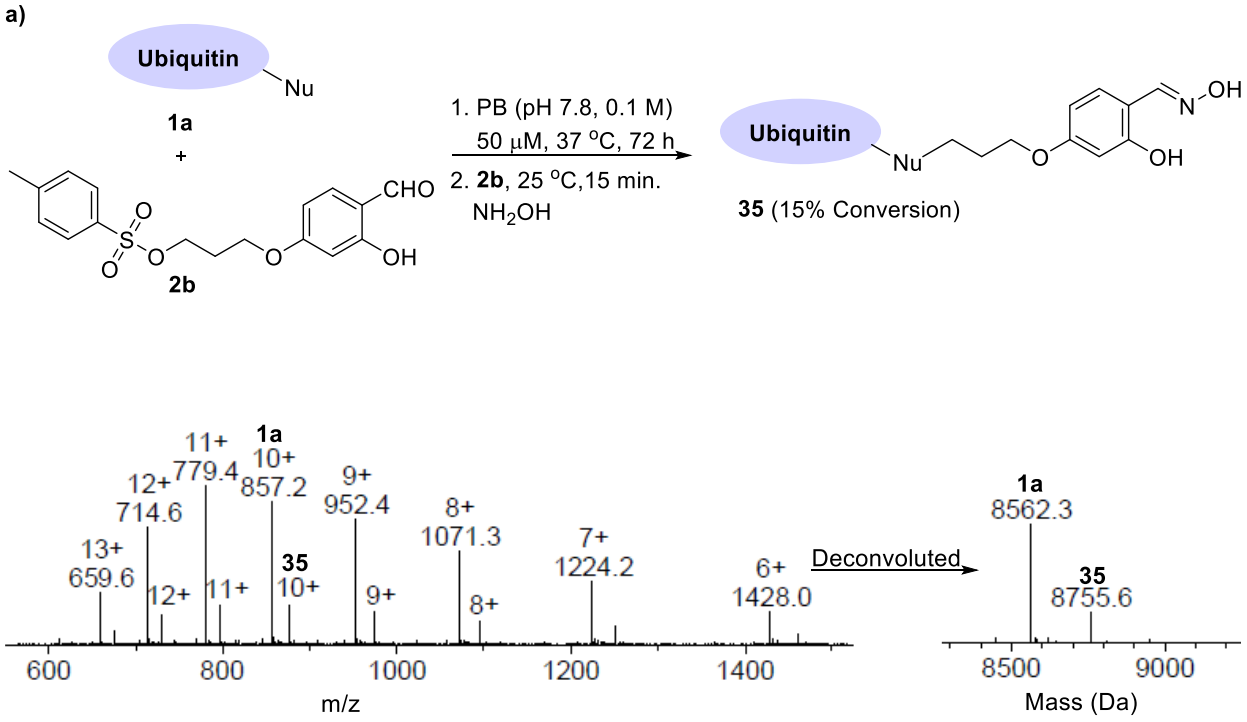

Figure S21. (a) Site-selective labeling of ubiquitin **1a** enabled by LDM reagent **2b** (25 equiv.). (b) ESI-MS spectrum of labeled ubiquitin (**35**).

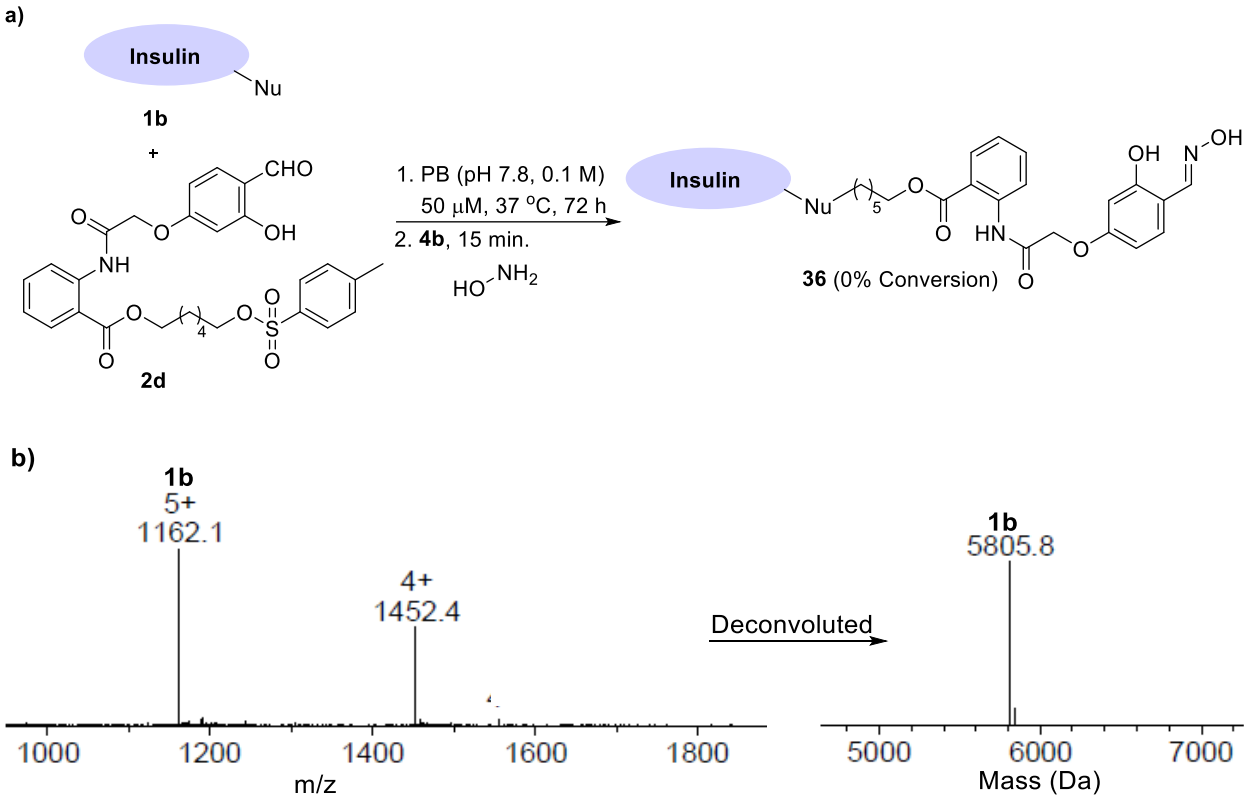

Figure S22. (a) Site-selective labeling of insulin **1b** enabled by LDM reagent **2d** (25 equiv.). (b) ESI-MS spectrum of labeled insulin (**36**).

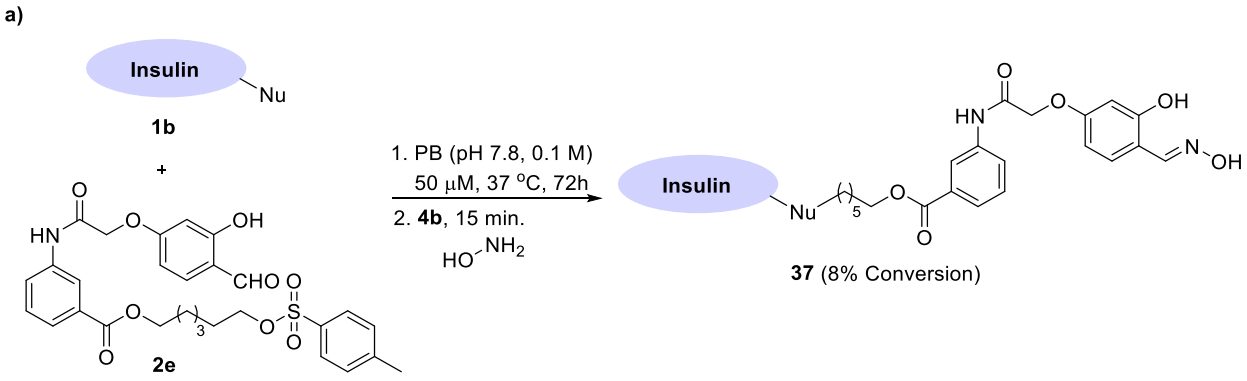

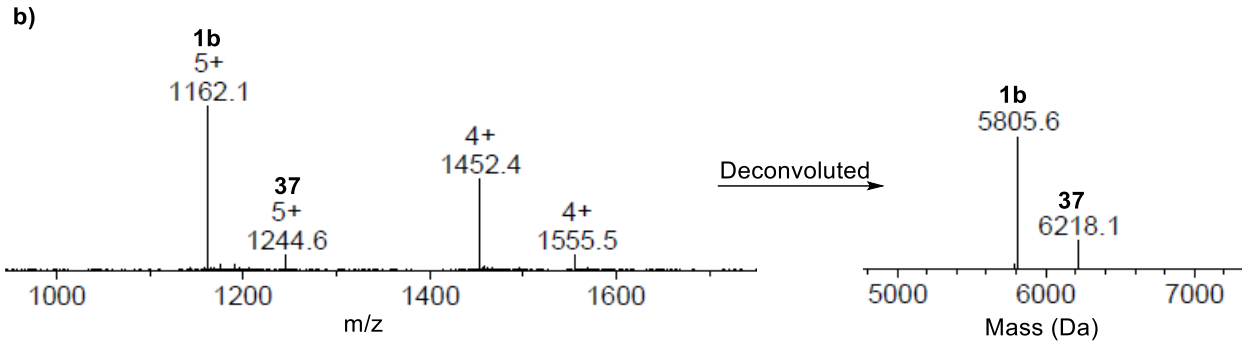

Figure S23. (a) Site-selective labeling of insulin **1b** enabled by LDM reagent **2e** (25 equiv.). (b) ESI-MS spectrum of labeled insulin (**37**).

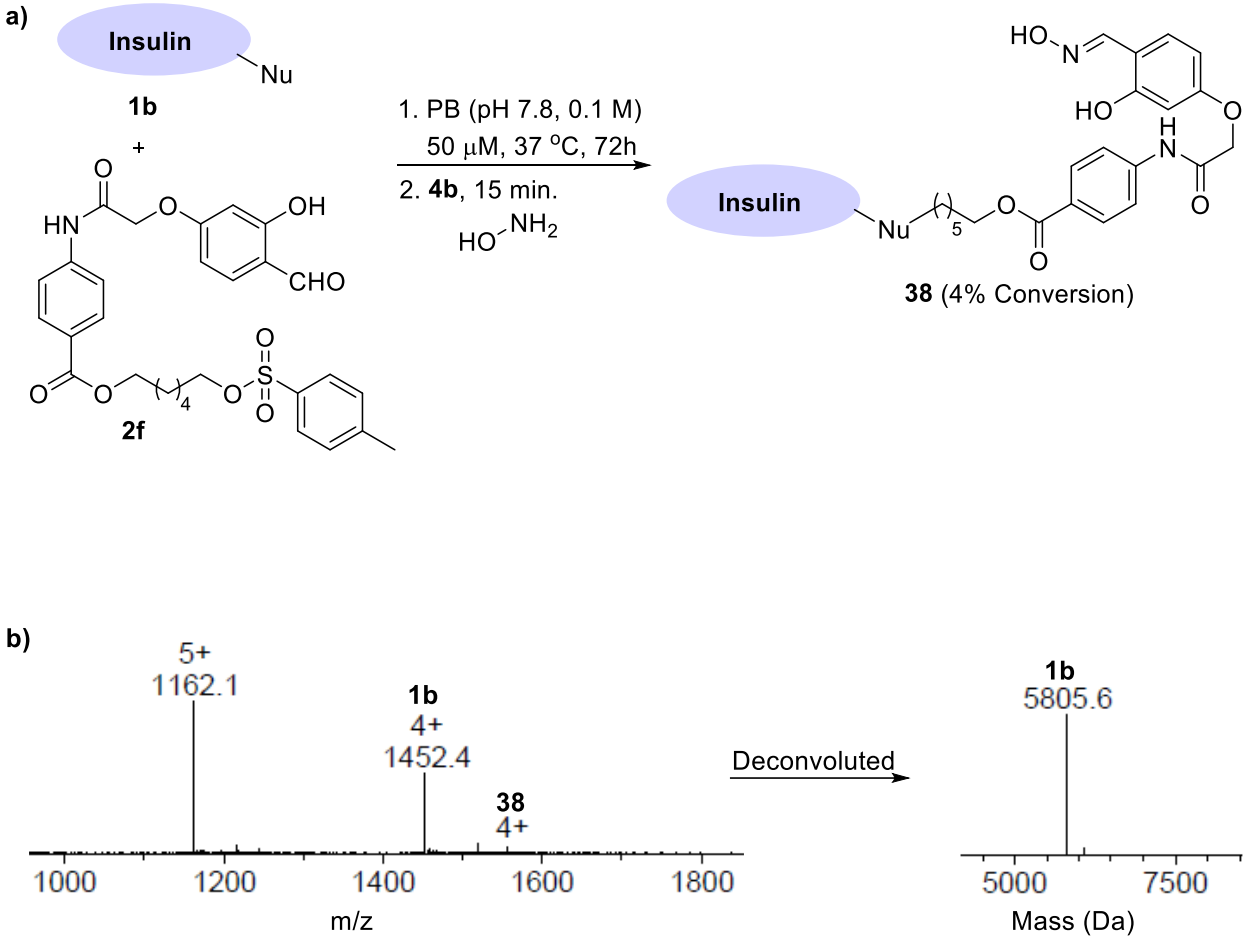

Figure S24. (a) Site-selective labeling of insulin **1b** enabled by LDM reagent **2f** (25 equiv.). (b) ESI-MS spectrum of labeled insulin (**38**).

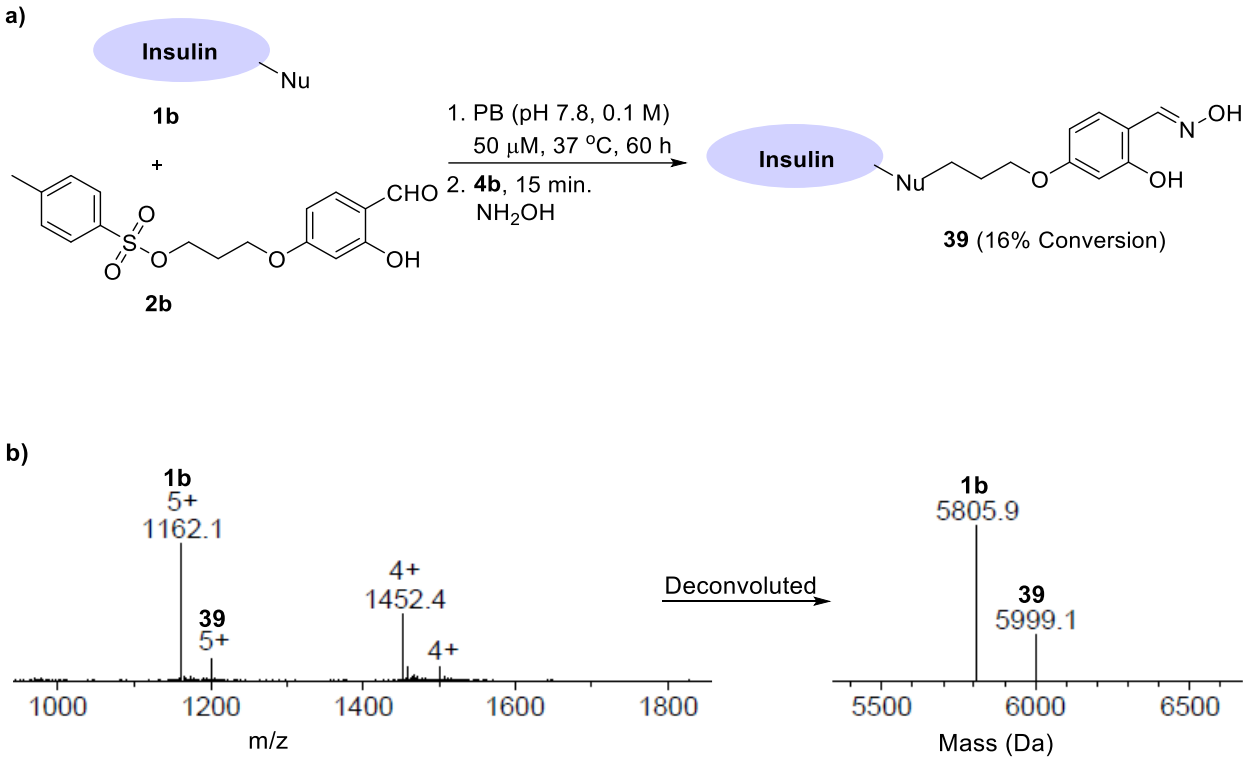

Figure S25. (a) Site-selective labeling of insulin **1b** enabled by LDM reagent **2b** (25 equiv.). (b) ESI-MS spectrum of labeled insulin (**39**).

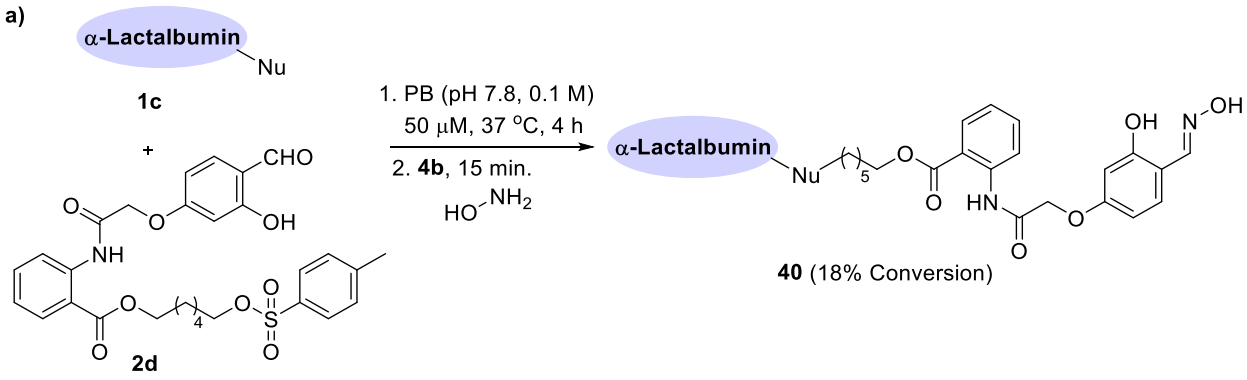

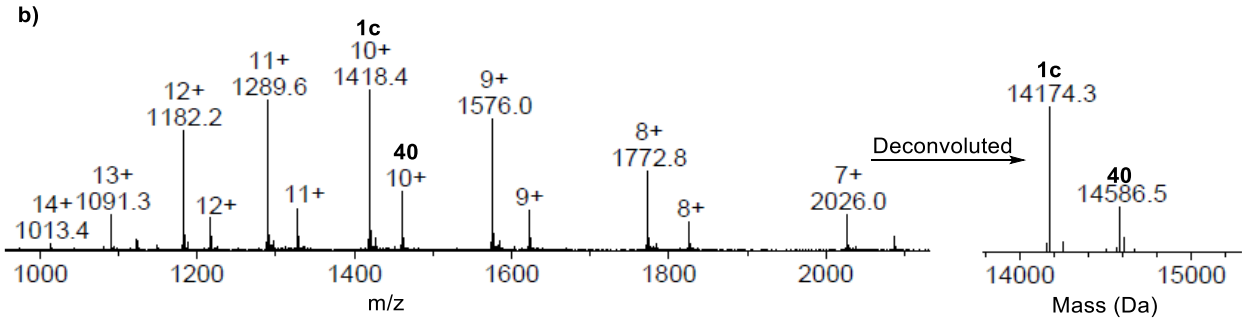

Figure S26. (a) Site-selective labeling of α-lactalbumin **1c** enabled by LDM reagent **2d** (25 equiv.). (b) ESI-MS spectrum of labeled α-lactalbumin (**40**).

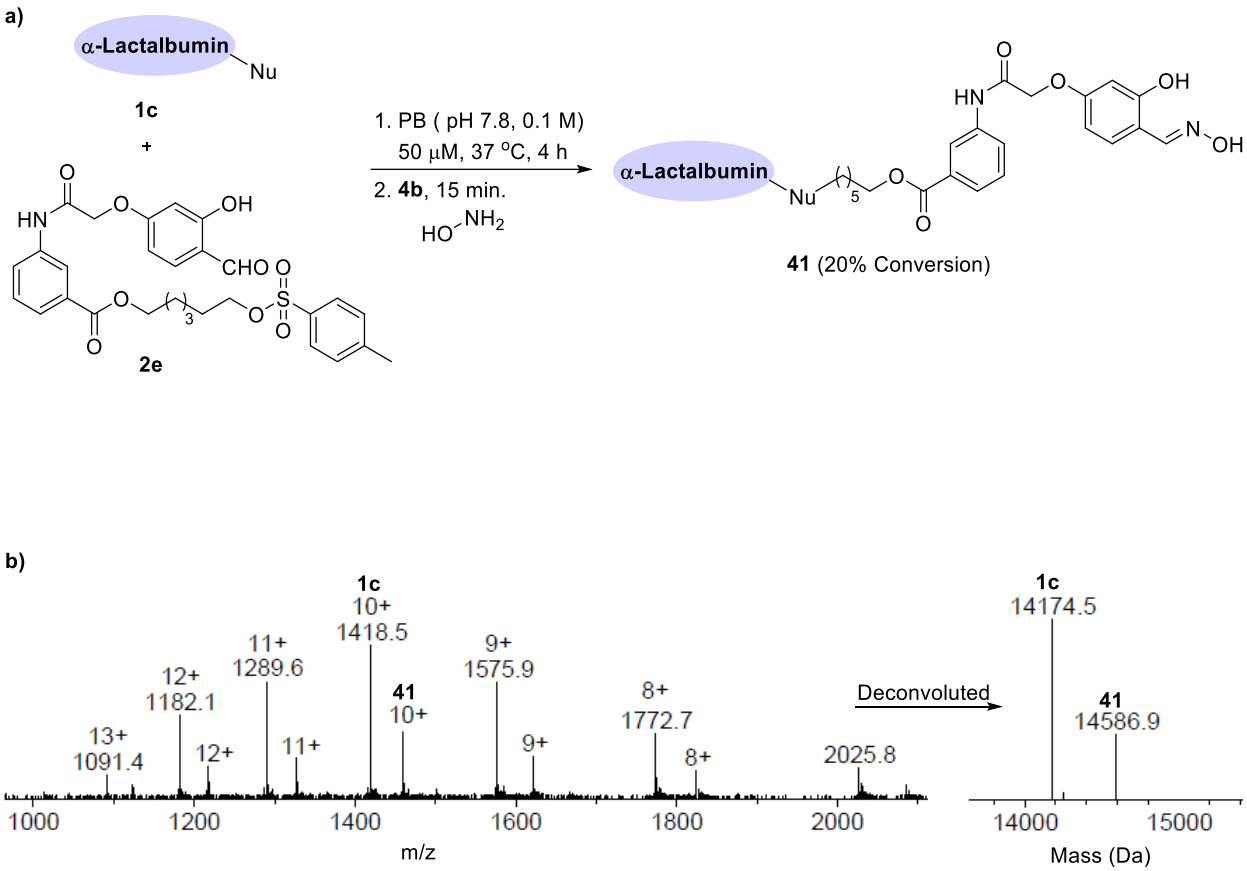

Figure S27. (a) Site-selective labeling of α-lactalbumin **1c** enabled by LDM reagent **2e** (25 equiv.). (b) ESI-MS spectrum of labeled α-lactalbumin (**41**).

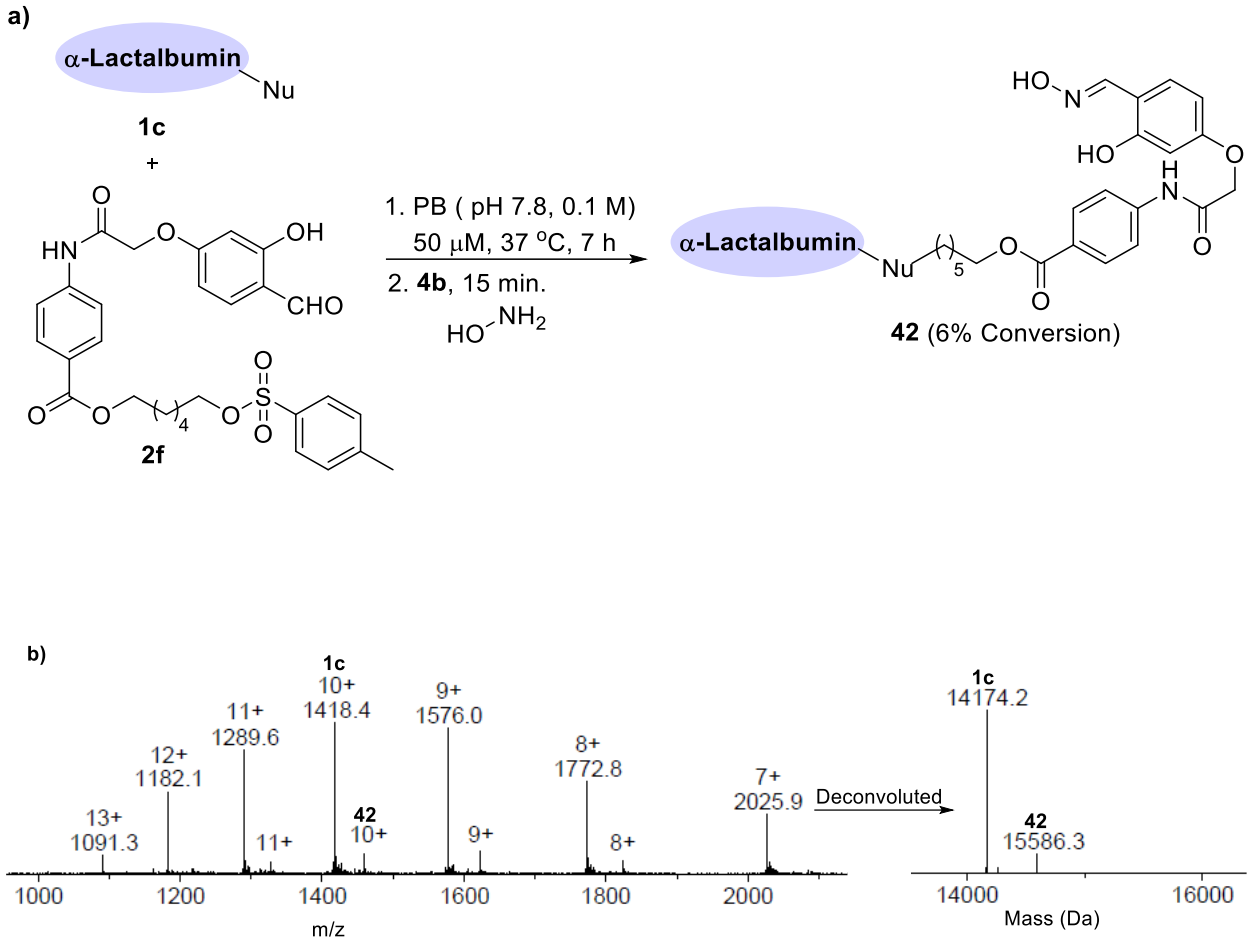

Figure S28. (a) Site-selective labeling of α-lactalbumin **1c** enabled by LDM reagent **2f** (25 equiv.). (b) ESI-MS spectrum of labeled α-lactalbumin (**42**).

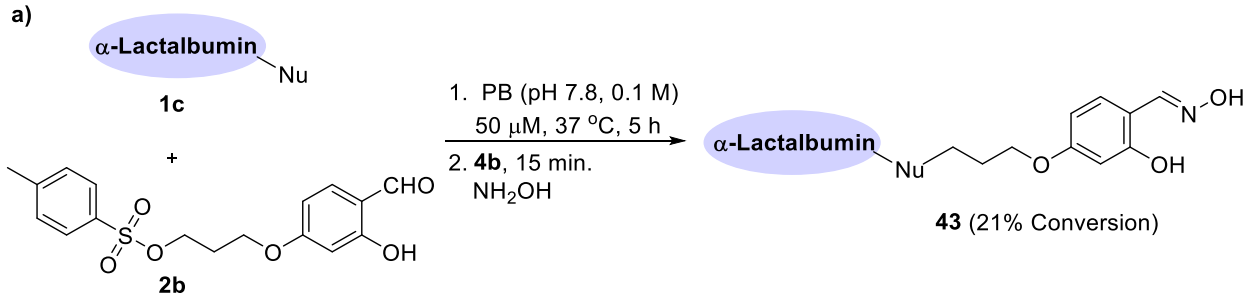

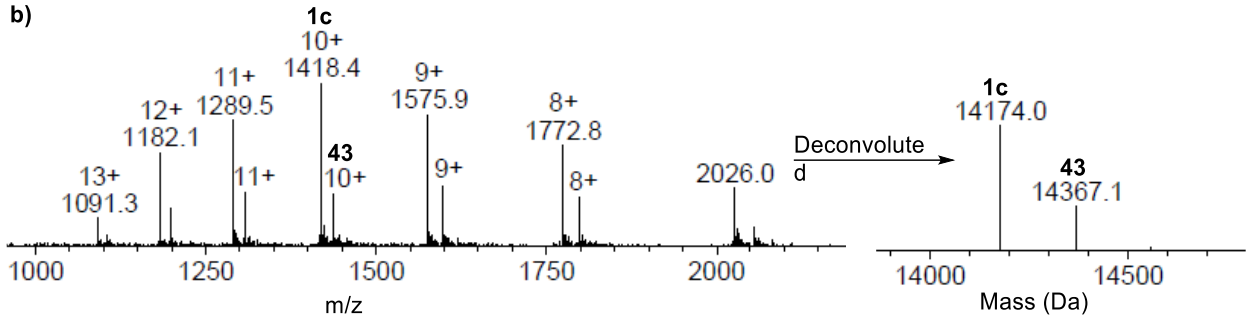

Figure S29. (a) Site-selective labeling of α-lactalbumin **1c** enabled by LDM reagent **2b** (25 equiv.). (b) ESI-MS spectrum of labeled α-lactalbumin (**43**).

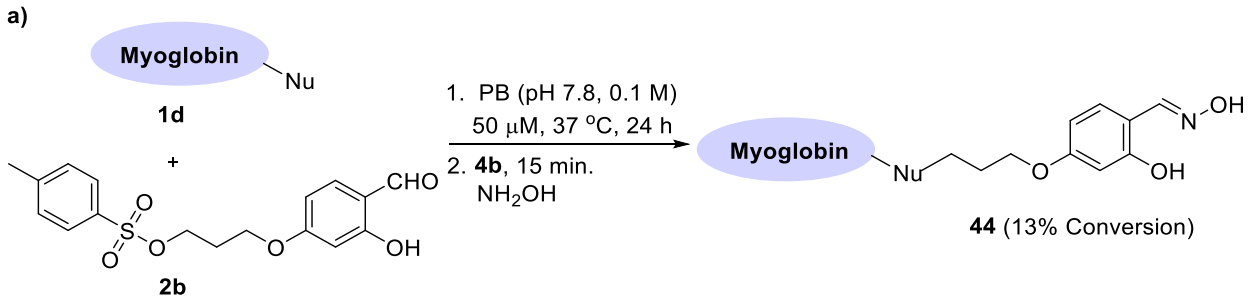

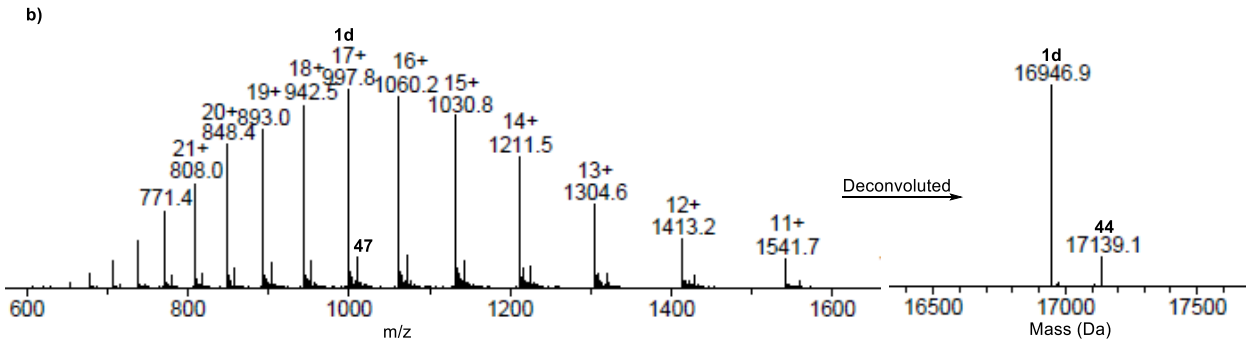

Figure S30. (a) Site-selective labeling of myoglobin **1d** enabled by LDM reagent **2b** (25 equiv.). (b) ESI-MS spectrum of labeled myoglobin (**44**).

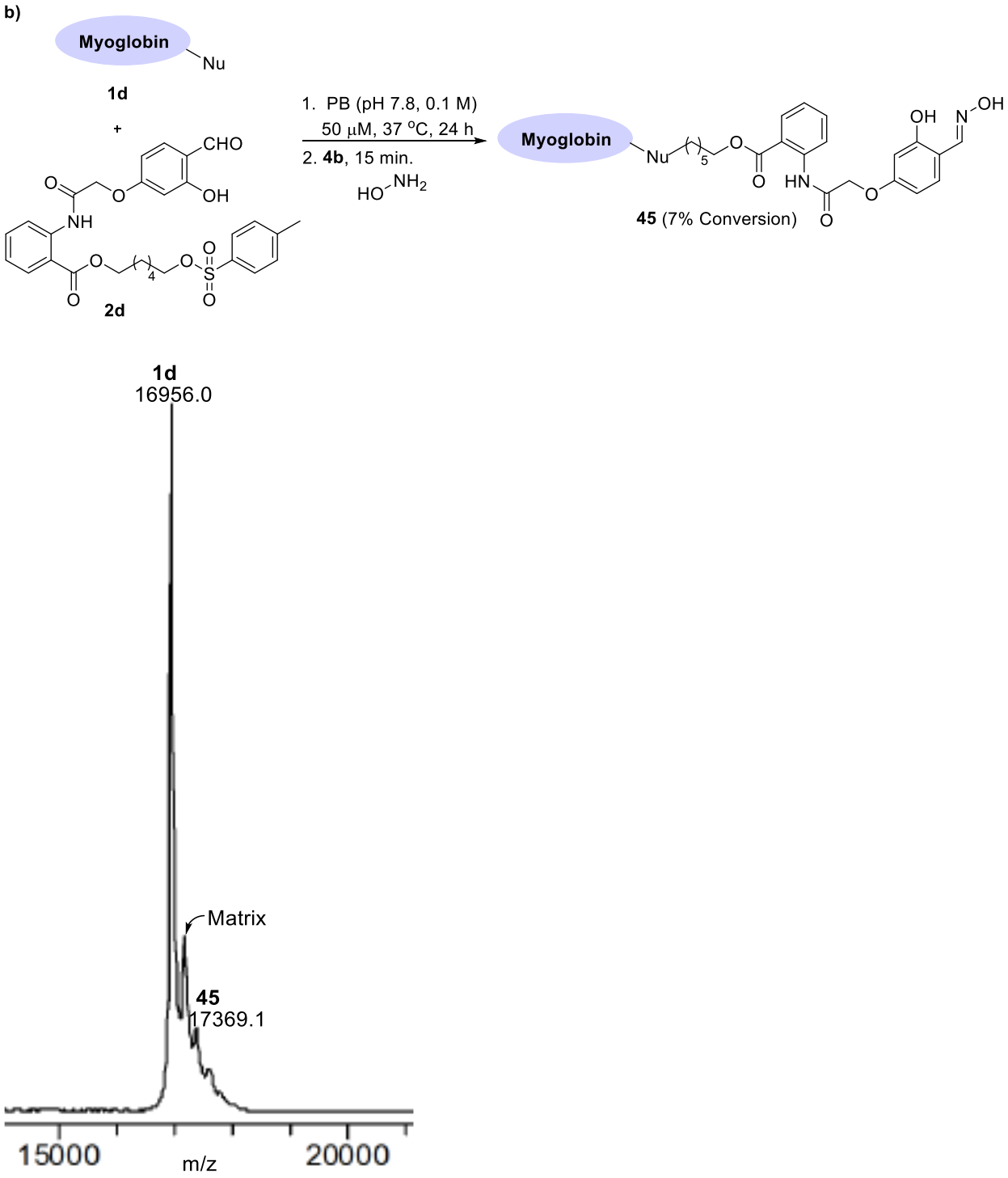

Figure S31. (a) Site-selective labeling of myoglobin **1d** enabled by LDM reagent **2d** (25 equiv.). (b) MALDI-ToF-MS spectrum of labeled myoglobin (**45**).

a)

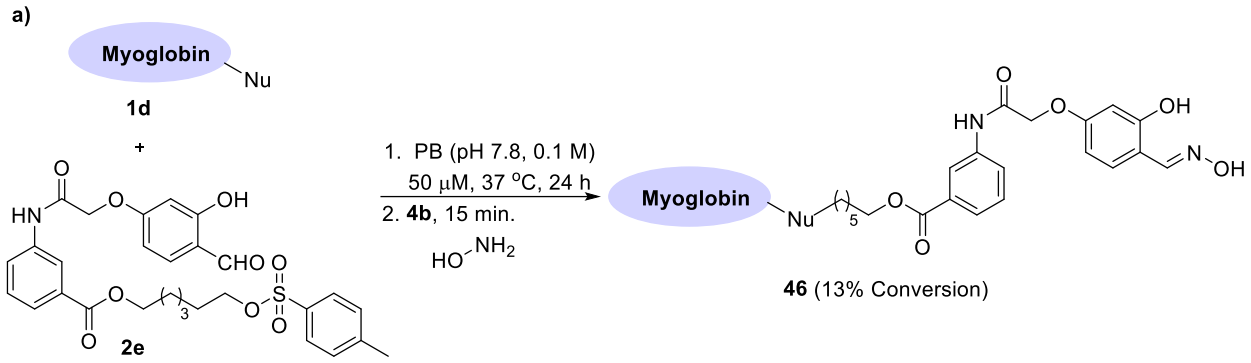
Myoglobin
Nu
1d
+
HN
O
O
OH
CHO
O
O
3
O
S
O
O
2e
1. PB (pH 7.8, 0.1 M)
50 μM, 37 °C, 24 h
2. 4b, 15 min.
HO
NH2
Myoglobin
Nu
5
O
O
HN
O
O
OH
N
OH
46 (13% Conversion)

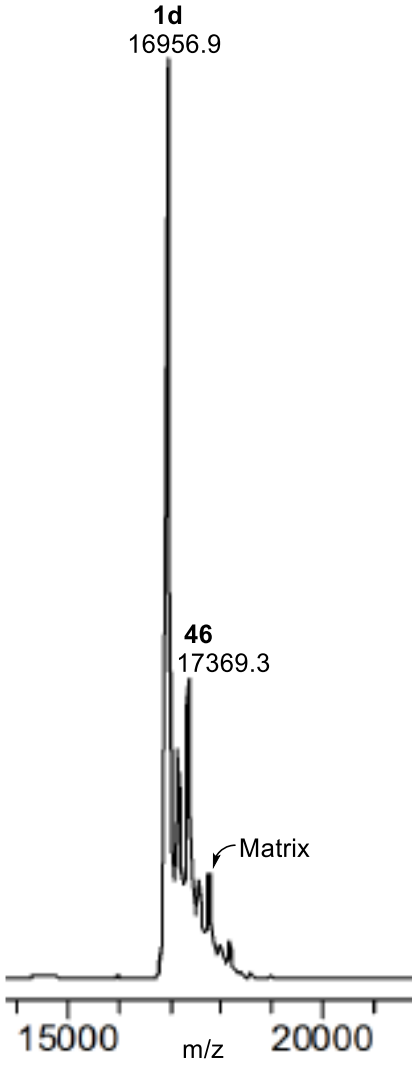
1d
16956.9
46
17369.3
Matrix
15000
m/z
20000

Figure S32. (a) Site-selective labeling of myoglobin **1d** enabled by LDM reagent **2e** (25 equiv.). (b) MALDI-ToF-MS spectrum of labeled myoglobin (**46**).

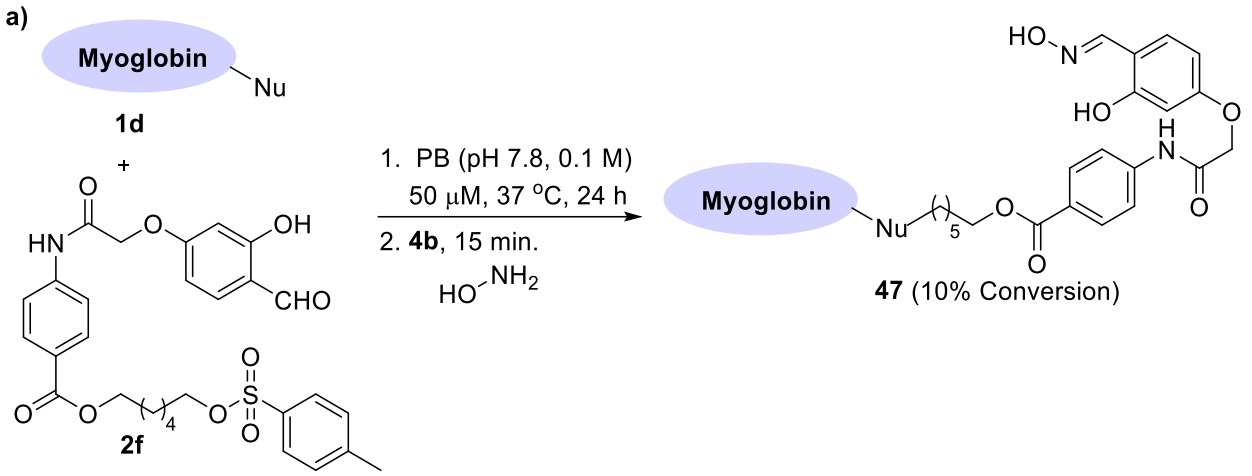

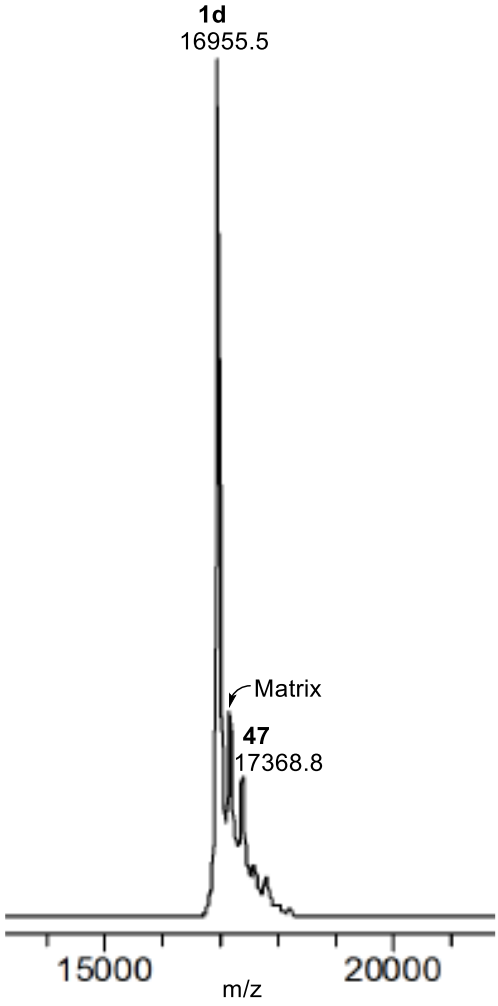

Figure S33. (a) Site-selective labeling of myoglobin **1d** enabled by LDM reagent **2f** (25 equiv.). (b) MALDI-ToF-MS spectrum of labeled myoglobin (**47**).

5b. Circular dichroism spectra of protein

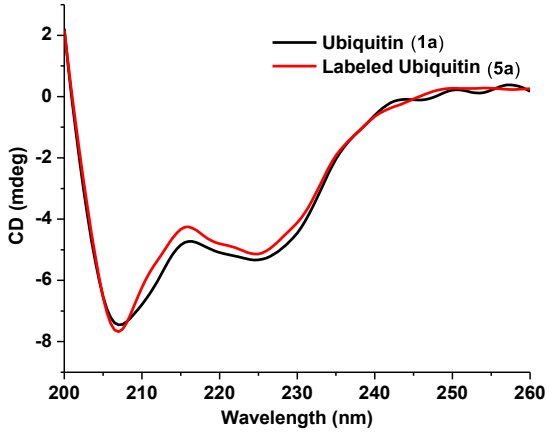

Figure S34. Circular Dichroism (CD) spectra of ubiquitin (**1a**) and labeled ubiquitin (**5a**) in phosphate buffer (0.1 M, pH 7.0) at concentration 0.1 mg/ml.

5c. Fluorescence spectra of coumarin tagged ubiquitin

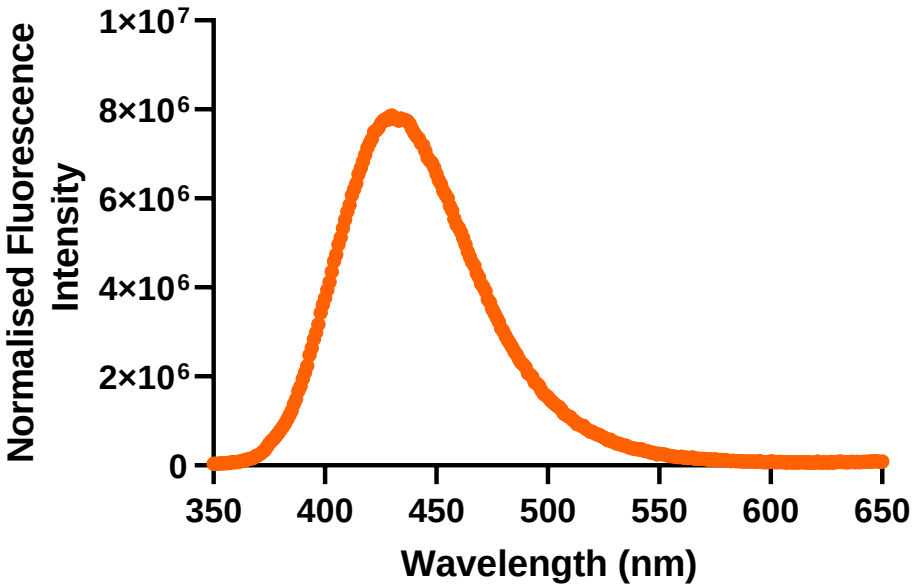

Figure S35. Steady-state fluorescence spectra of coumarin tagged ubiquitin (**6c**) in phosphate buffer (0.1 M, pH 7.0). **6c** exhibits emission band peaked at 428 nm (excitation at 333 nm). For MS data, see Scheme 4.

6. Spectral data

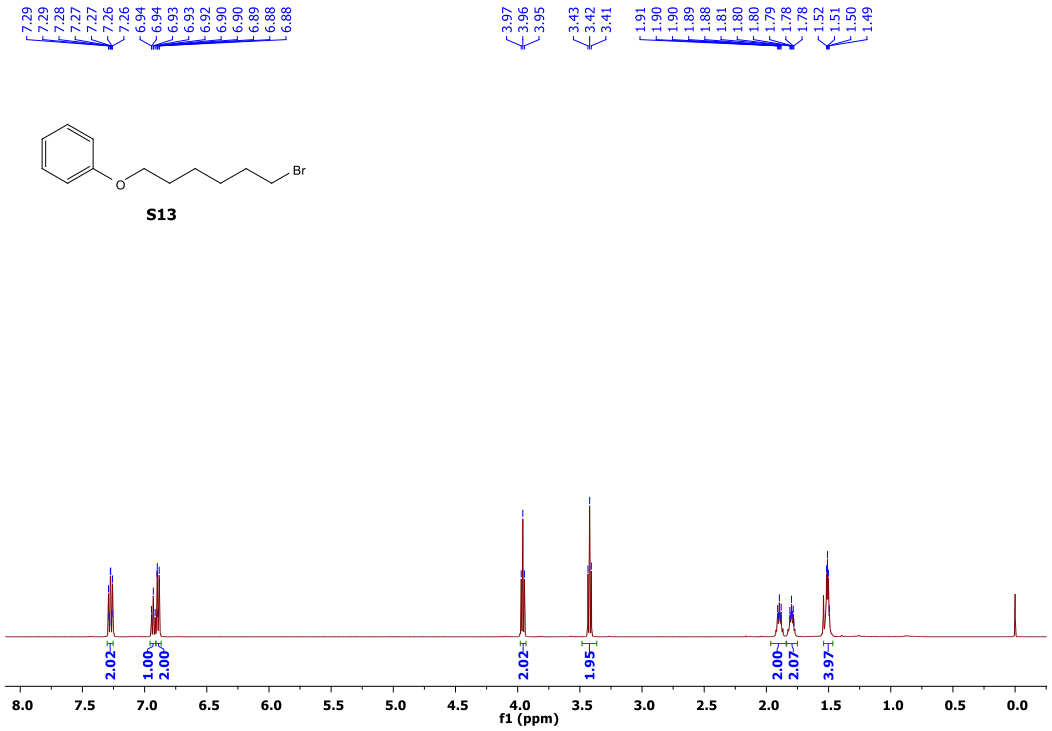

Figure S36. ^{1}H-NMR spectrum of compound **S13.**

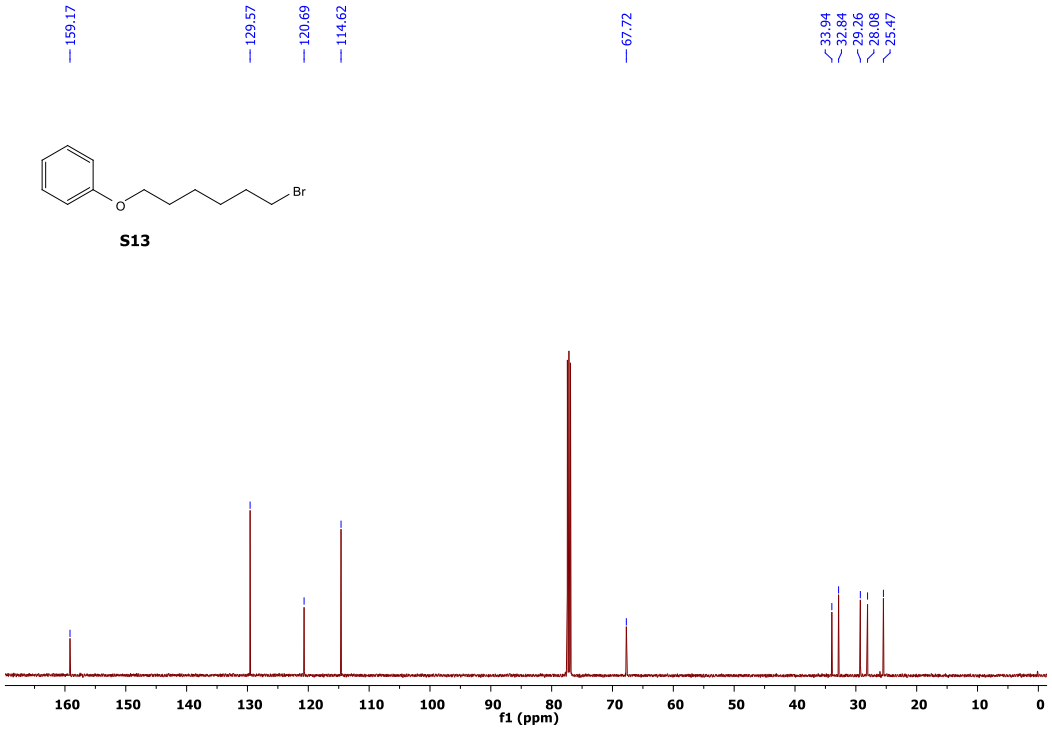

Figure S37. ^{13}C-NMR spectrum of compound **S13.**

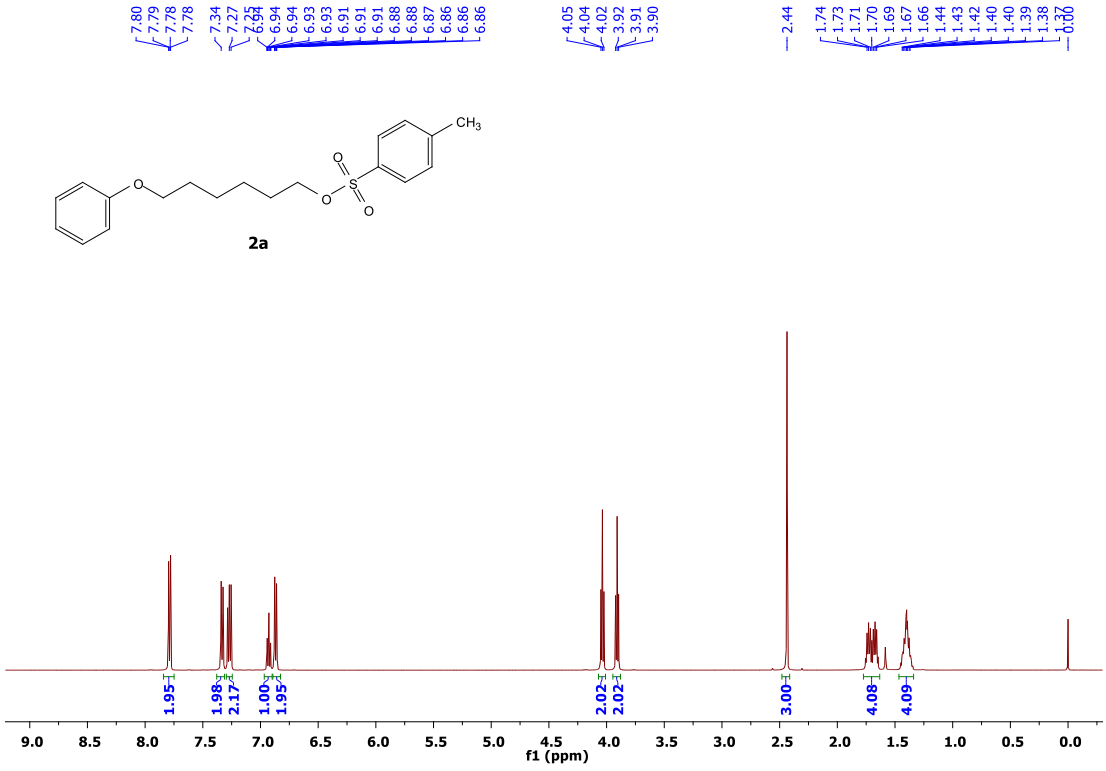

Figure S38. ^{1}H-NMR spectrum of compound **2a.**

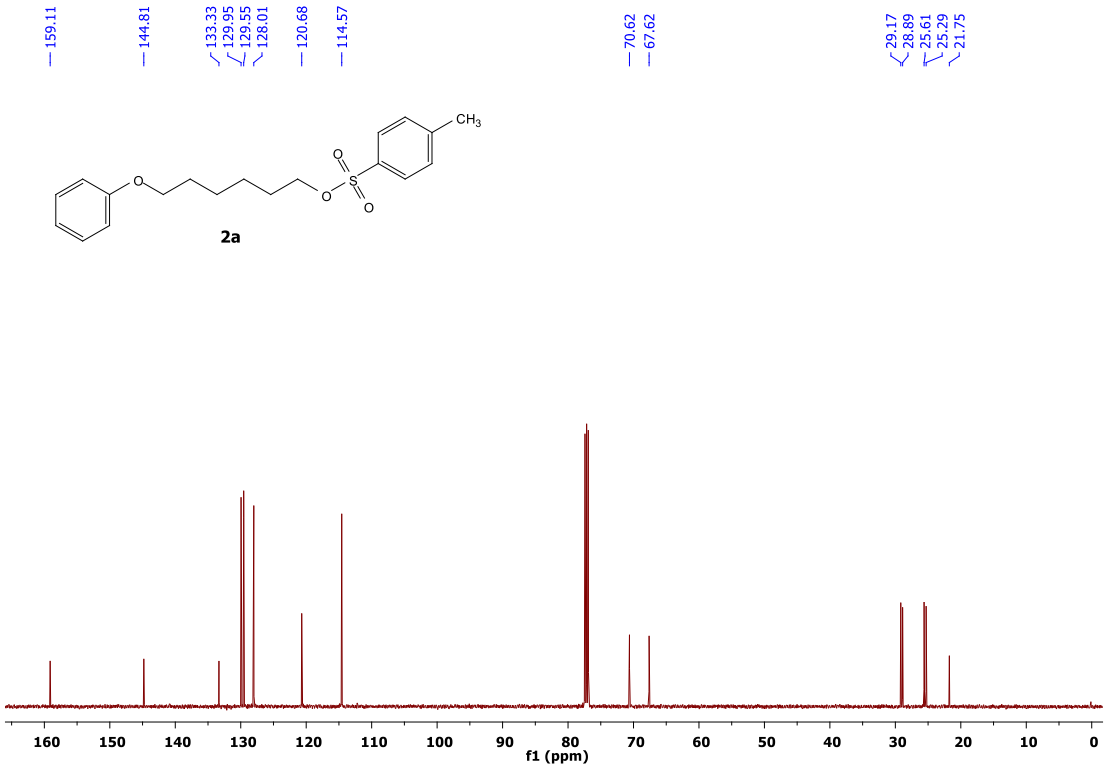

Figure S39. ^{13}C-NMR spectrum of compound **2a.**

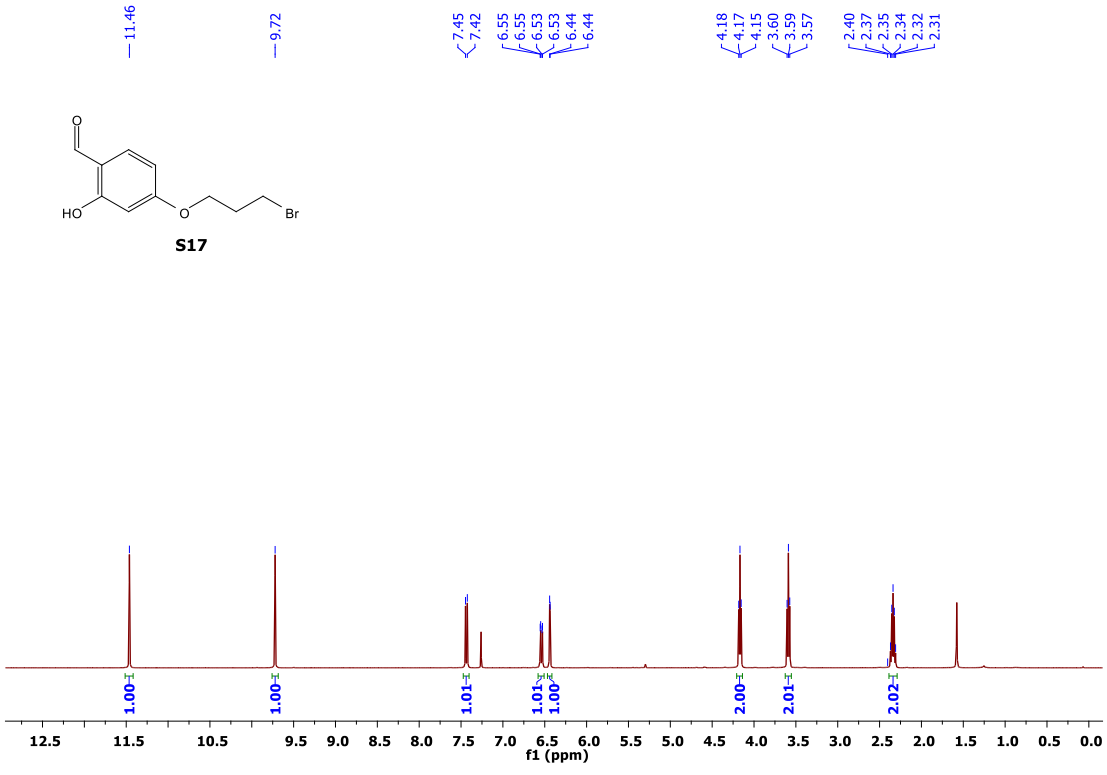

Figure S40. ^{1}H-NMR spectrum of compound **S17.**

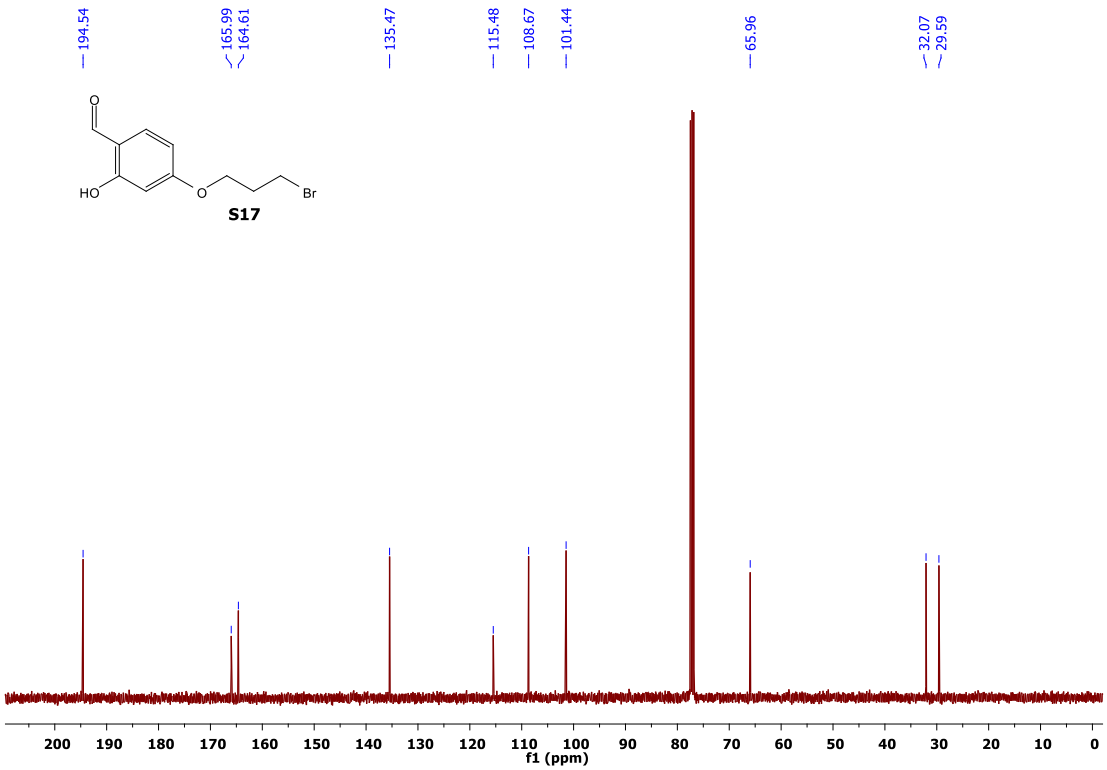

Figure S41. ^{13}C-NMR spectrum of compound **S17.**

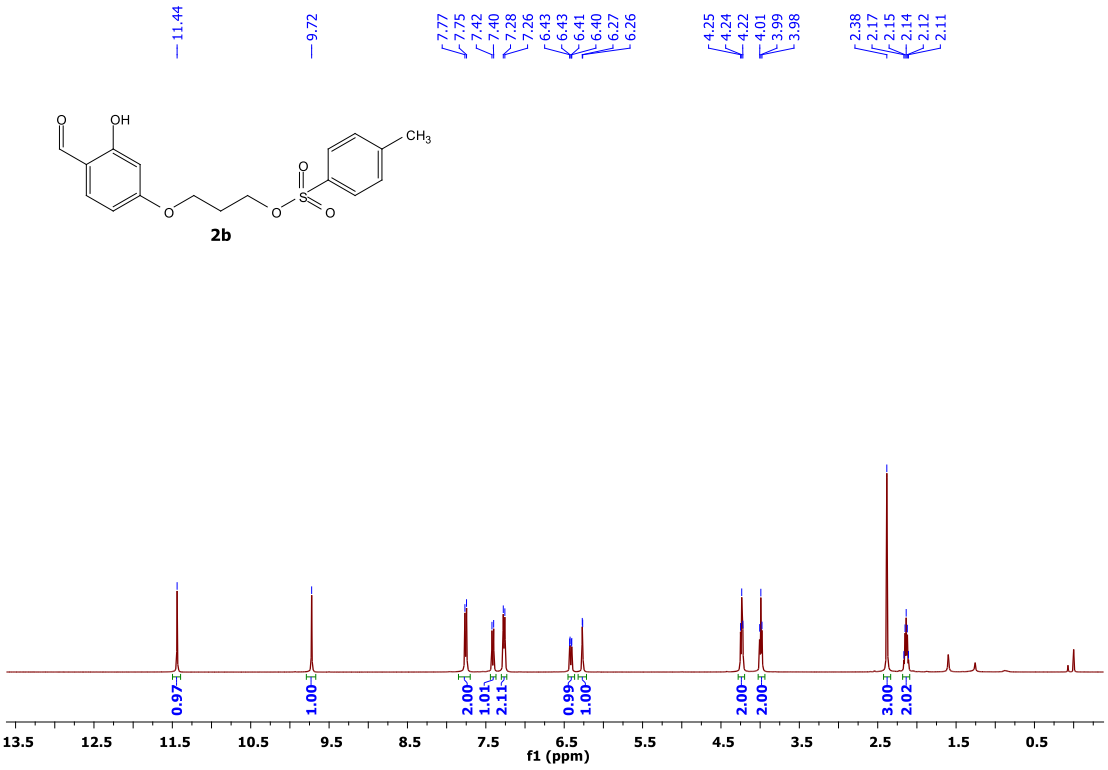

Figure S42. ^{1}H-NMR spectrum of compound **2b.**

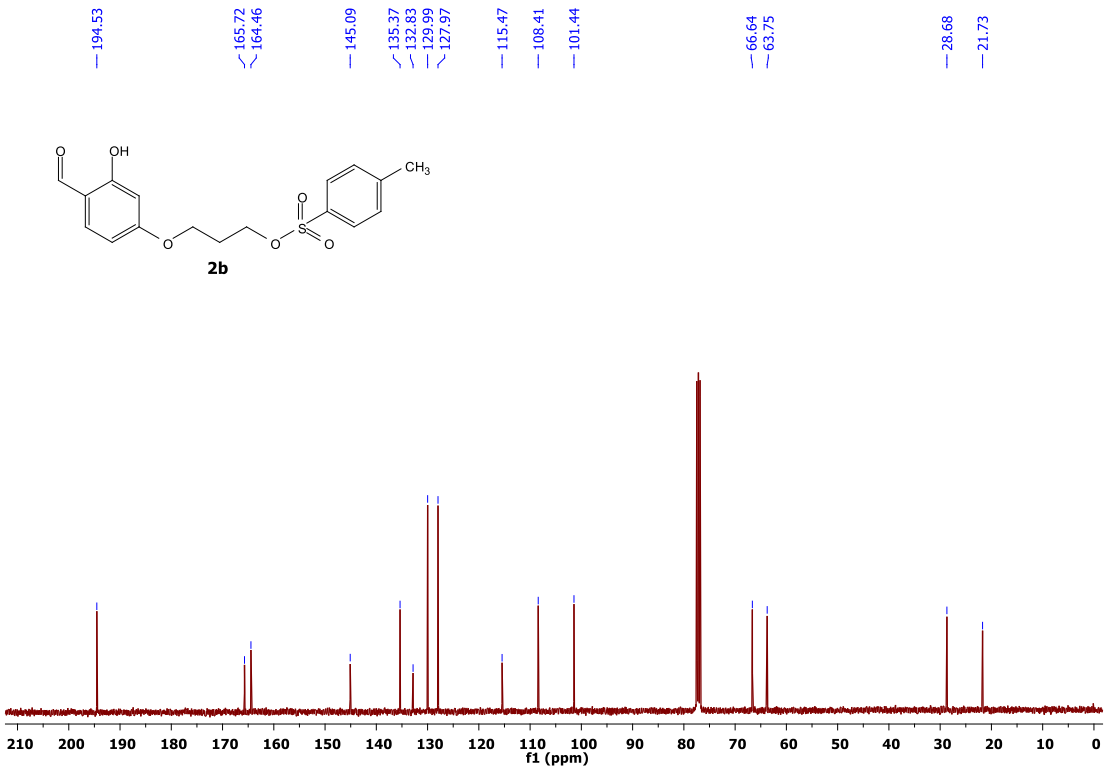

Figure S43. ^{13}C-NMR spectrum of compound **2b.**

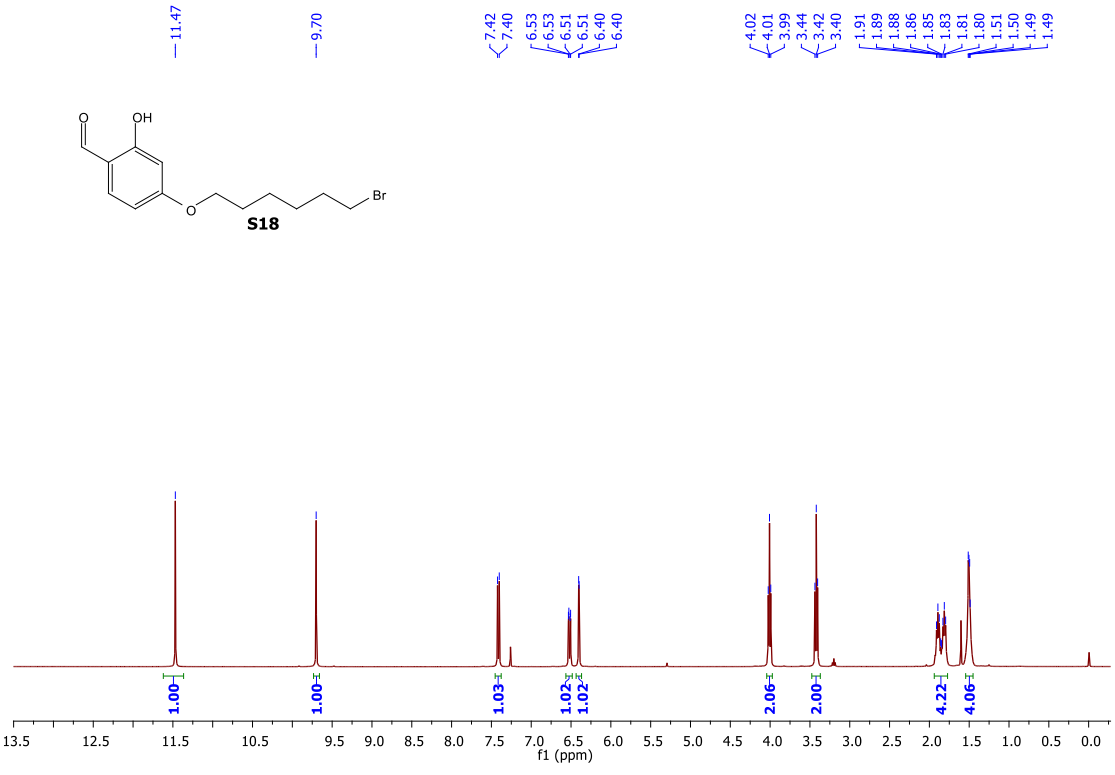

Figure S44. ^{1}H-NMR spectrum of compound **S18.**

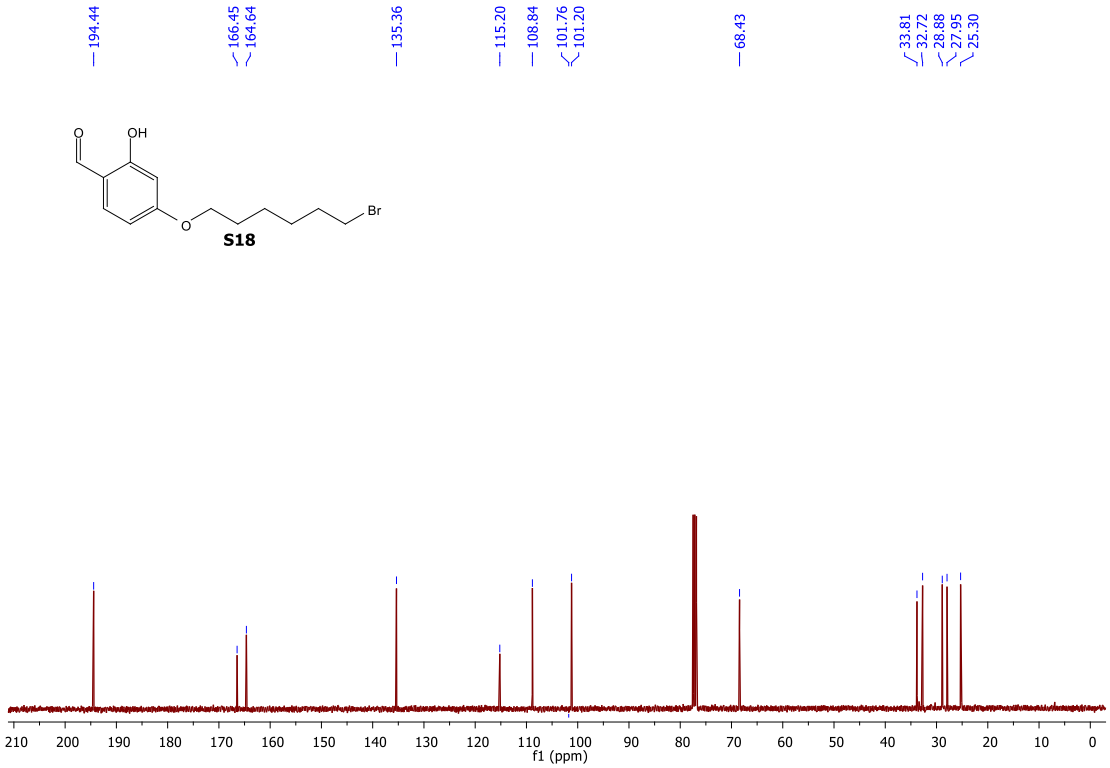

Figure S45. ^{13}C-NMR spectrum of compound **S18.**

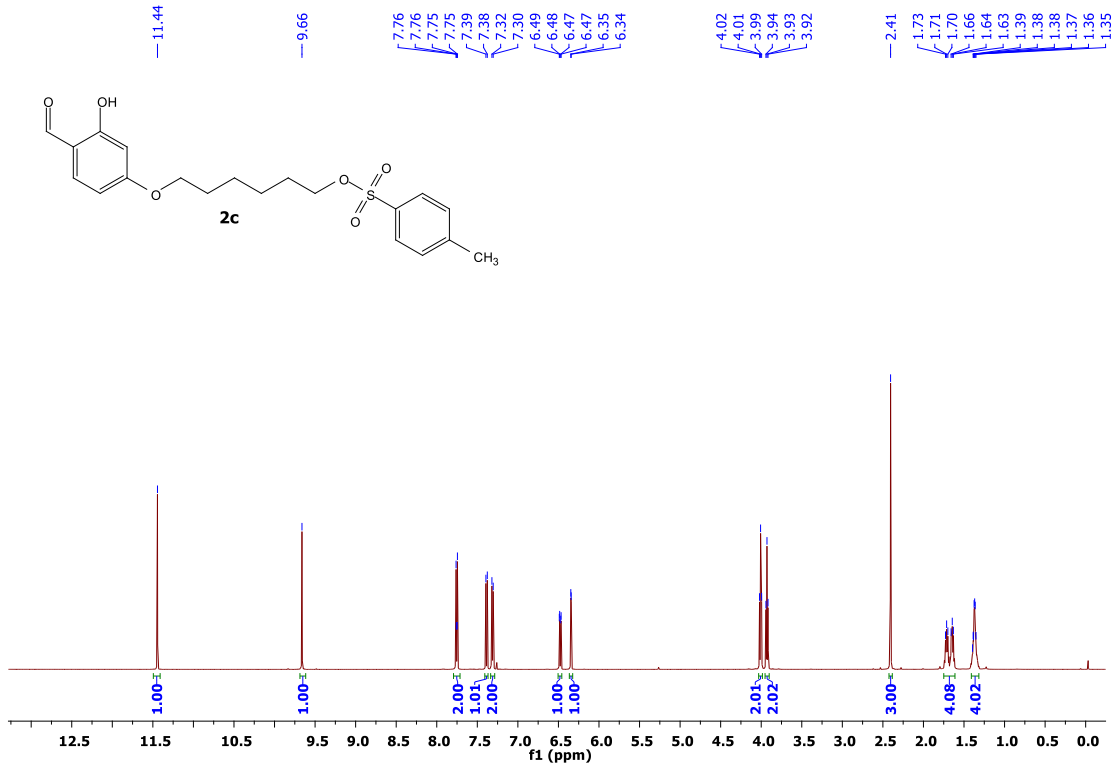

Figure S46. ^{1}H-NMR spectrum of compound **2c.**

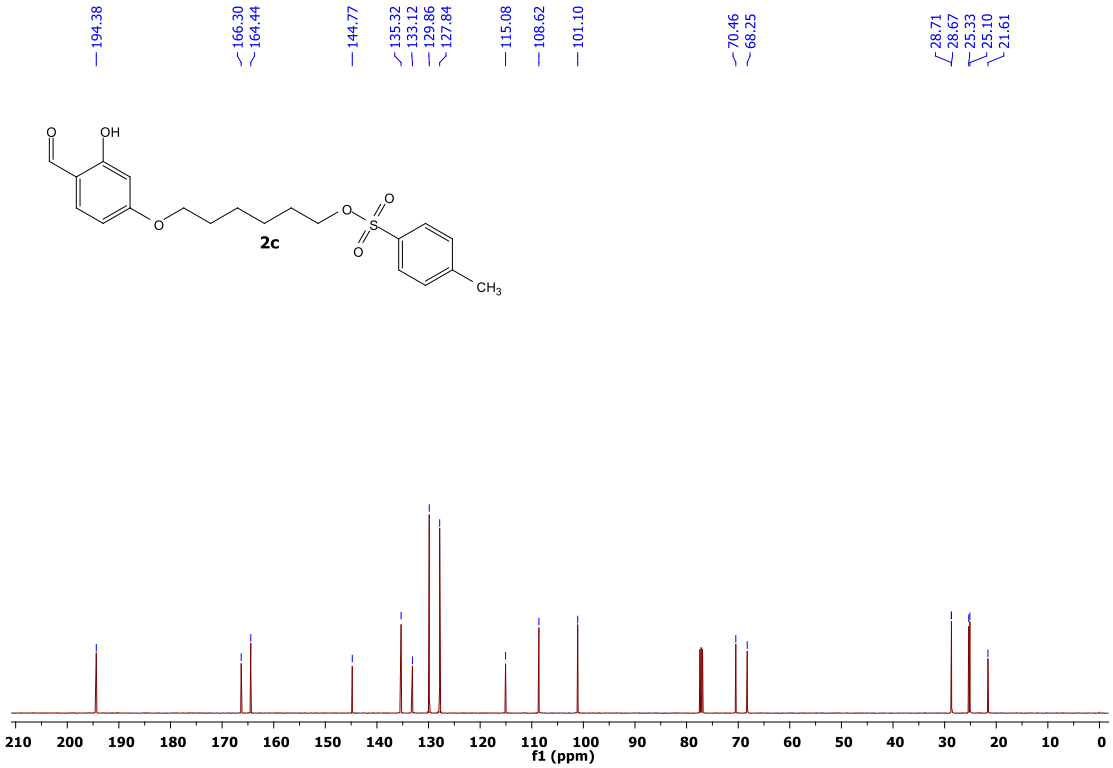

Figure S47. ^{13}C-NMR spectrum of compound **2c.**

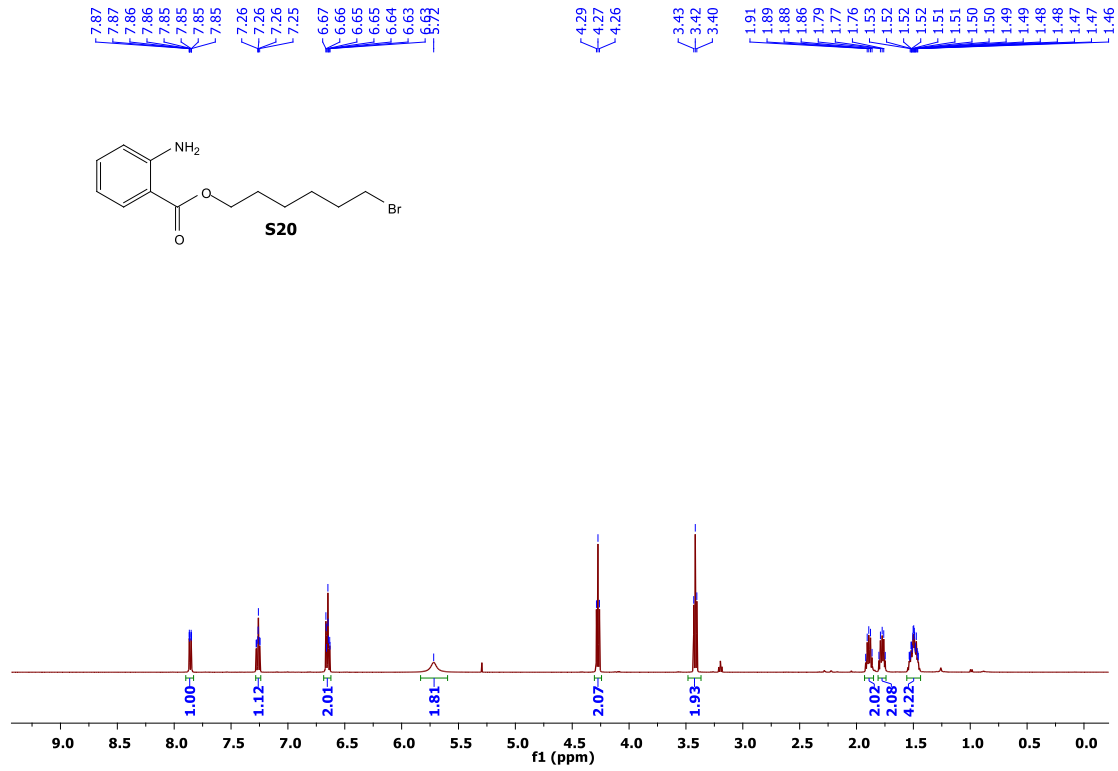

Figure S48. ^{1}H-NMR spectrum of compound **S20.**

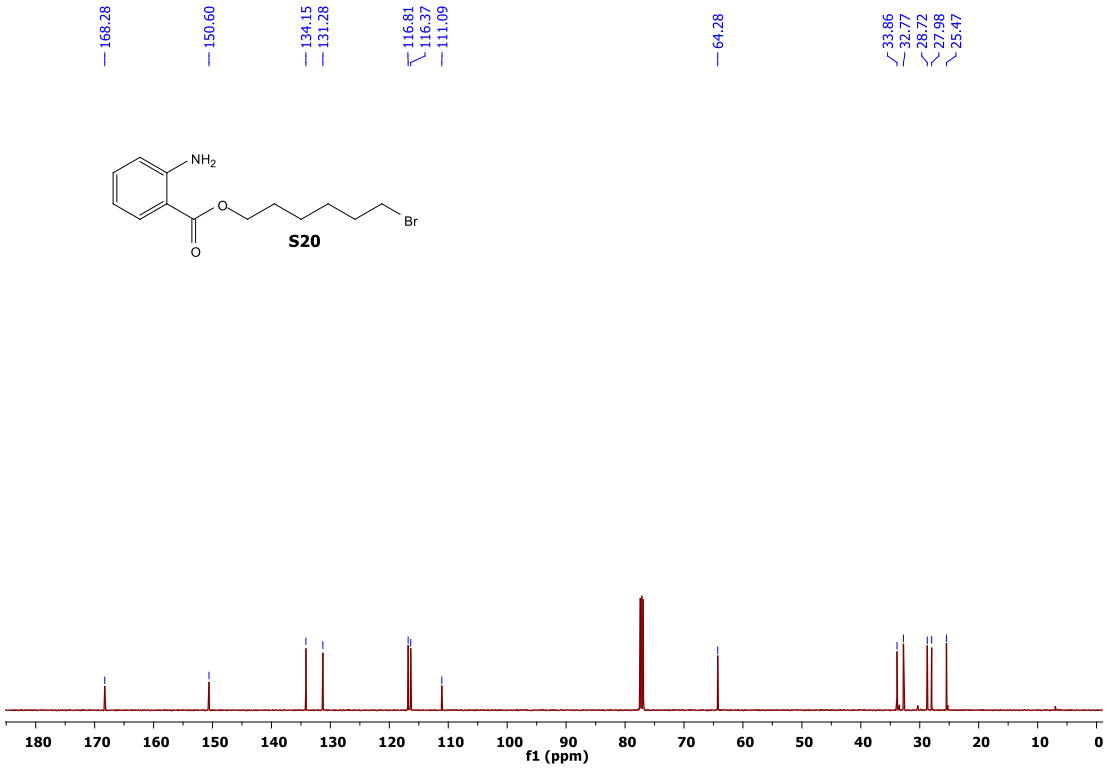

Figure S49. ^{13}C-NMR spectrum of compound **S20.**

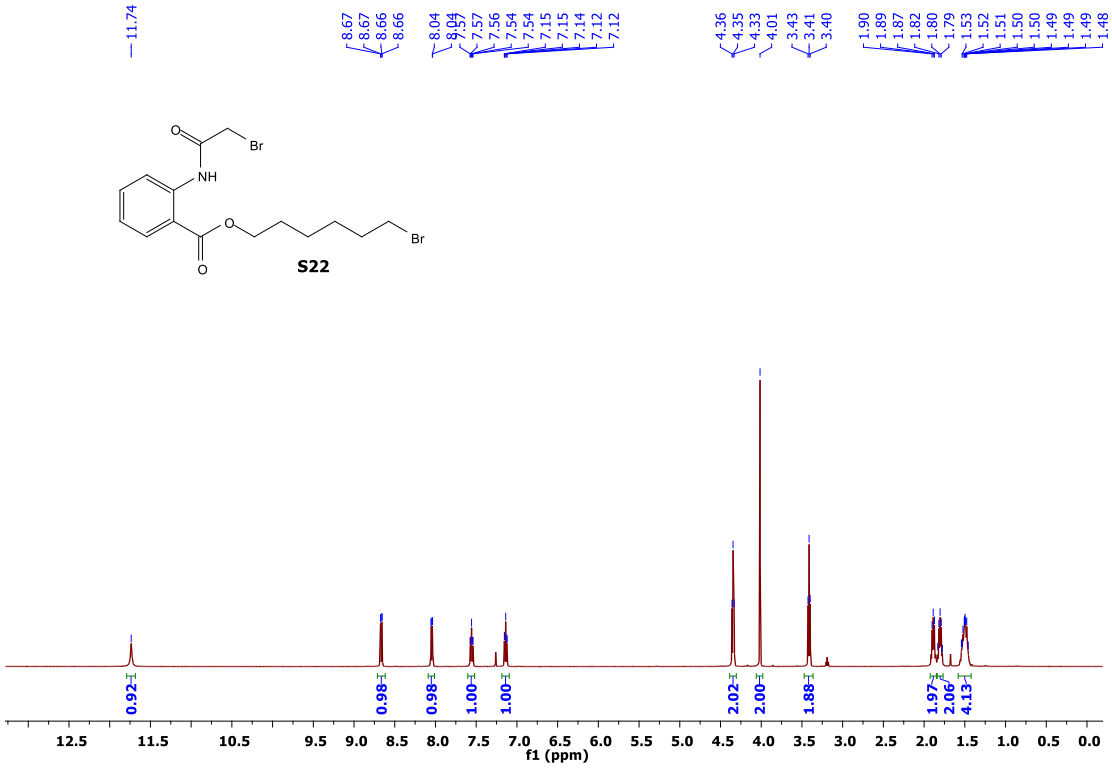

Figure S50. ^{1}H-NMR spectrum of compound **S22.**

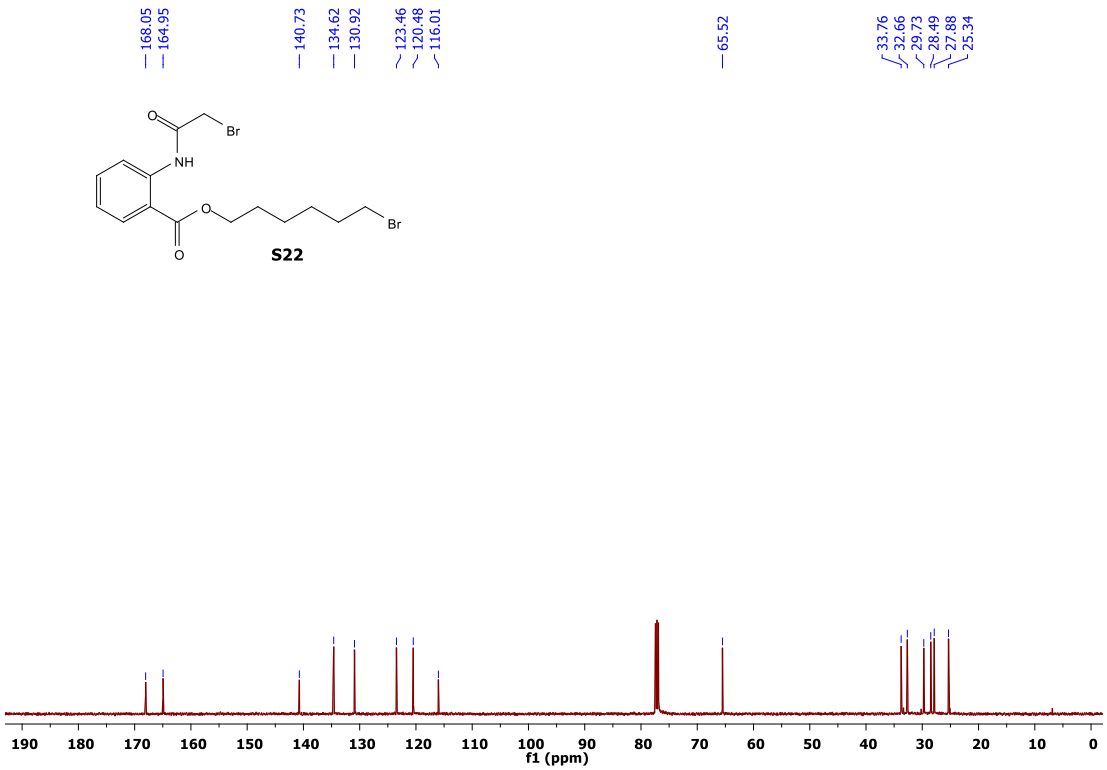

Figure S51. ^{13}C-NMR spectrum of compound **S22.**

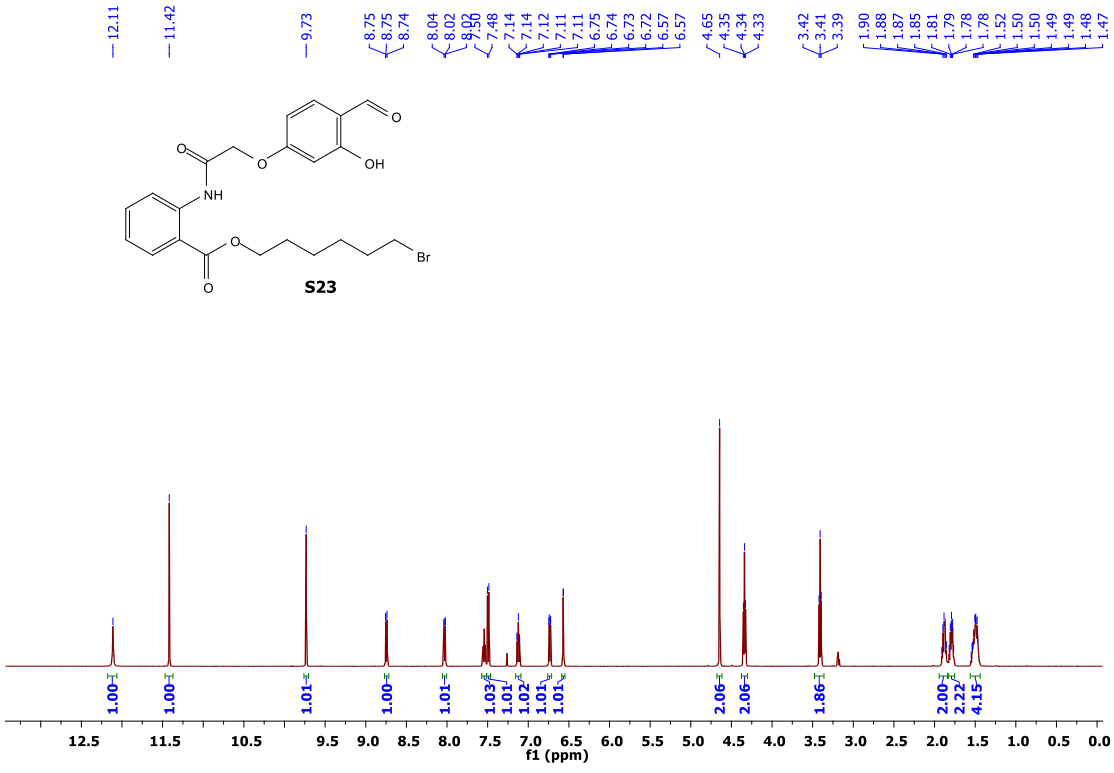

Figure S52. ^{1}H-NMR spectrum of compound **S23.**

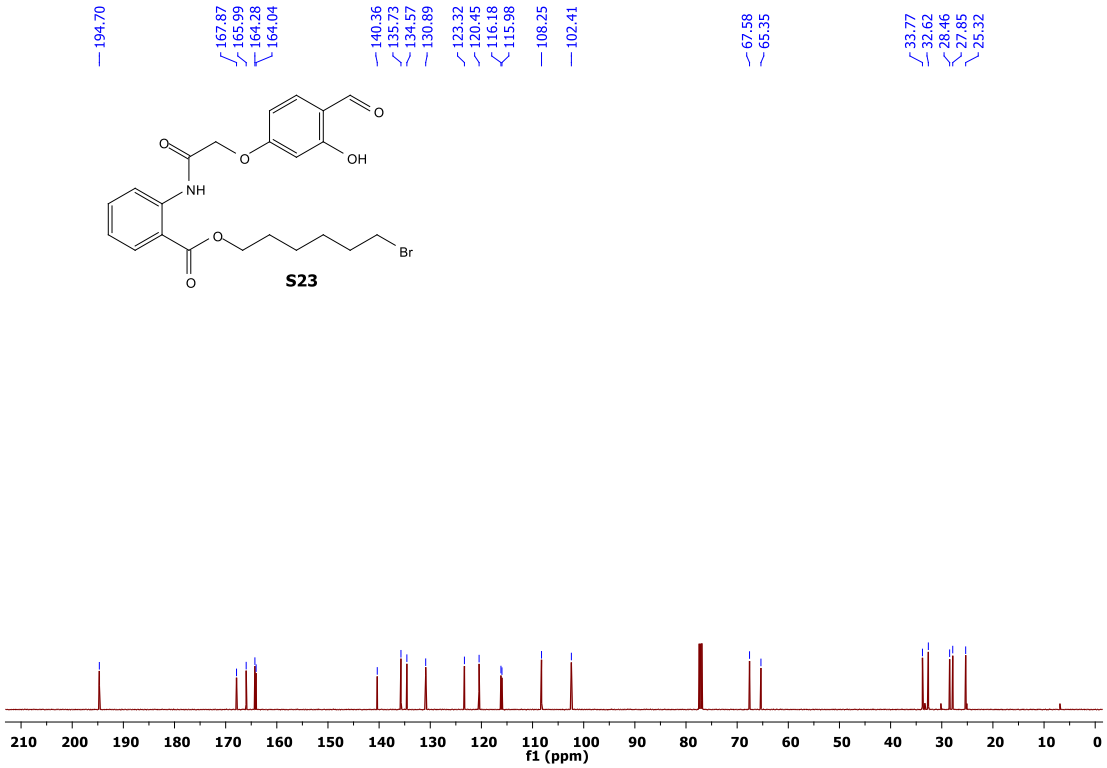

Figure S53. ^{13}C-NMR spectrum of compound **S23.**

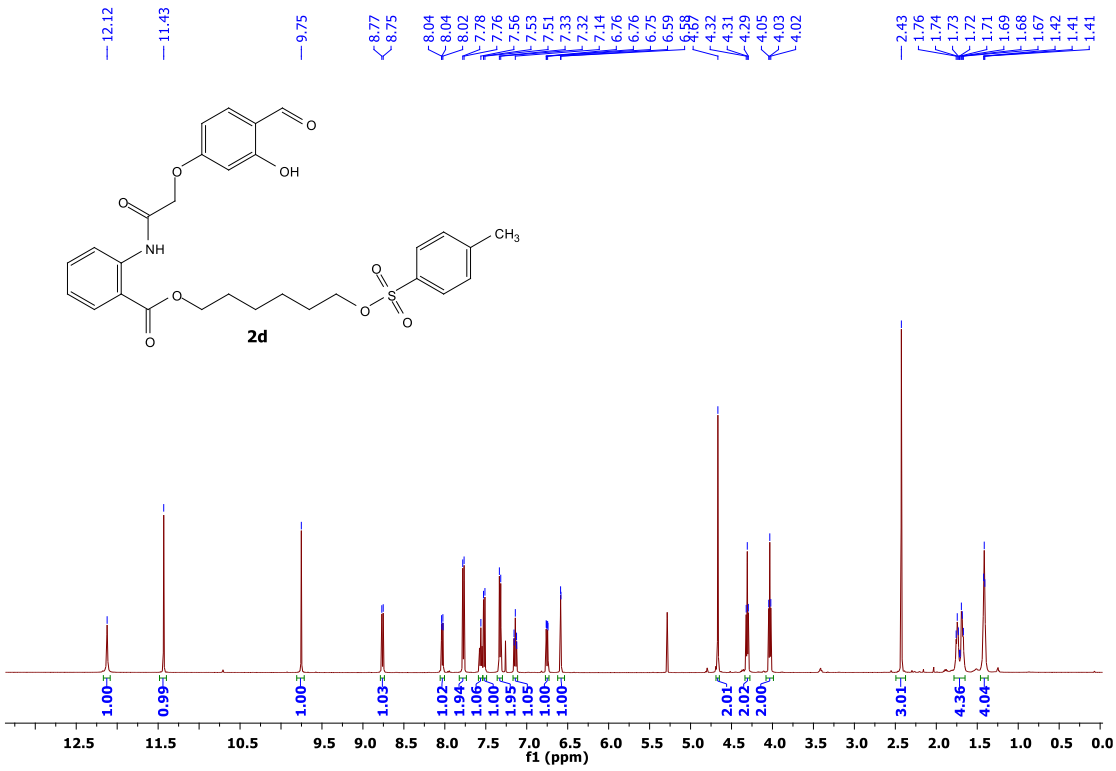

Figure S54. ^{1}H-NMR spectrum of compound **2d.**

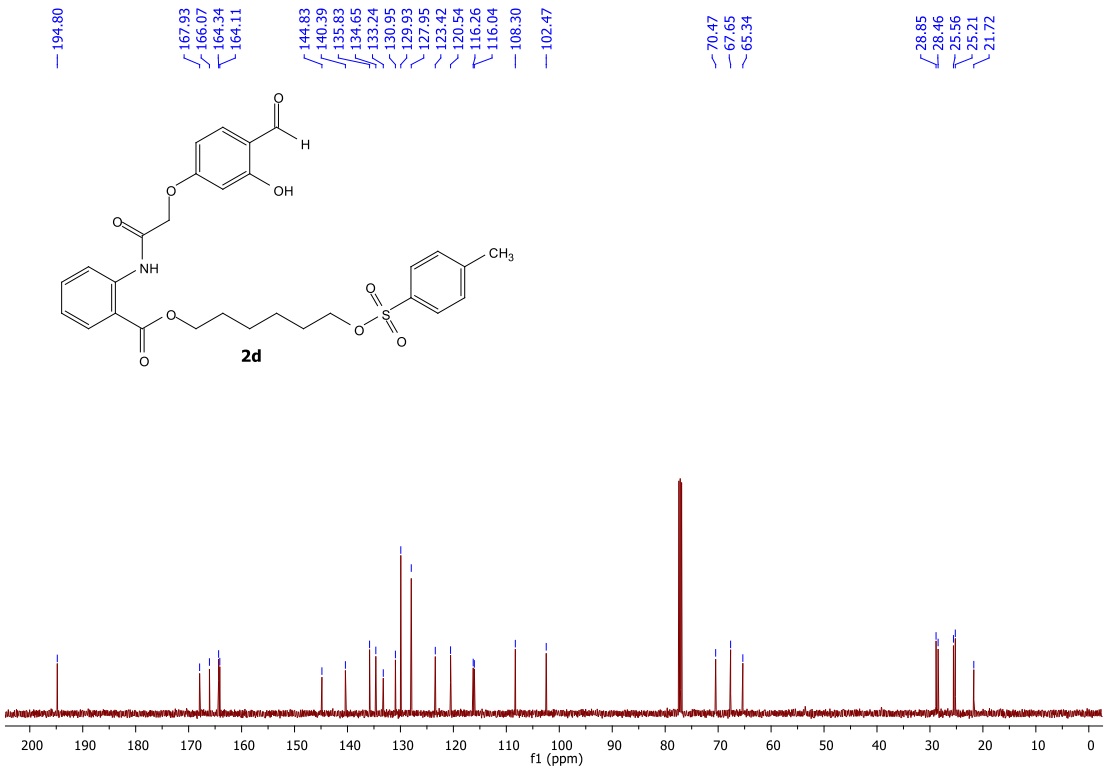

Figure S55. ^{13}C-NMR spectrum of compound **2d.**

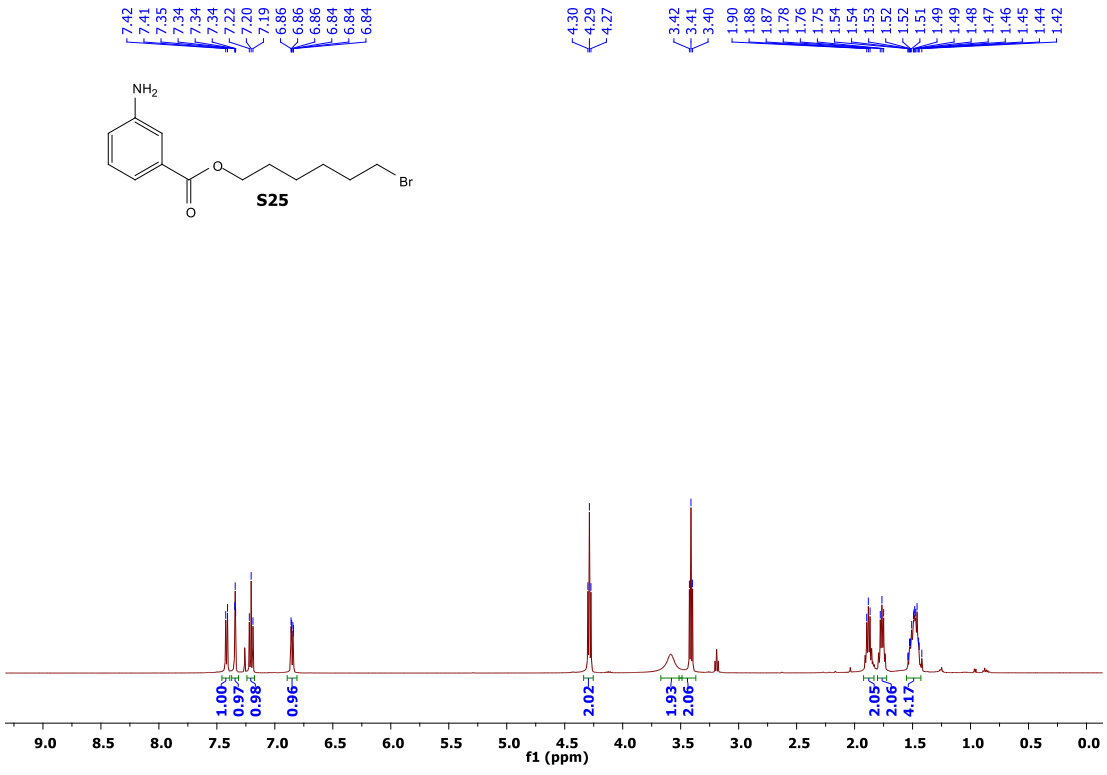

Figure S56. ^{1}H-NMR spectrum of compound **S25**

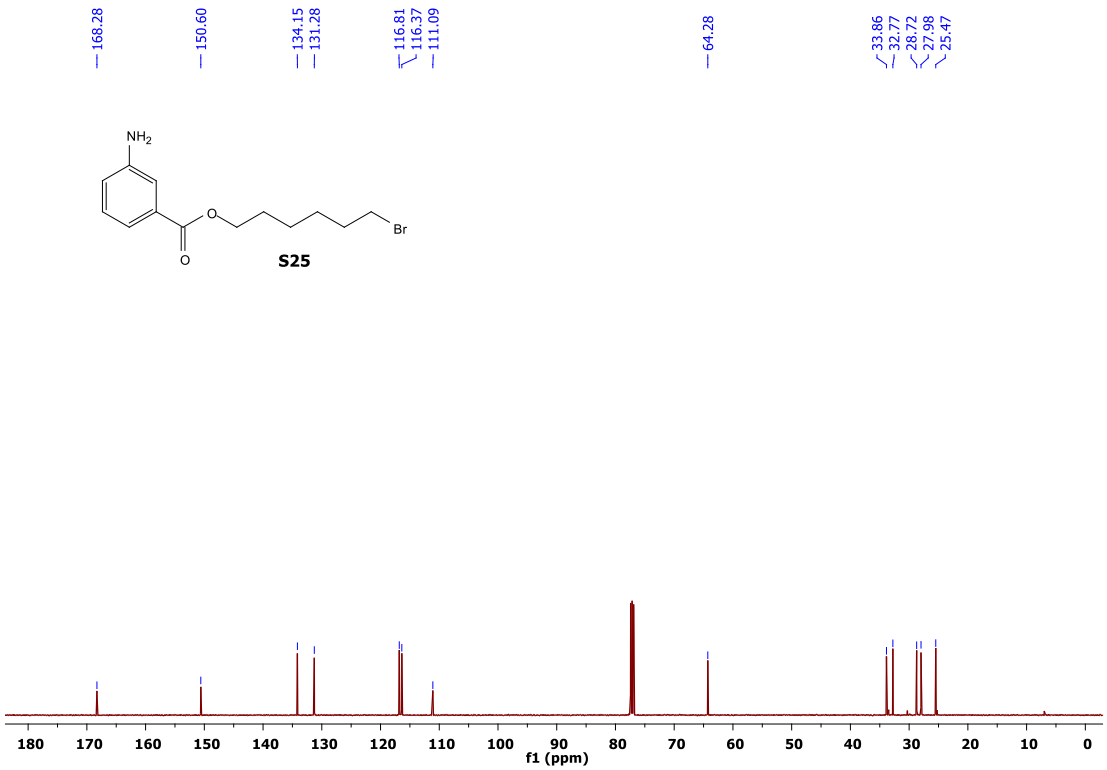

Figure S57. ^{13}C-NMR spectrum of compound **S25.**

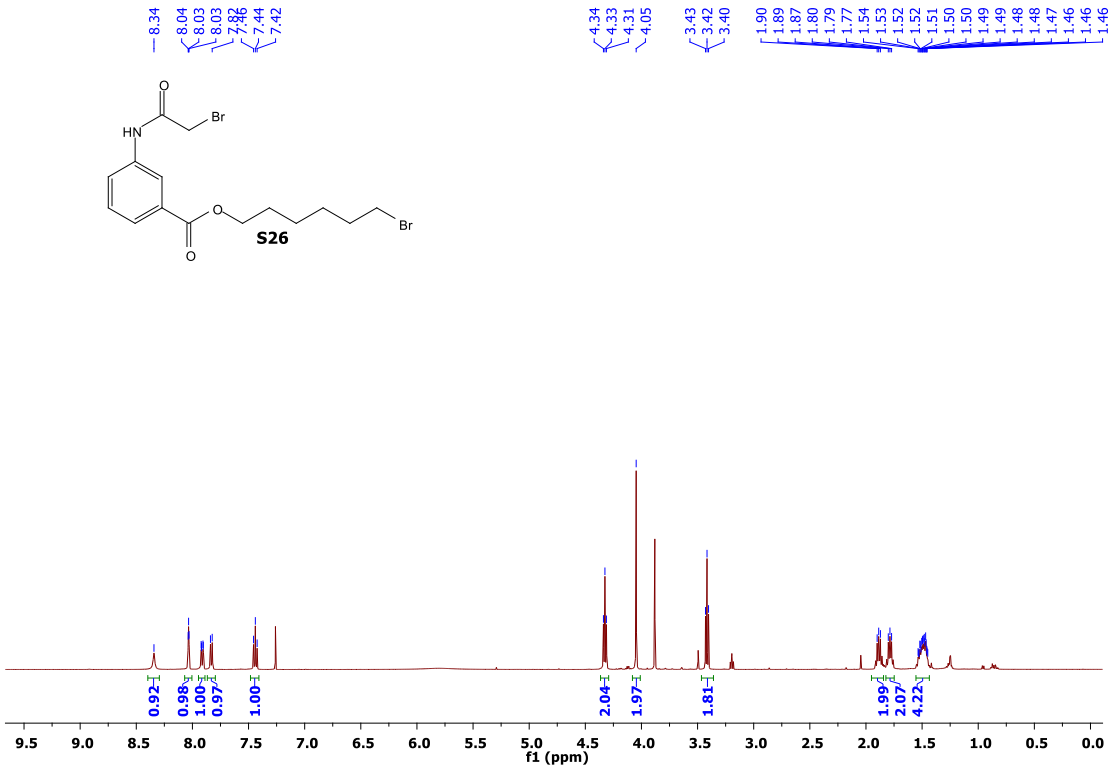

Figure S58. ^{1}H-NMR spectrum of compound **S26.**

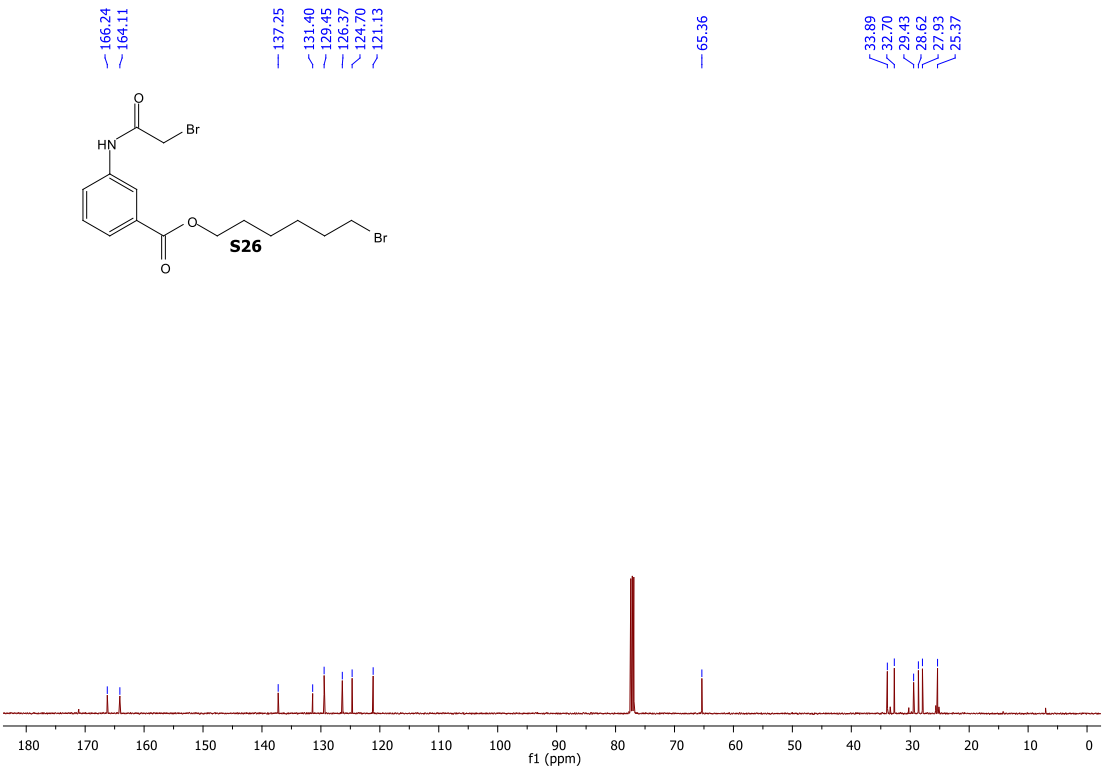

Figure S59. ^{13}C-NMR spectrum of compound **S26.**

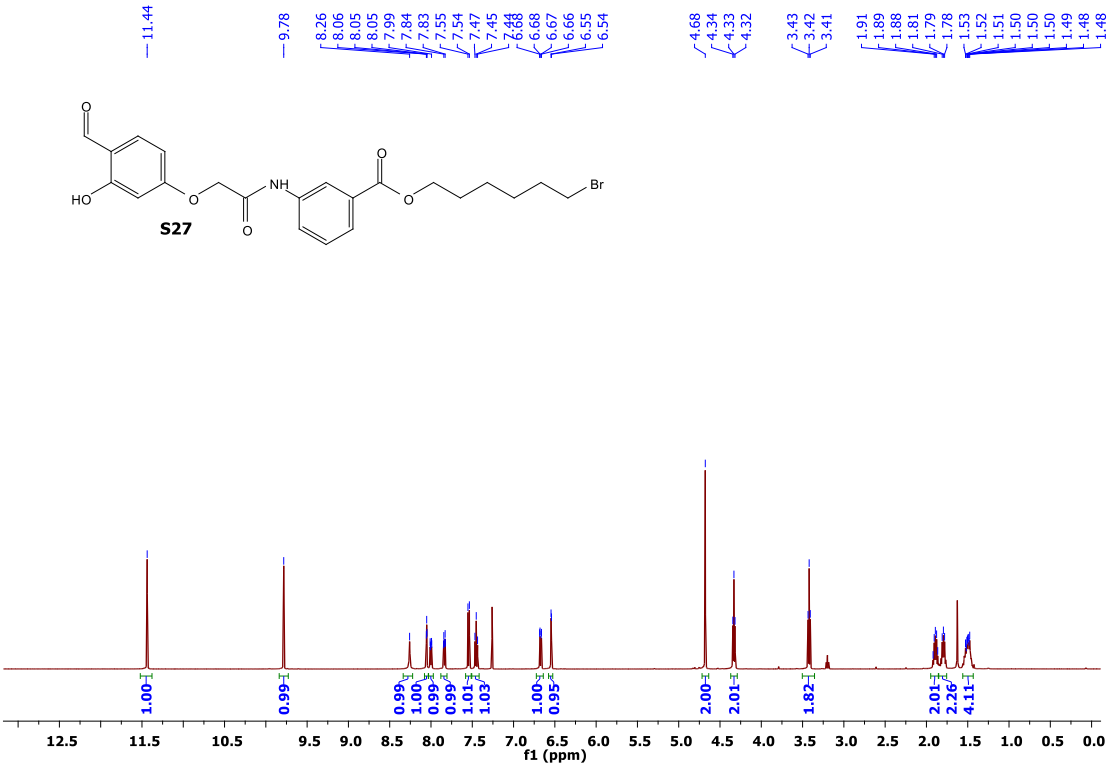

Figure S60. ^{1}H-NMR spectrum of compound **S27.**

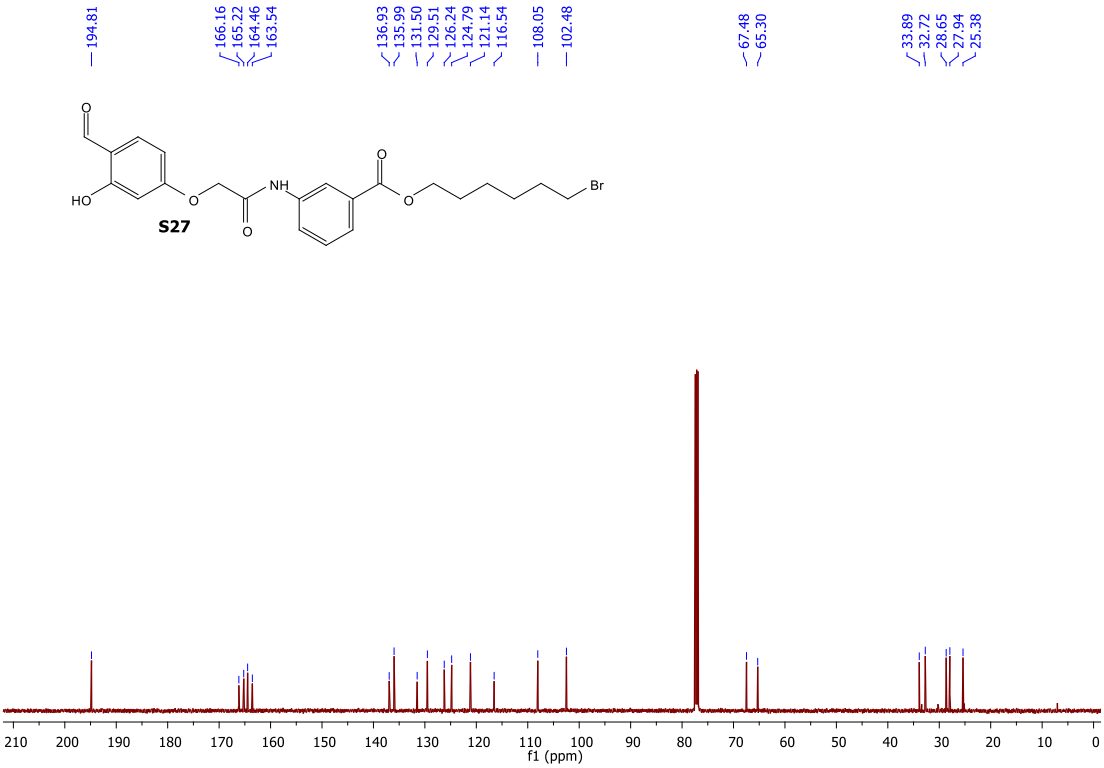

Figure S61. ^{13}C-NMR spectrum of compound **S27.**

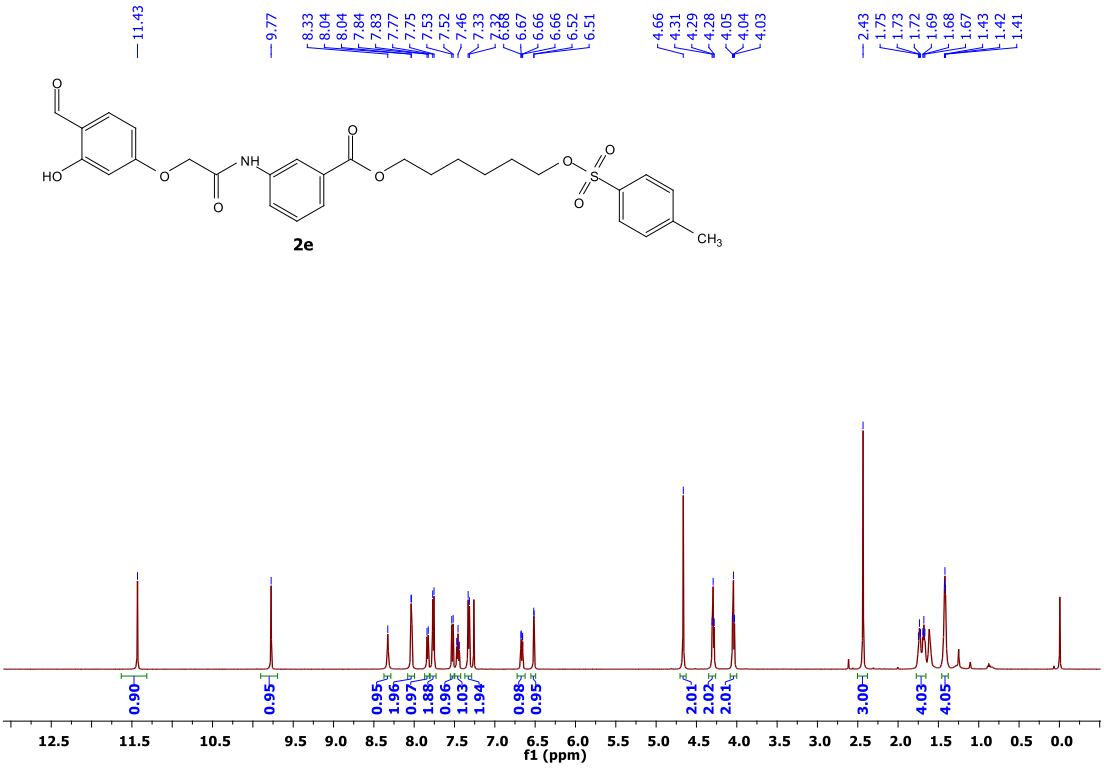

Figure S62. ^{1}H-NMR spectrum of compound **2e.**

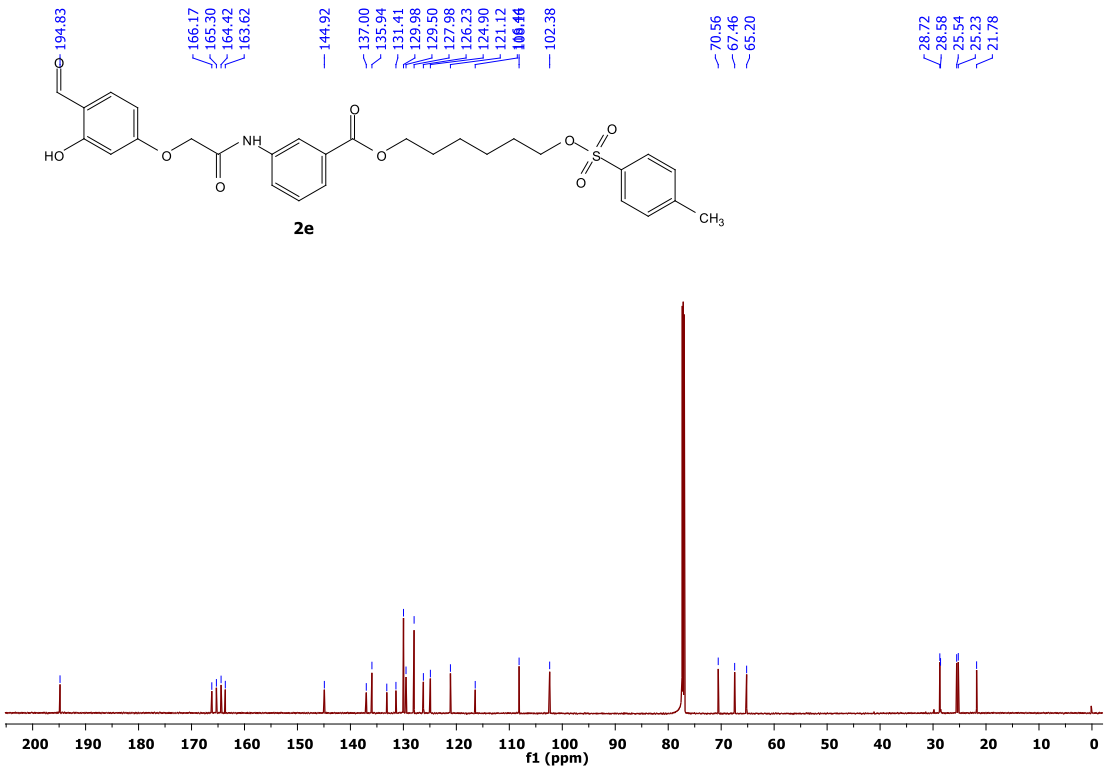

Figure S63. ^{13}C-NMR spectrum of compound **2e.**

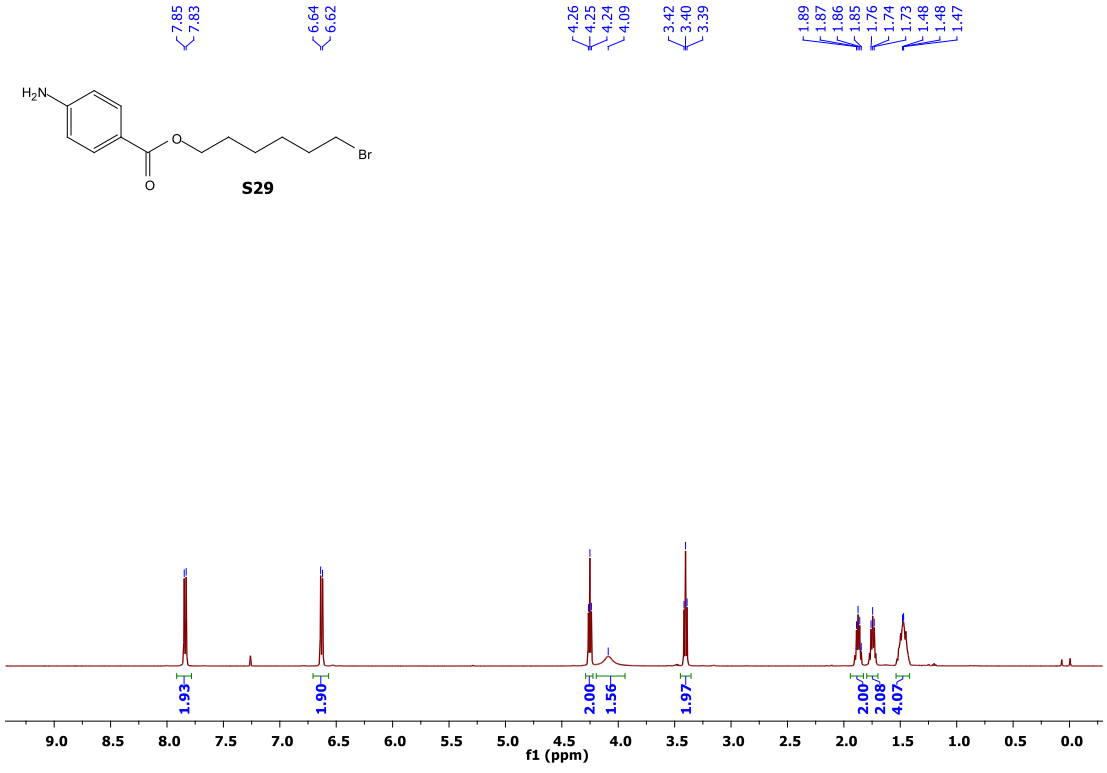

Figure S64. ^{1}H-NMR spectrum of compound **S29.**

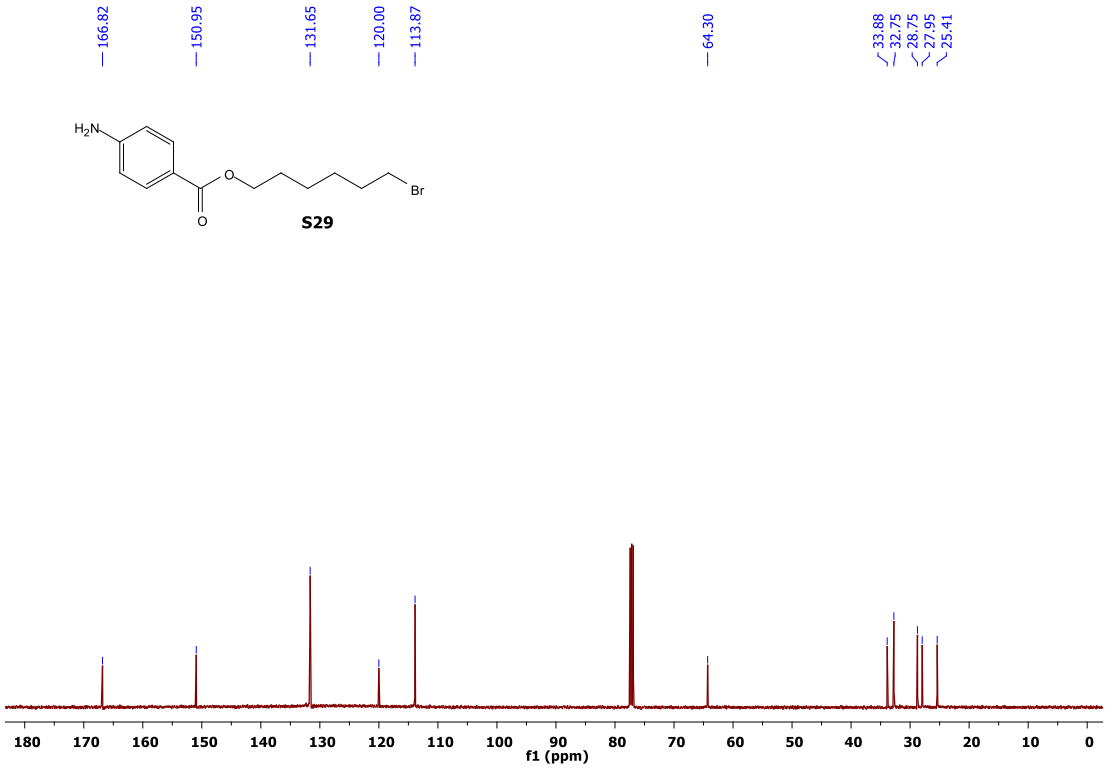

Figure S65. ^{13}C-NMR spectrum of compound **S29.**

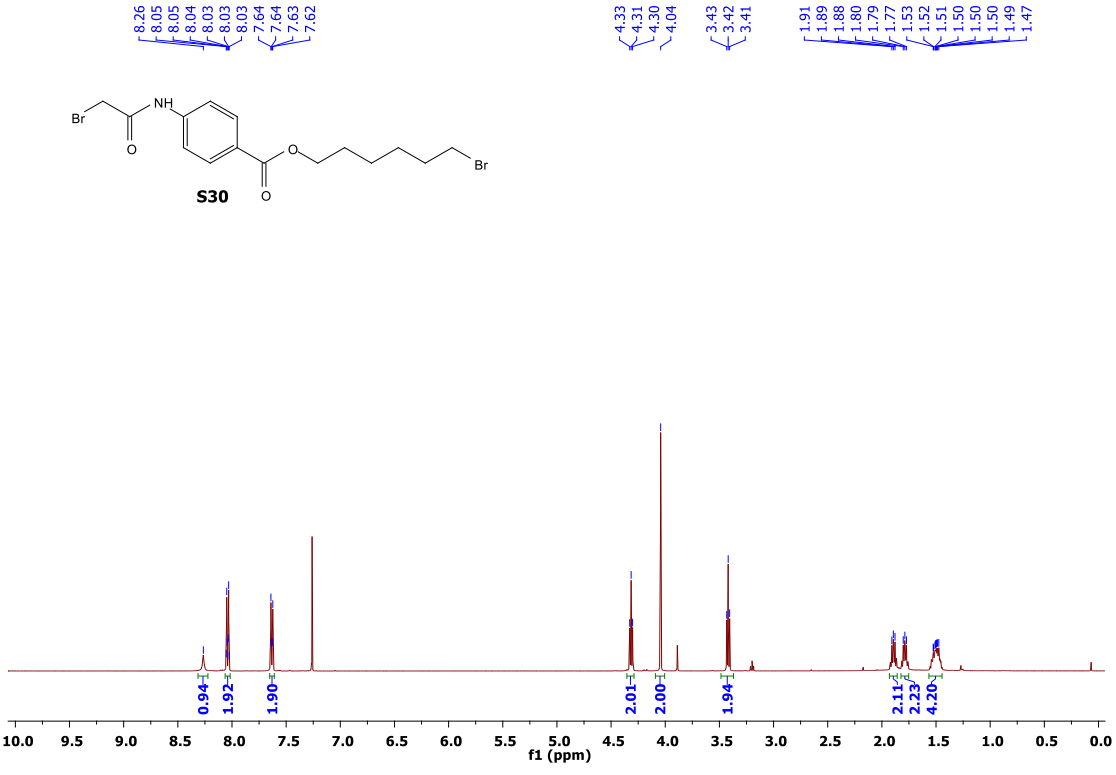

Figure S66. ^{1}H-NMR spectrum of compound **S30.**

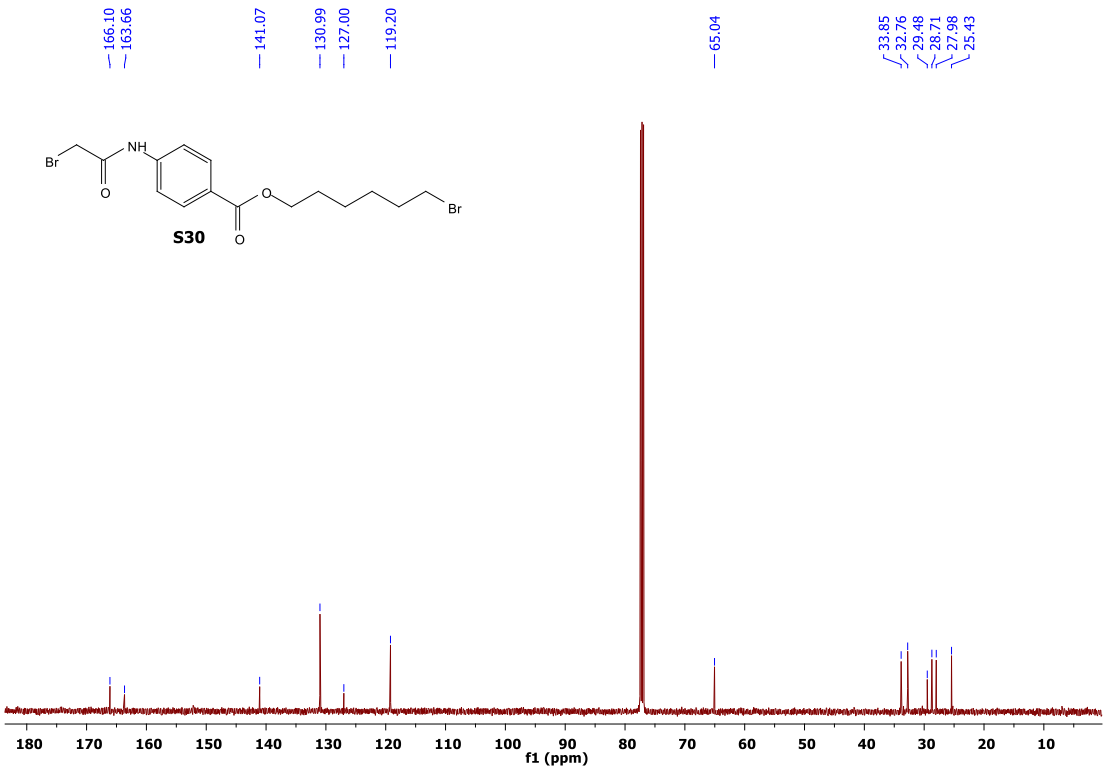

Figure S67. ^{13}C-NMR spectrum of compound **S30.**

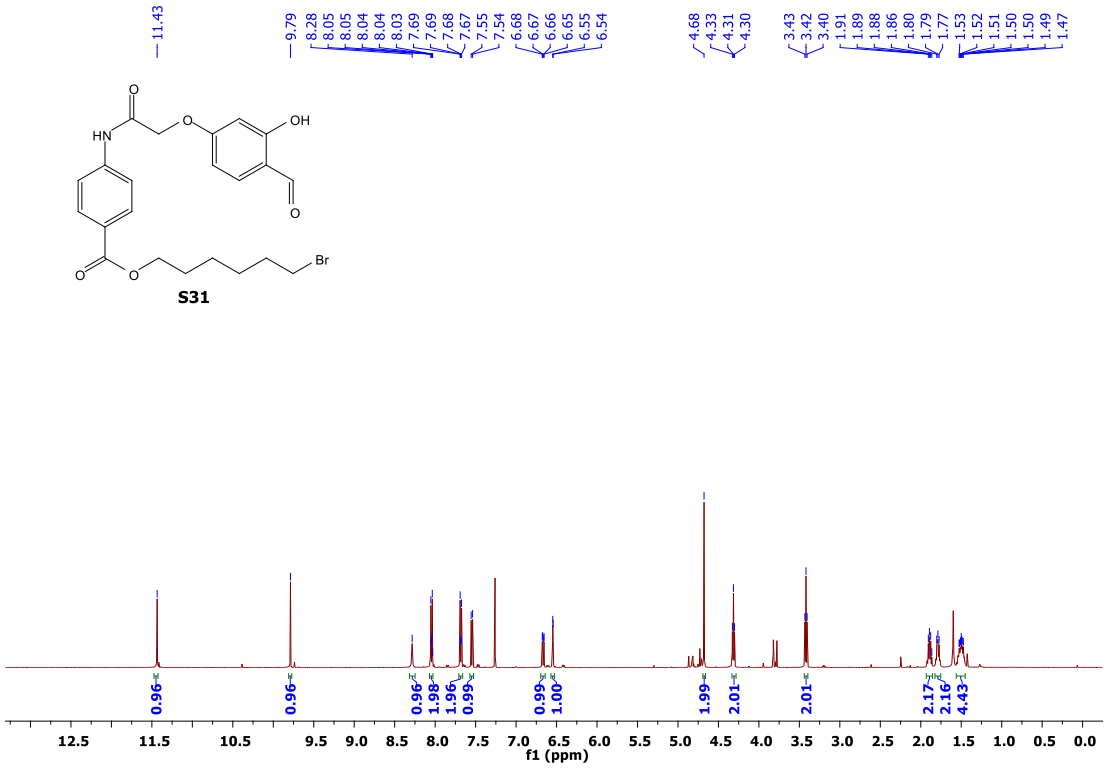

Figure S68. ^{1}H-NMR spectrum of compound **S31.**

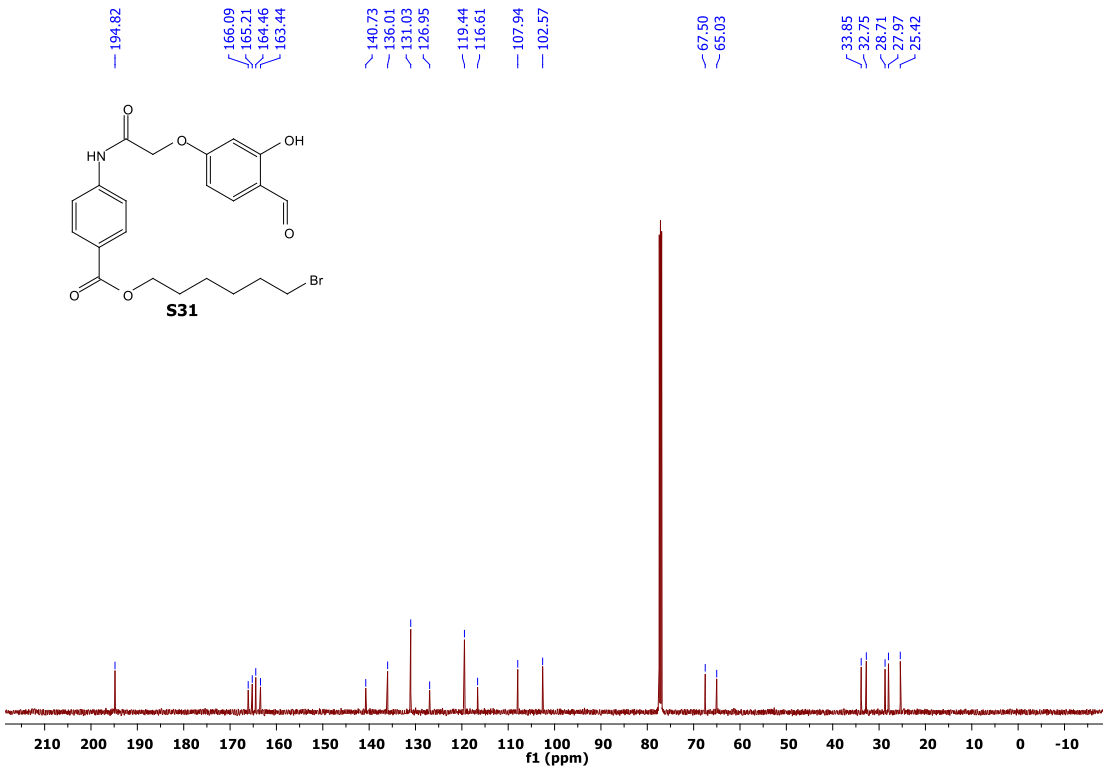

Figure S69. ^{13}C-NMR spectrum of compound **S31.**

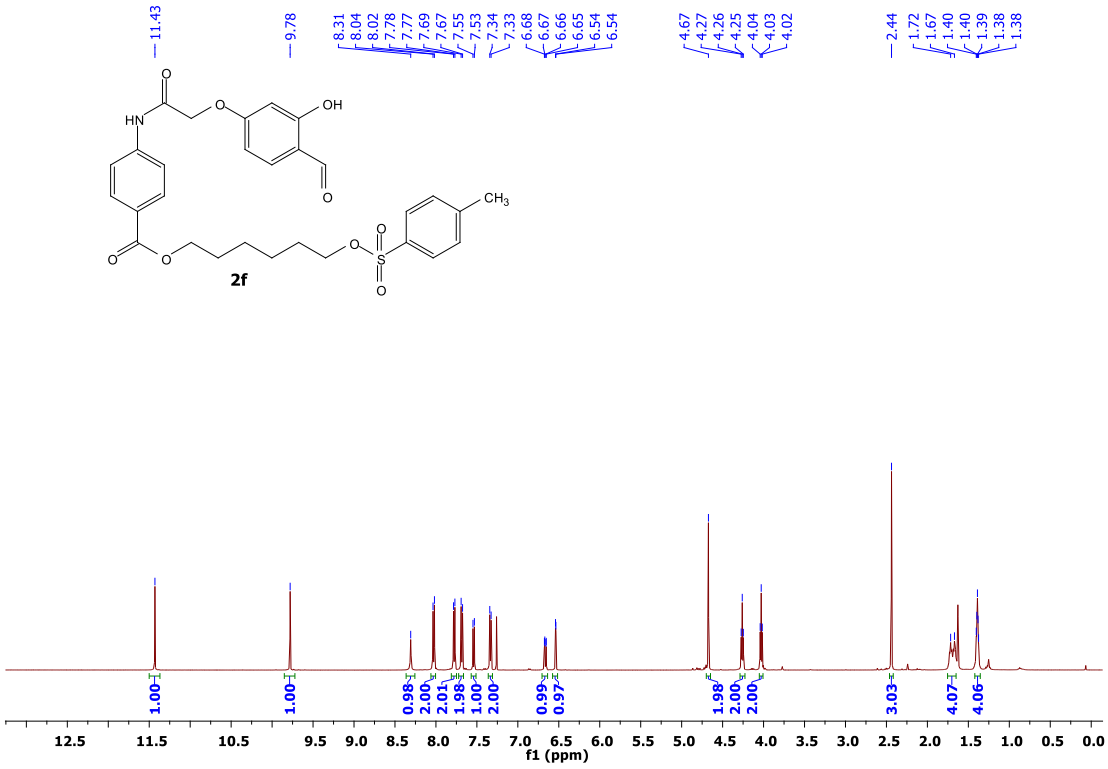

Figure S70. ^{1}H-NMR spectrum of compound **2f.**

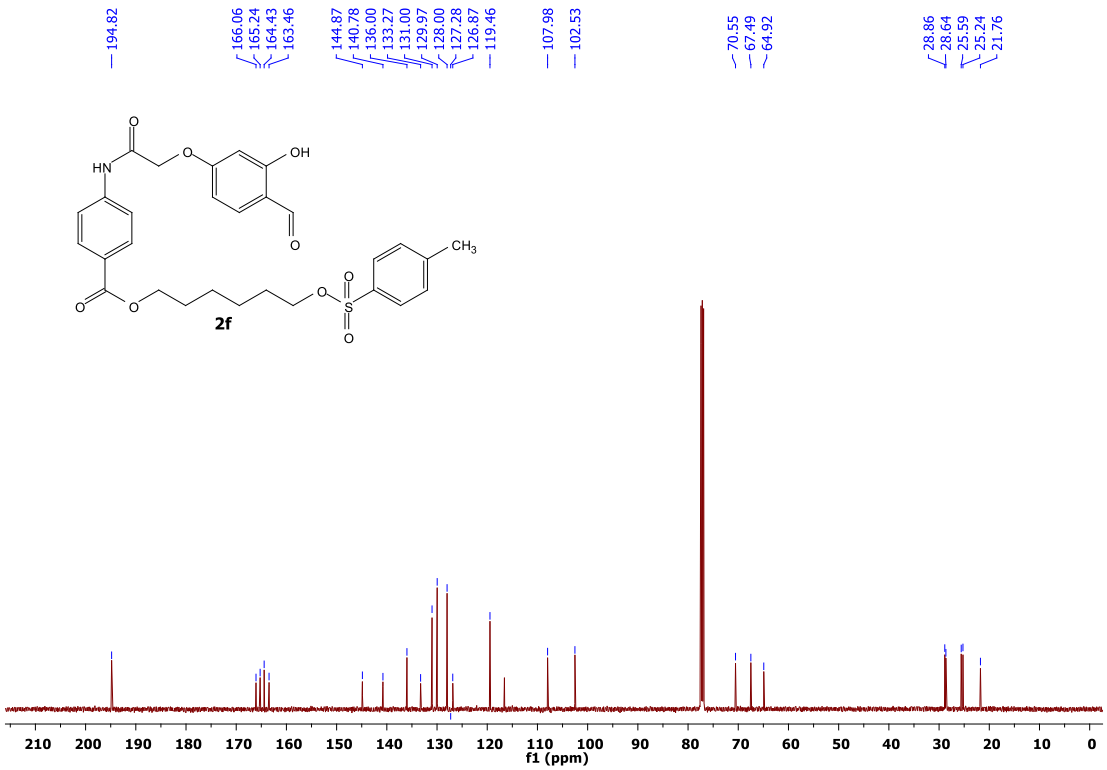

Figure S71. ^{13}C-NMR spectrum of compound **2f.**

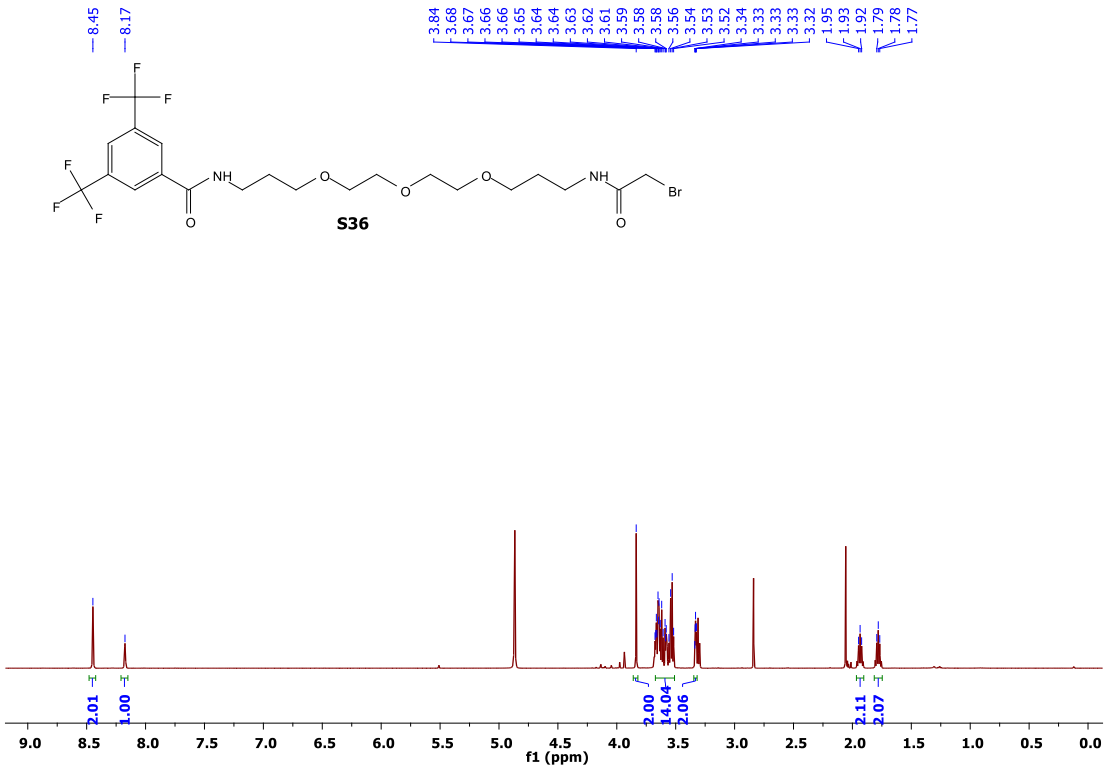

Figure S72. ^{1}H-NMR spectrum of compound **S36.**

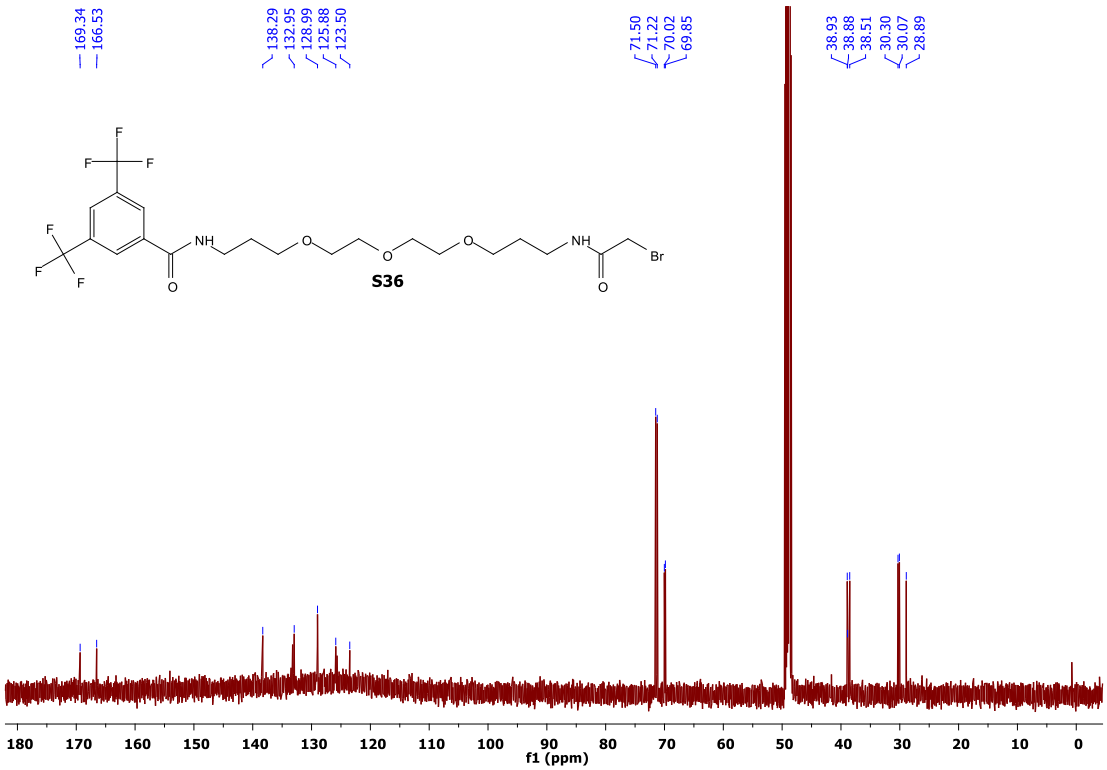

Figure S73. ^{13}C-NMR spectrum of compound **S36.**

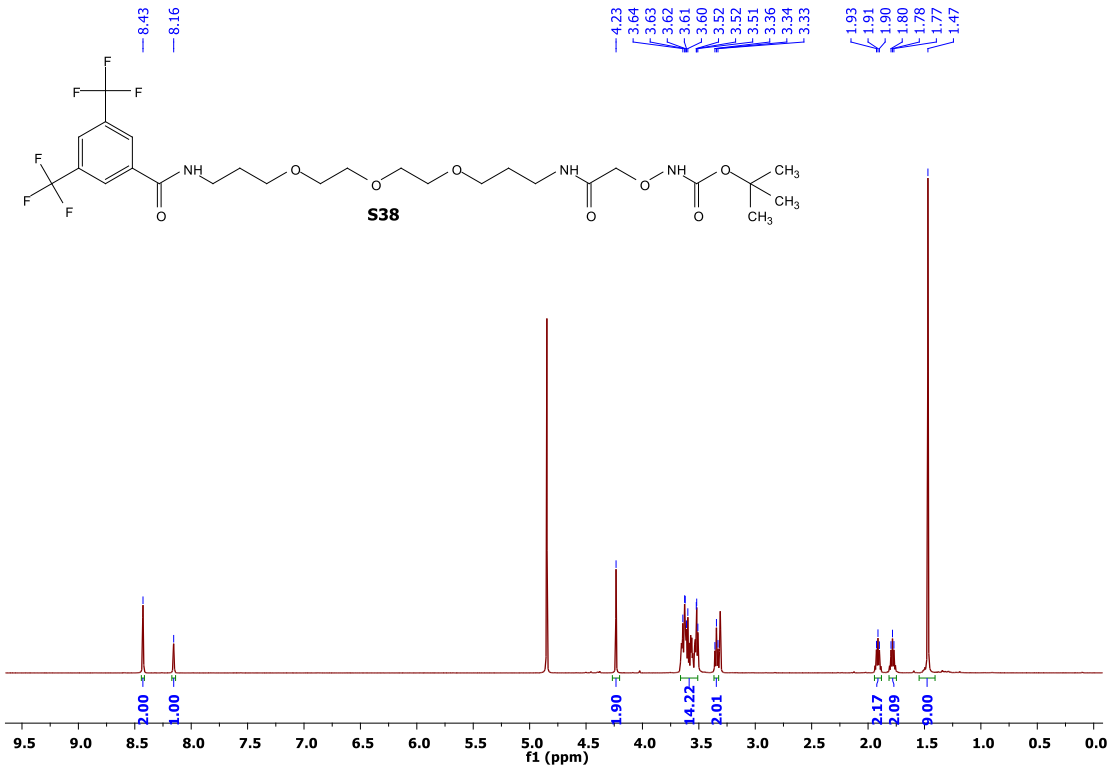

Figure S74. ^{1}H-NMR spectrum of compound **S38.**

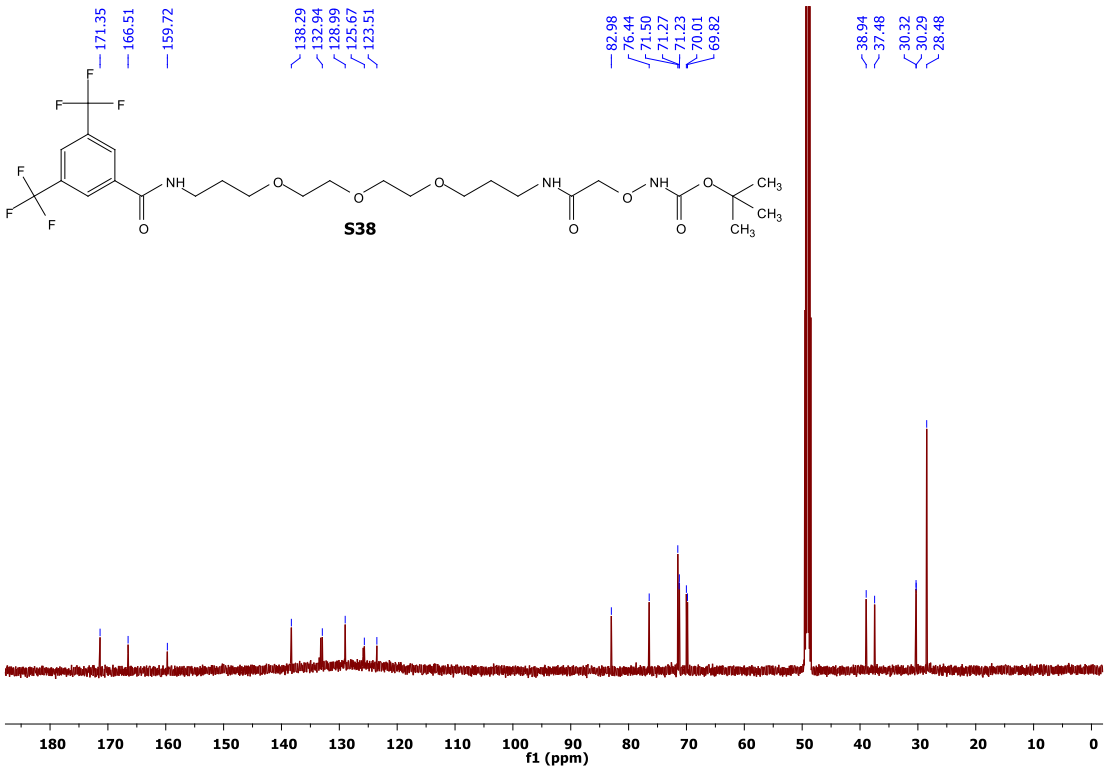

Figure S75. ^{13}C-NMR spectrum of compound **S38.**

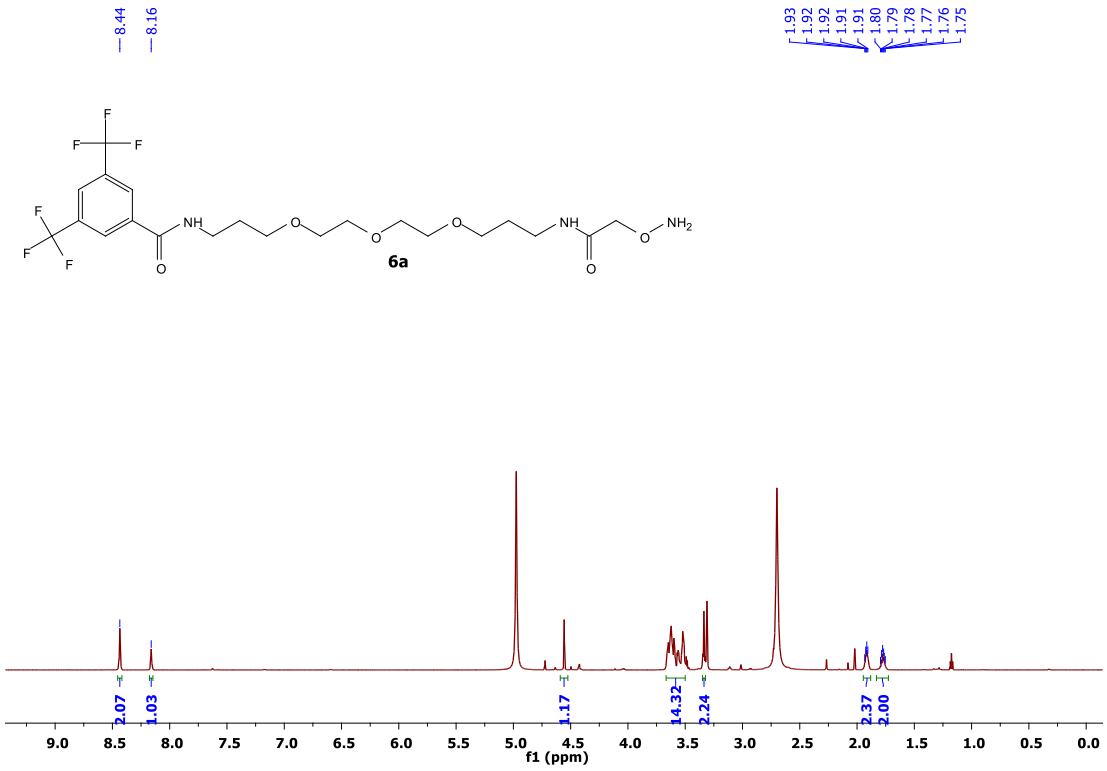

Figure S76. ^{1}H-NMR spectrum of compound **6a.**

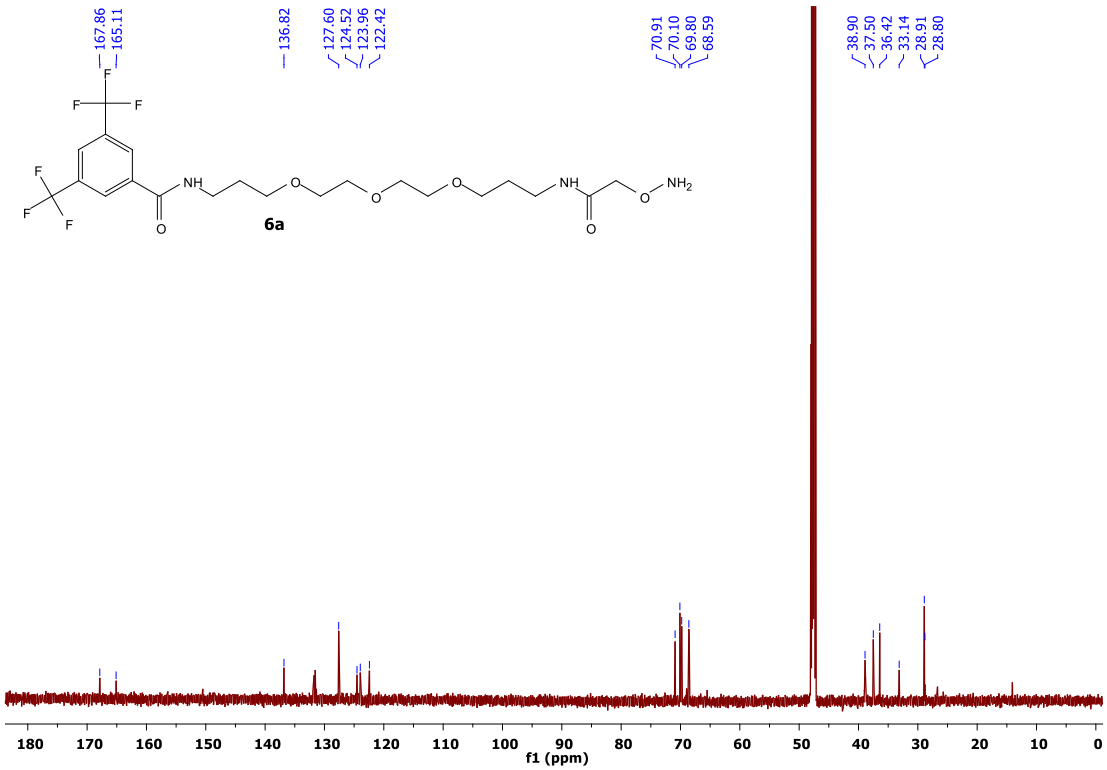

Figure S77. ^{13}C-NMR spectrum of compound **6a.**

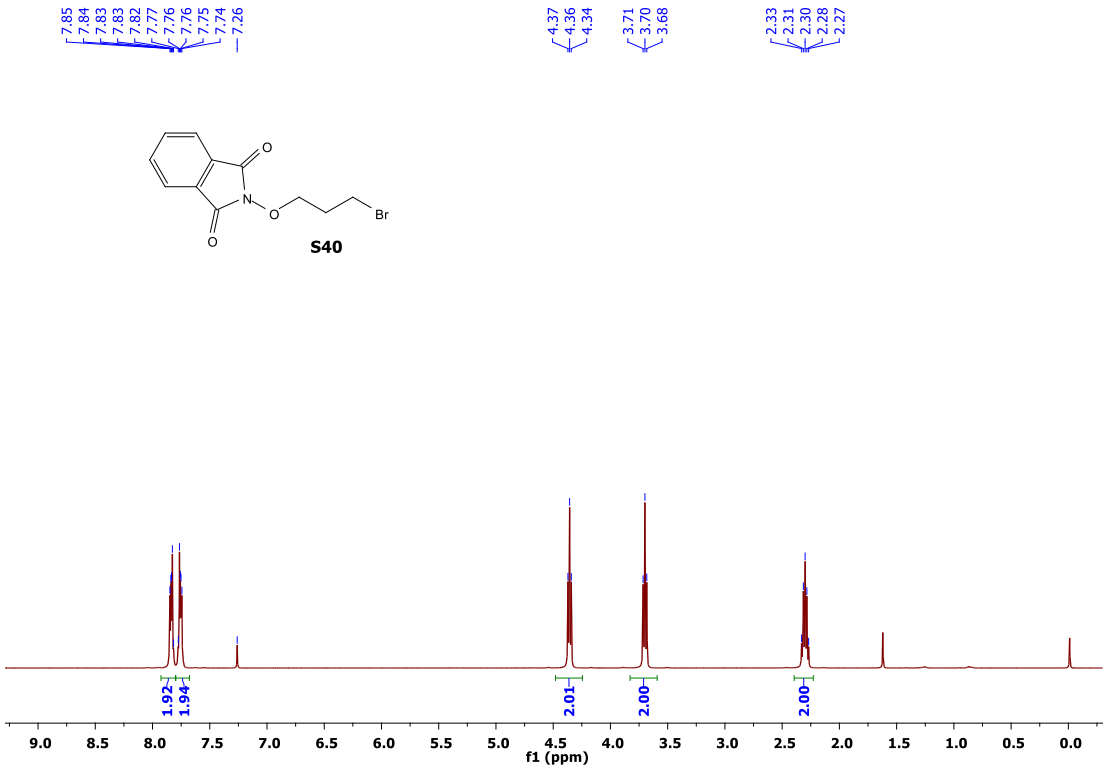

Figure S78. ^{1}H-NMR spectrum of compound **S40.**

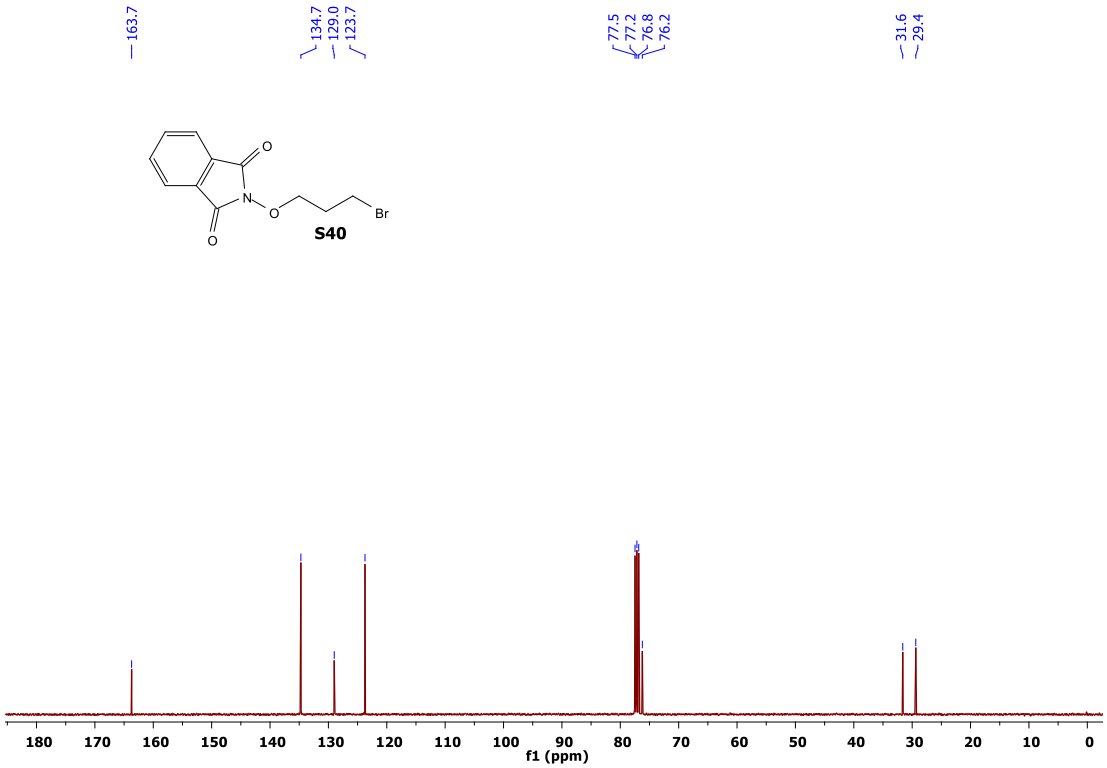

Figure S79. ^{13}C-NMR spectrum of compound **S40.**

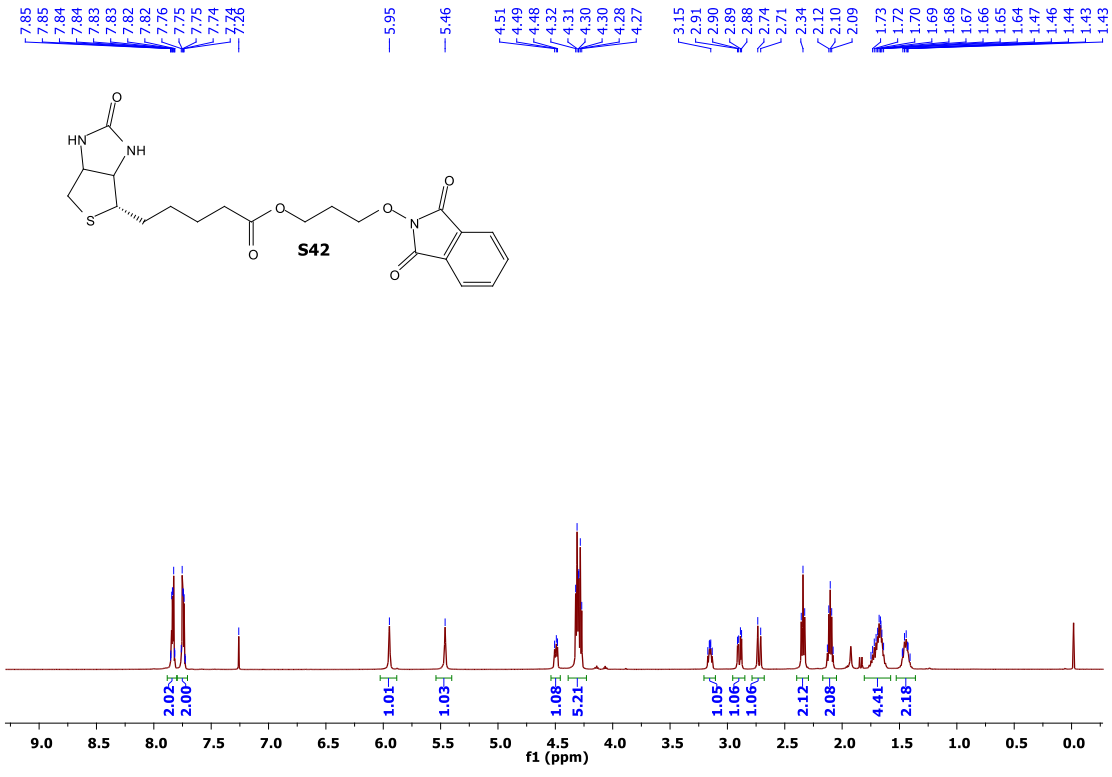

Figure S80. ^{1}H-NMR spectrum of compound **S42.**

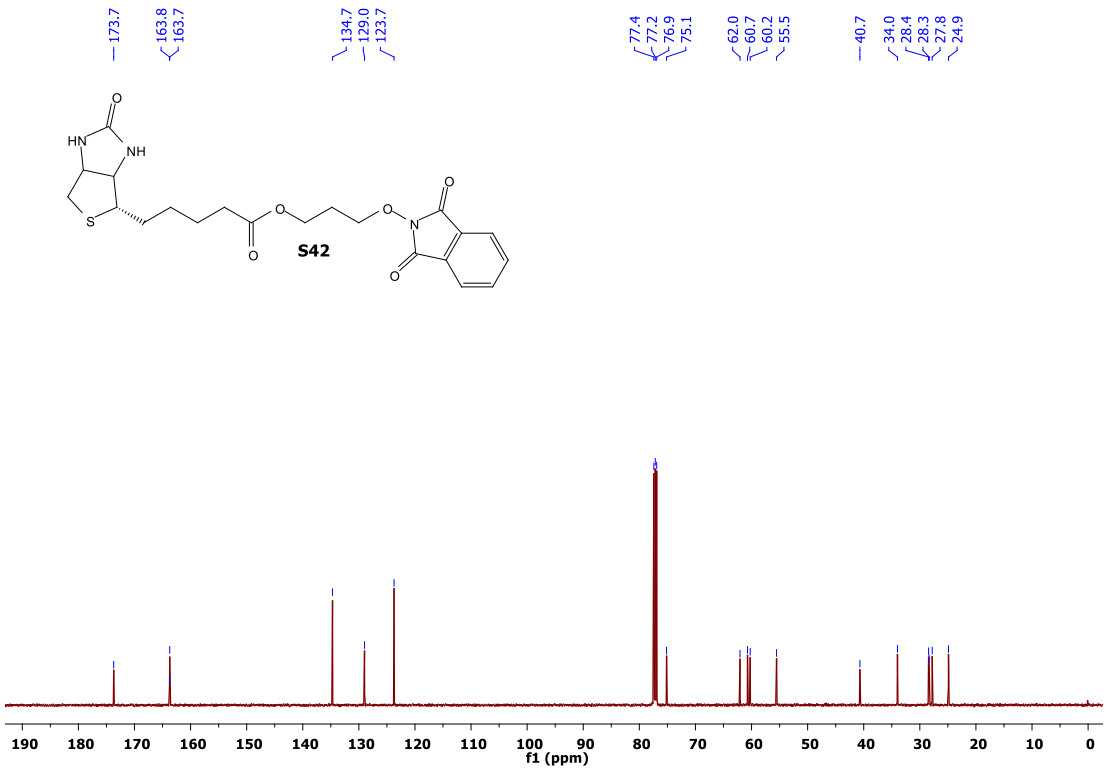

Figure S81. ^{13}C-NMR spectrum of compound **S42.**

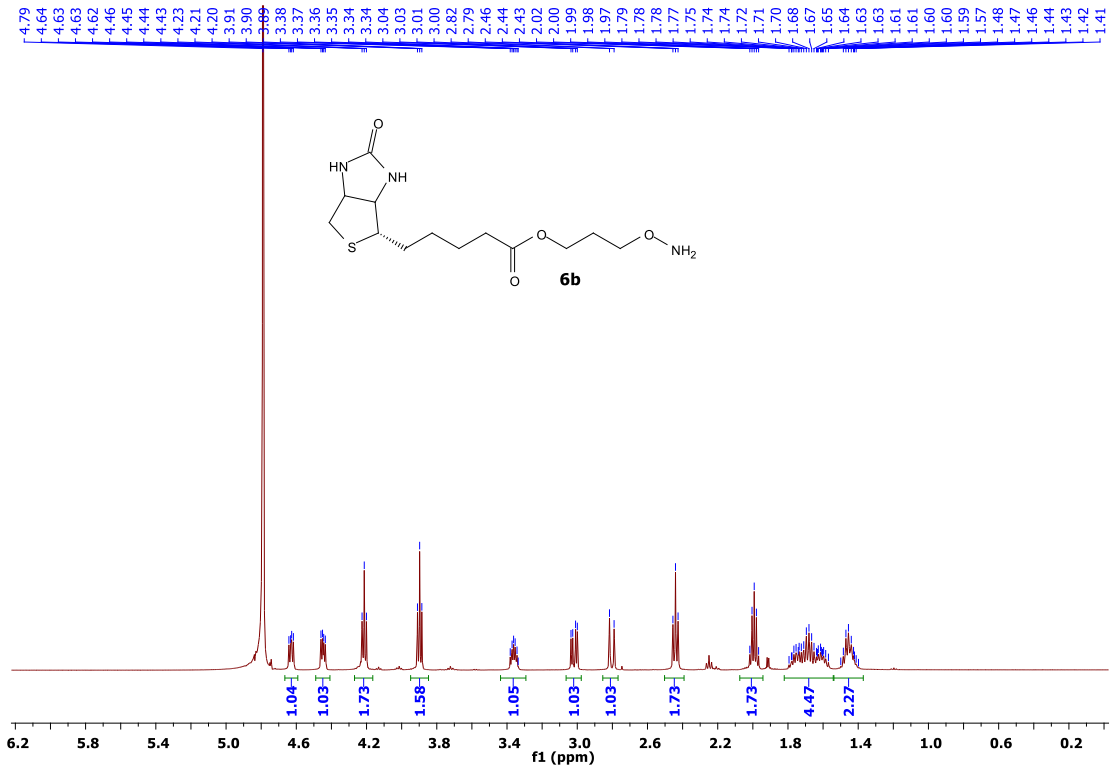

Figure S82. ^{1}H-NMR spectrum of compound **6b.**

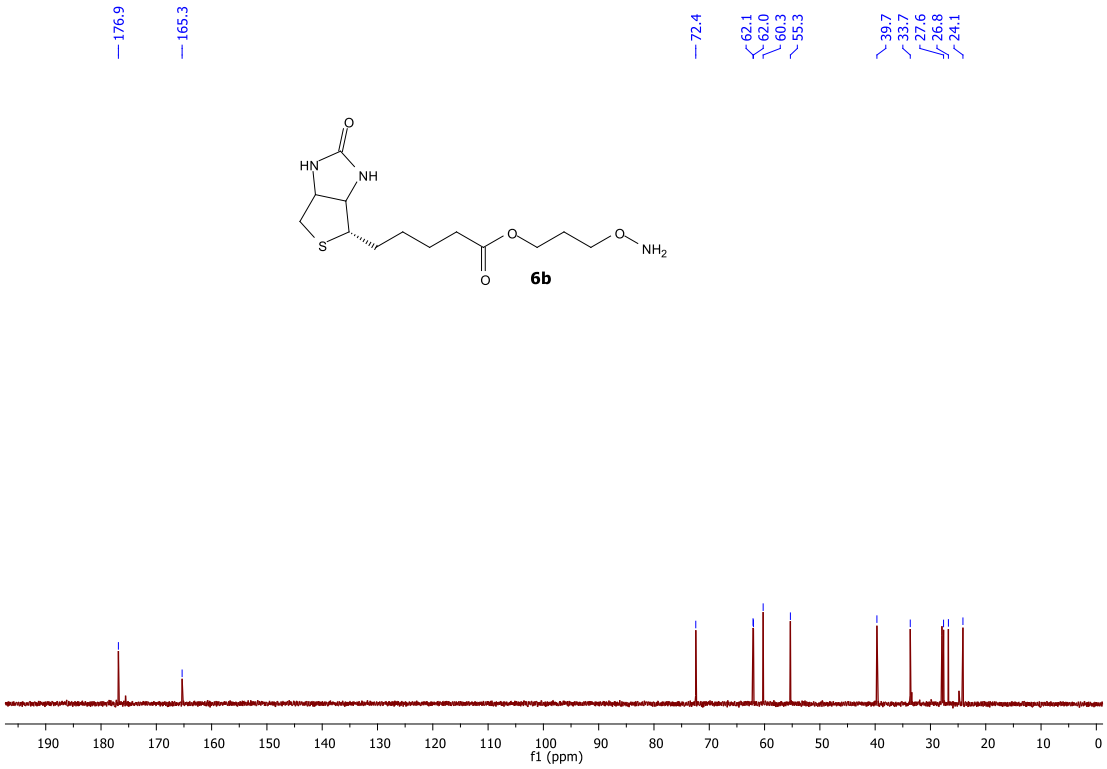

Figure S83. ^{13}C-NMR spectrum of compound **6b.**

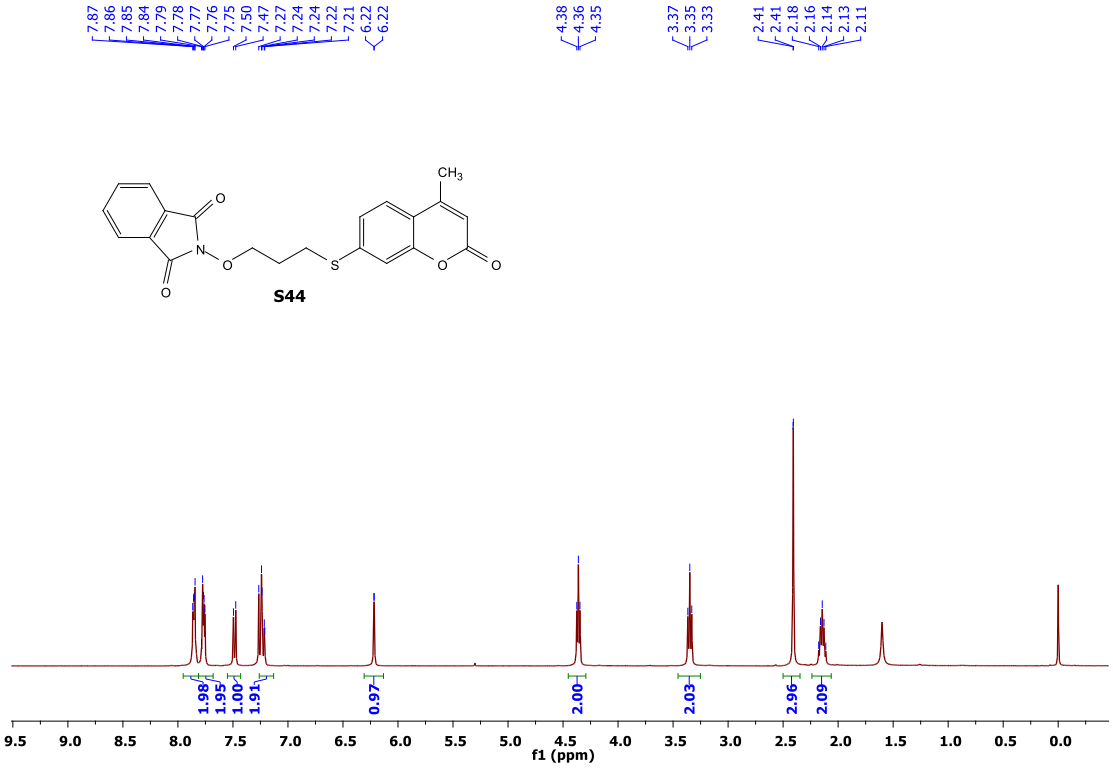

Figure S84. ^{1}H-NMR spectrum of compound **S44.**

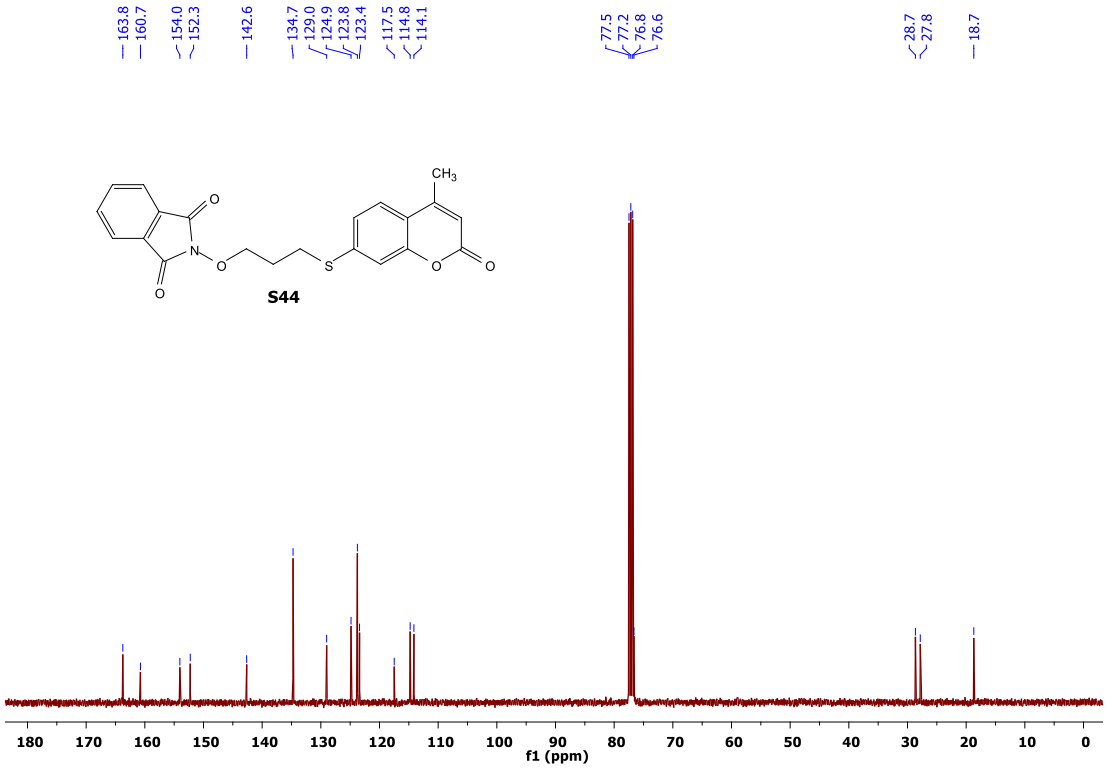

Figure S85. ^{13}C-NMR spectrum of compound **S44.**

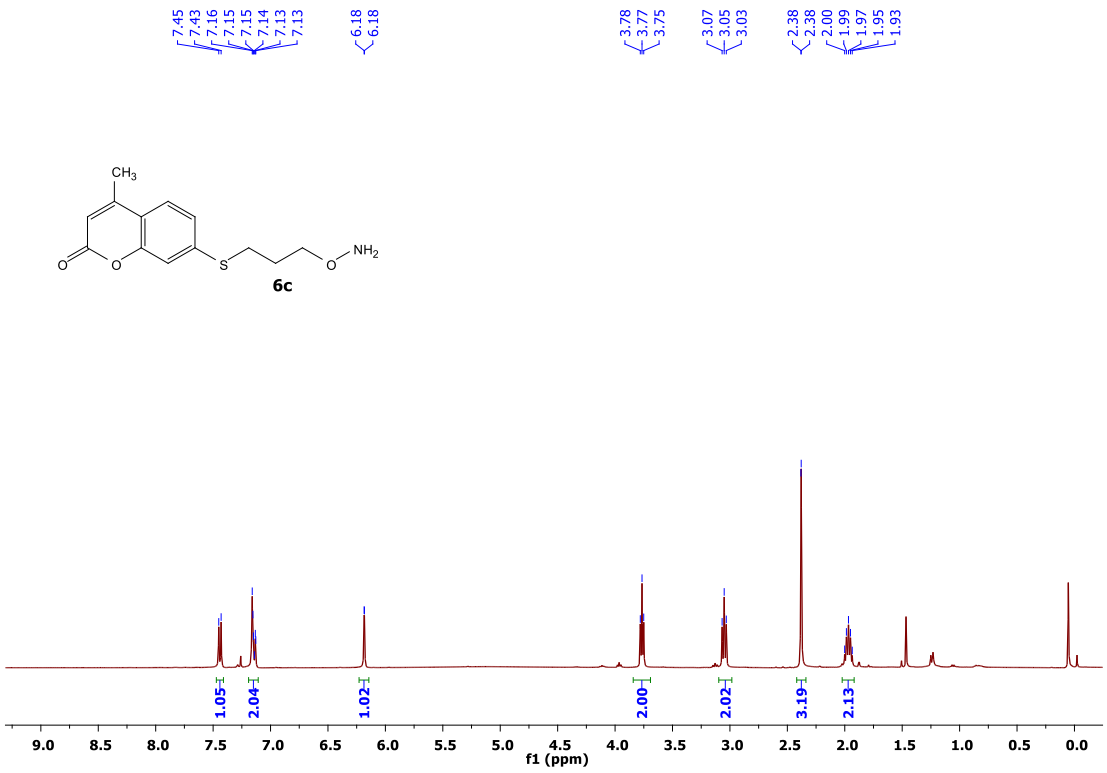

Figure S86. ^{1}H-NMR spectrum of compound **6c.**

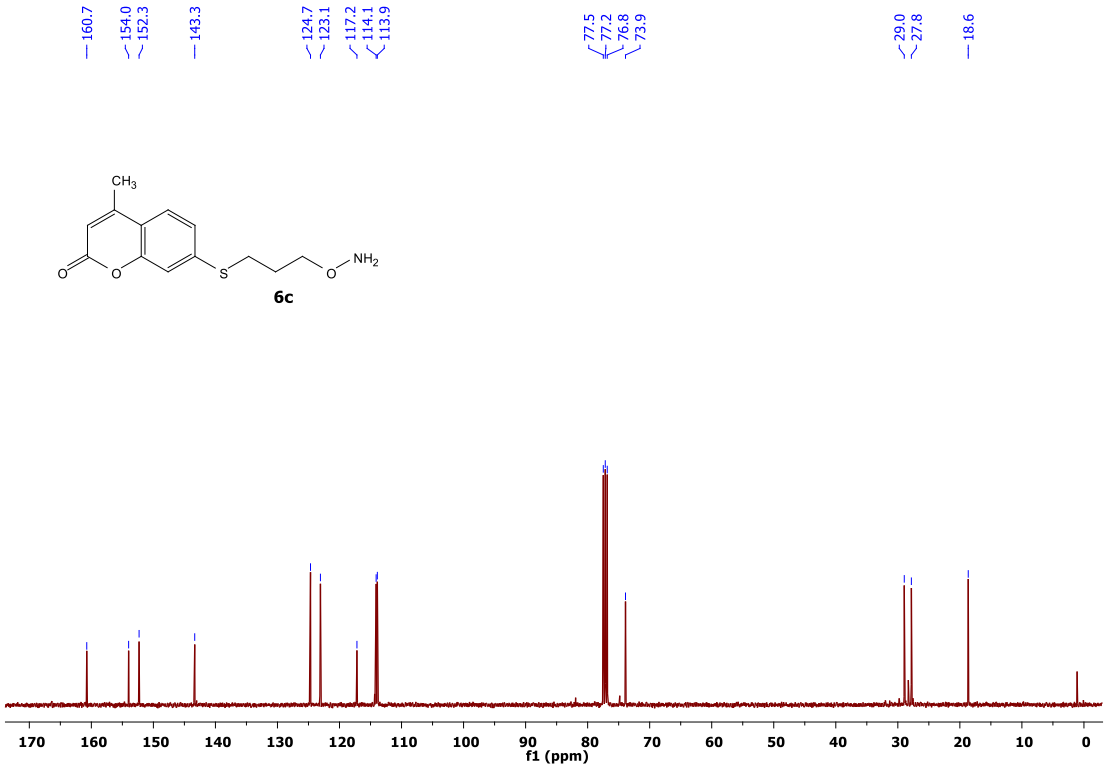

Figure S87. ^{13}C-NMR spectrum of compound **6c.**

7. Additional discussion

[1] Reaction of proteins with higher concentration of alkylating reagent 2a.

The reactions were performed with a higher concentration of electrophile (**2a**, 1000-5000 equivalents) with different proteins. In the case of α-lactalbumin and myoglobin, we noted ~5% conversion with 5000 equivalents of alkylating reagent **2a**. For α-lactalbumin, E1 is labeled preferentially in contrast to H107 by LDM reagent **2c**. Further, E18 is labeled for myoglobin (H116 with **2c**), validating the reagent's promiscuity. These observations are also supported by the reaction between ubiquitin and reagent **2c** that renders the modification of glutamic acid, aspartic acid, and histidine (entry 4, Table S7).

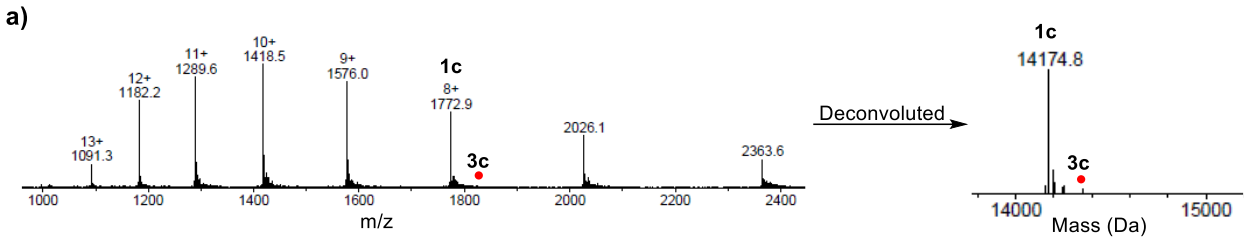

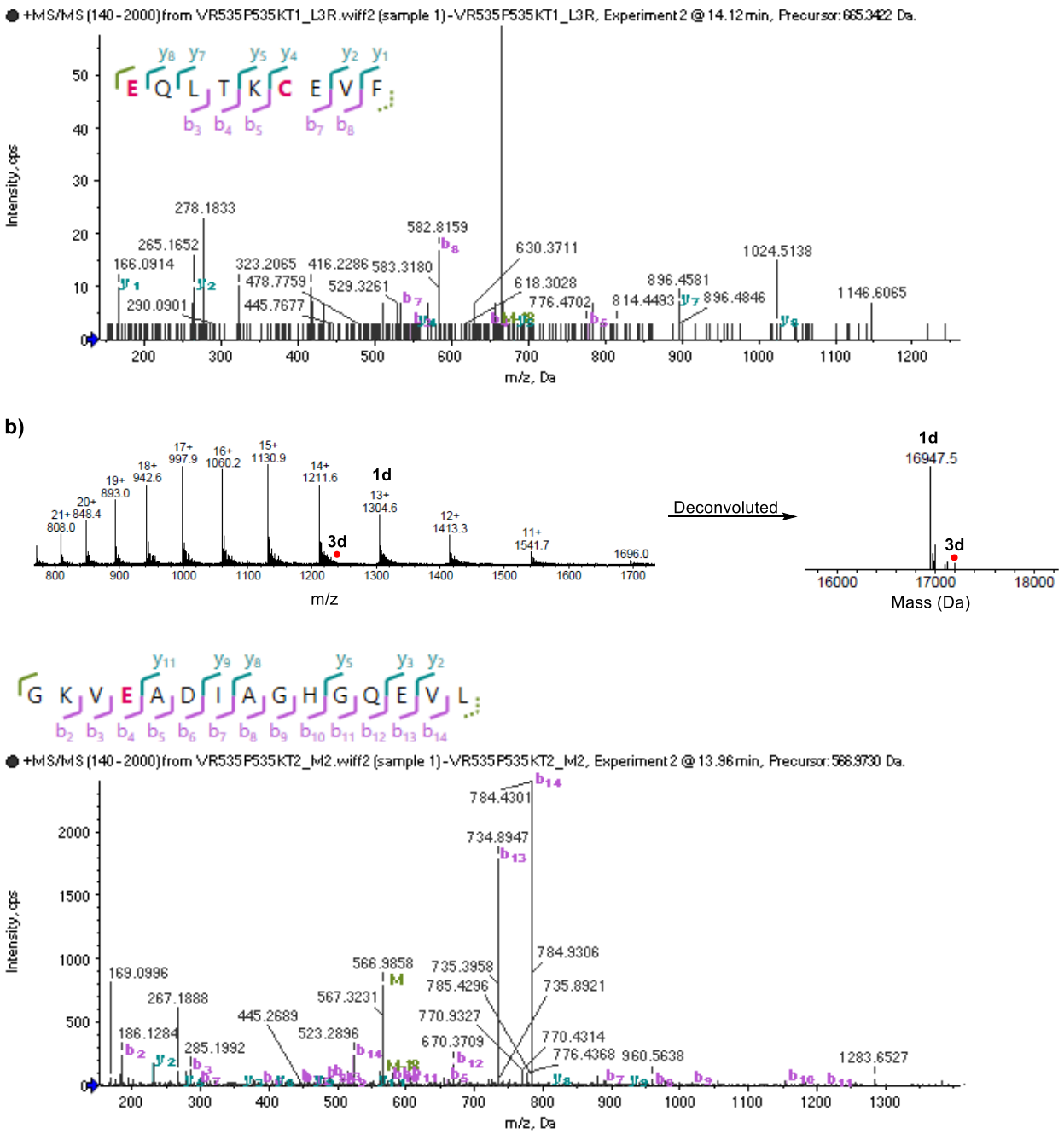

Figure S88. (a) α-Lactalbumin labeling with **2a**: MS and MS-MS. (b) Myoglobin labeling with **2a**: MS and MS-MS.

[2] Reaction of ubiquitin (1a) with LDM reagent (2c)

Table S5. Effect of LDM reagent concentration on protein bioconjugation.

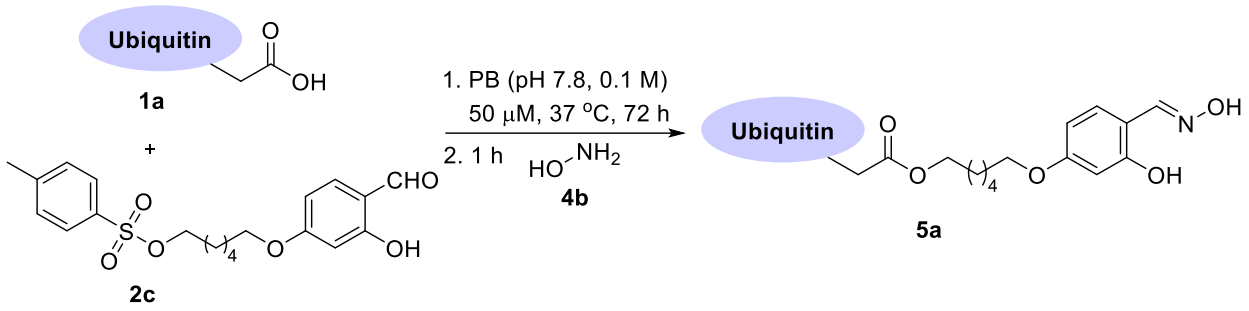

S. No.	Equivalents (2c)	% Conversion[a]		Site(s) of modification
		Mono-labeled	Bis-labeled	
1	25	37[b]	0	D32
2	50	46	0	D32
3	100	43	***6***	D32, ***D58***
4	250	35	***5***	D32, ***D58***
5	500	25	0	D32
6	1000	17	0	D32

[a]% Conversion was determined by ESI-MS. [b]In another trial; 42% conversion was observed under these conditions.

We treated ubiquitin with higher equivalents of LDM reagent (**2c**, Table S5). The experiments in this series were performed from a common stock solution of protein and reagent. At first, 25 equivalents of reagent **2c** resulted in 37% labeling of D32. The increase in relative stoichiometry (50 equivalents) led to increased conversions (46%) while retaining the singles-site D32 labeling. A further increase to 100 and 200 equivalents resulted in 5-6% bis-labeled product along with the mono-labeled bioconjugates (43% and 35%, respectively). In both cases, D58 was labeled in addition to D32. Interestingly, 500 and 1000 equivalents of reagent led to a considerable drop in conversions (25% and 17%, respectively) while regaining the single-site selectivity.

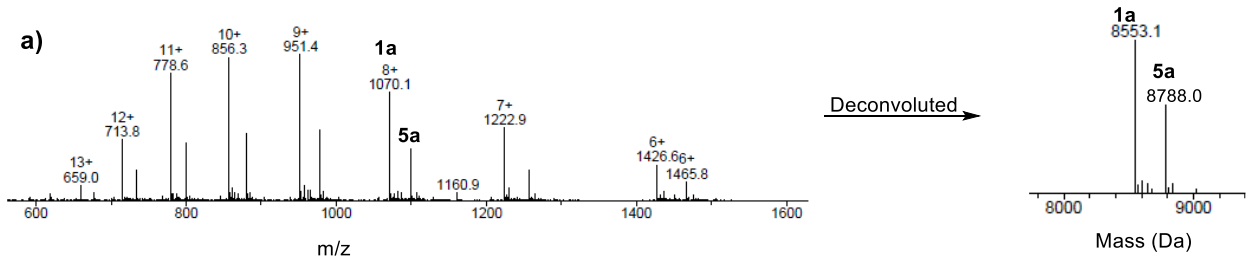

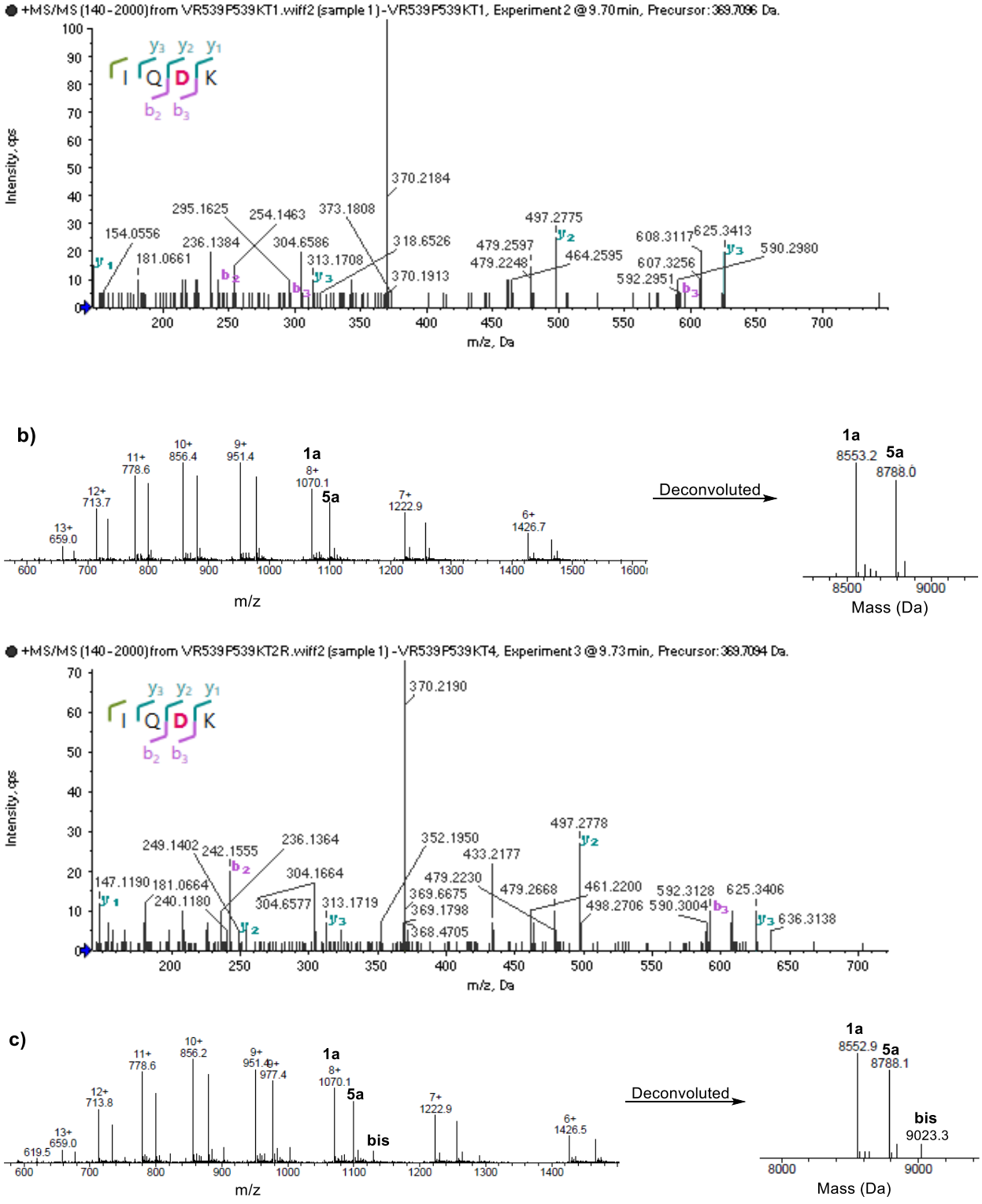
+MS/MS (140 - 2000) from VR539P539KT1.wiff2 (sample 1) - VR539P539KT1, Experiment 2 @ 9.70 min, Precursor: 369.7096 Da.
Intensity, cps
m/z, Da
370.2184
295.1625
254.1463
373.1808
497.2775
154.0556
236.1384
304.6586
318.6526
479.2597
608.3117
625.3413
590.2980
181.0661
313.1708
479.2248
464.2595
607.3256
370.1913
592.2951
b)
m/z
1a
5a
Deconvoluted
8553.2
8788.0
Mass (Da)
+MS/MS (140 - 2000) from VR539P539KT2R.wiff2 (sample 1) - VR539P539KT4, Experiment 3 @ 9.73 min, Precursor: 369.7094 Da.
Intensity, cps
m/z, Da
370.2190
497.2778
249.1402
242.1555
236.1364
352.1950
433.2177
304.1664
147.1190
181.0664
240.1180
304.6577
313.1719
479.2230
479.2668
461.2200
592.3128
625.3406
369.6675
369.1798
498.2706
590.3004
636.3138
368.4705
c)
m/z
1a
5a
bis
Deconvoluted
8552.9
8788.1
9023.3
Mass (Da)

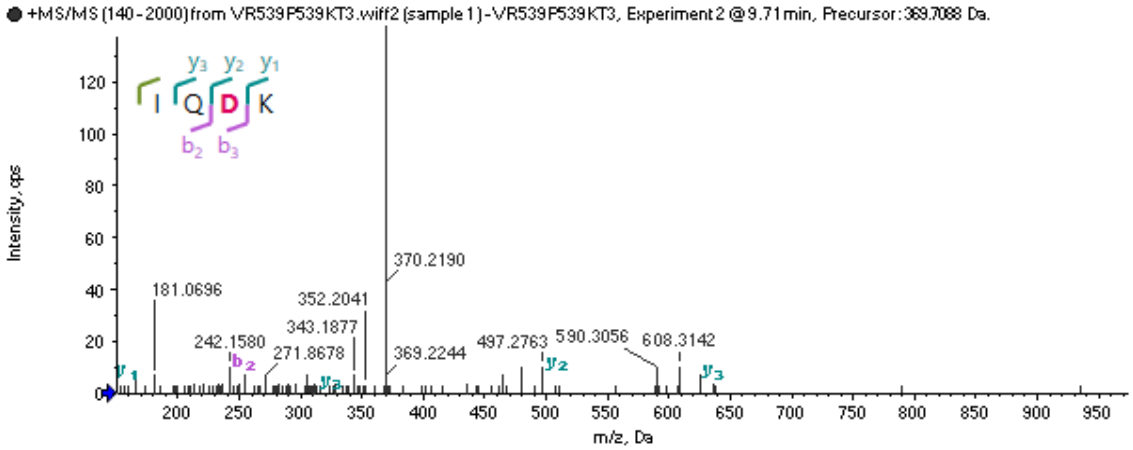
+MS/MS (140 - 2000) from VR539P539KT3.wiff2 (sample 1) - VR539P539KT3, Experiment 2 @ 9.71 min, Precursor: 369.7088 Da.
I Q D K
Intensity, cps
m/z, Da
370.2190
181.0696
352.2041
343.1877
242.1580
271.8678
369.2244
497.2763
590.3056
608.3142

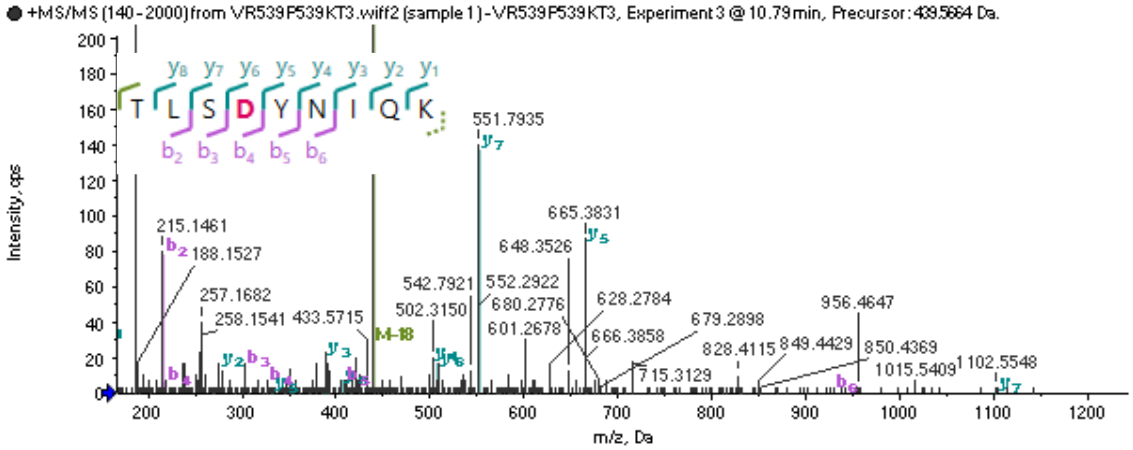
+MS/MS (140 - 2000) from VR539P539KT3.wiff2 (sample 1) - VR539P539KT3, Experiment 3 @ 10.79 min, Precursor: 439.5664 Da.
T L S D Y N I Q K
Intensity, cps
m/z, Da
551.7935
665.3831
648.3526
215.1461
188.1527
542.7921
552.2922
257.1682
258.1541
433.5715
502.3150
680.2776
628.2784
601.2678
679.2898
956.4647
666.3858
828.4115
849.4429
850.4369
715.3129
1015.5409
1102.5548

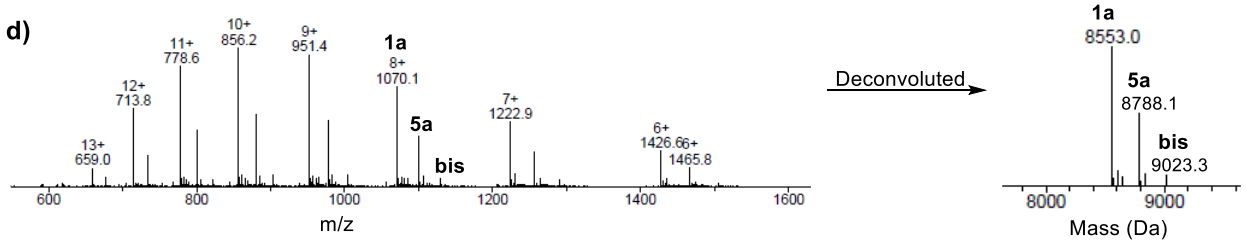
d)
m/z
13+ 659.0
12+ 713.8
11+ 778.6
10+ 856.2
9+ 951.4
1a
8+ 1070.1
5a
bis
7+ 1222.9
6+ 1426.66+ 1465.8
Deconvoluted
1a 8553.0
5a 8788.1
bis 9023.3
Mass (Da)

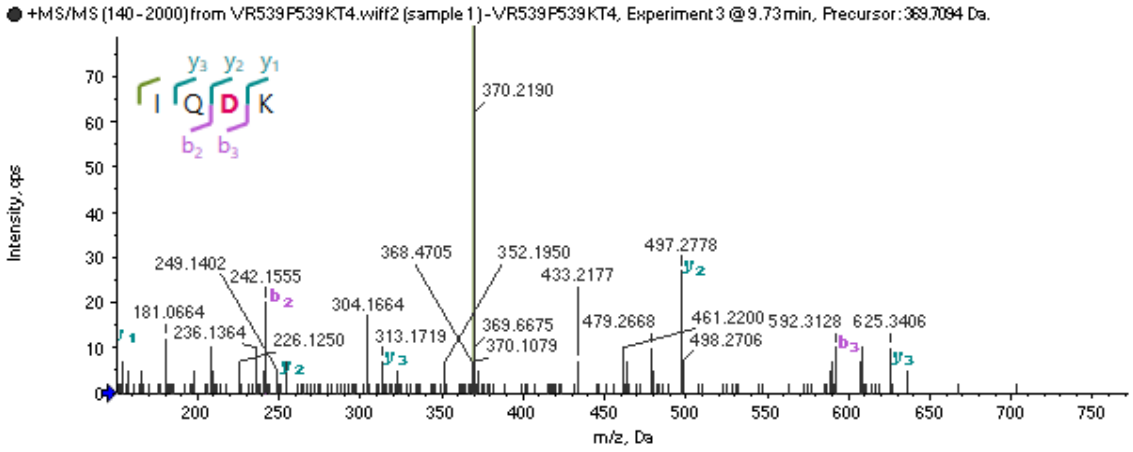
+MS/MS (140 - 2000) from VR539P539KT4.wiff2 (sample 1) - VR539P539KT4, Experiment 3 @ 9.73 min, Precursor: 369.7094 Da.
Intensity, cps
m/z, Da
I Q D K
370.2190
249.1402
242.1555
368.4705
352.1950
433.2177
497.2778
181.0664
236.1364
226.1250
304.1664
313.1719
369.6675
370.1079
479.2668
461.2200
498.2706
592.3128
625.3406

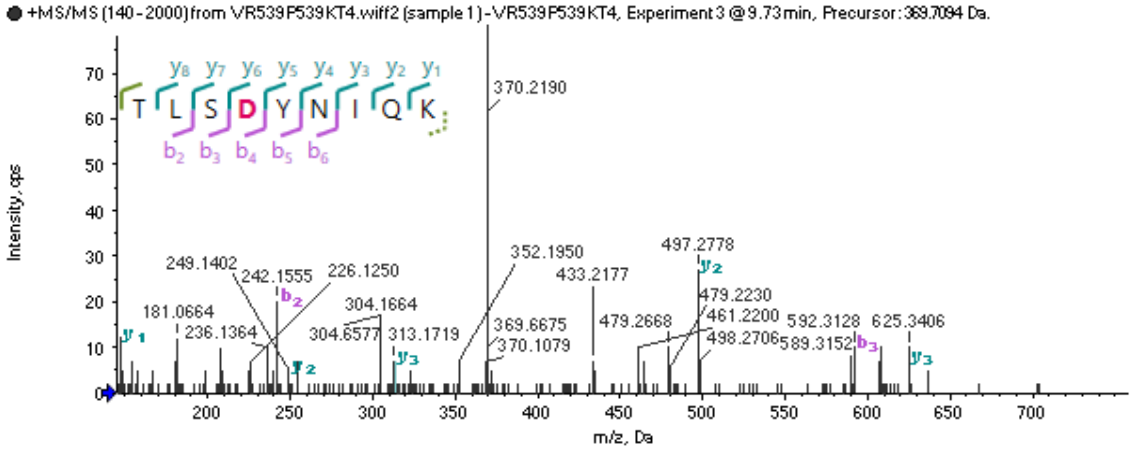
+MS/MS (140 - 2000) from VR539P539KT4.wiff2 (sample 1) - VR539P539KT4, Experiment 3 @ 9.73 min, Precursor: 369.7094 Da.
Intensity, cps
m/z, Da
T L S D Y N I Q K
370.2190
249.1402
242.1555
226.1250
352.1950
433.2177
497.2778
479.2230
181.0664
236.1364
304.1664
304.6577
313.1719
369.6675
370.1079
479.2668
461.2200
498.2706
589.3152
592.3128
625.3406

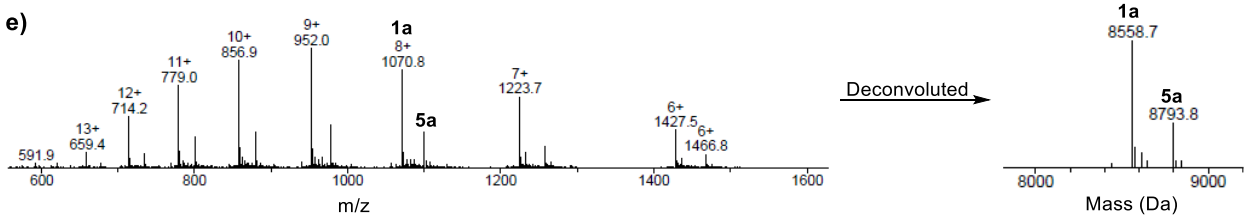
e)
m/z
591.9
659.4
714.2
779.0
856.9
952.0
1070.8
1223.7
1427.5
1466.8
1a
5a
Deconvoluted
8558.7
8793.8
Mass (Da)

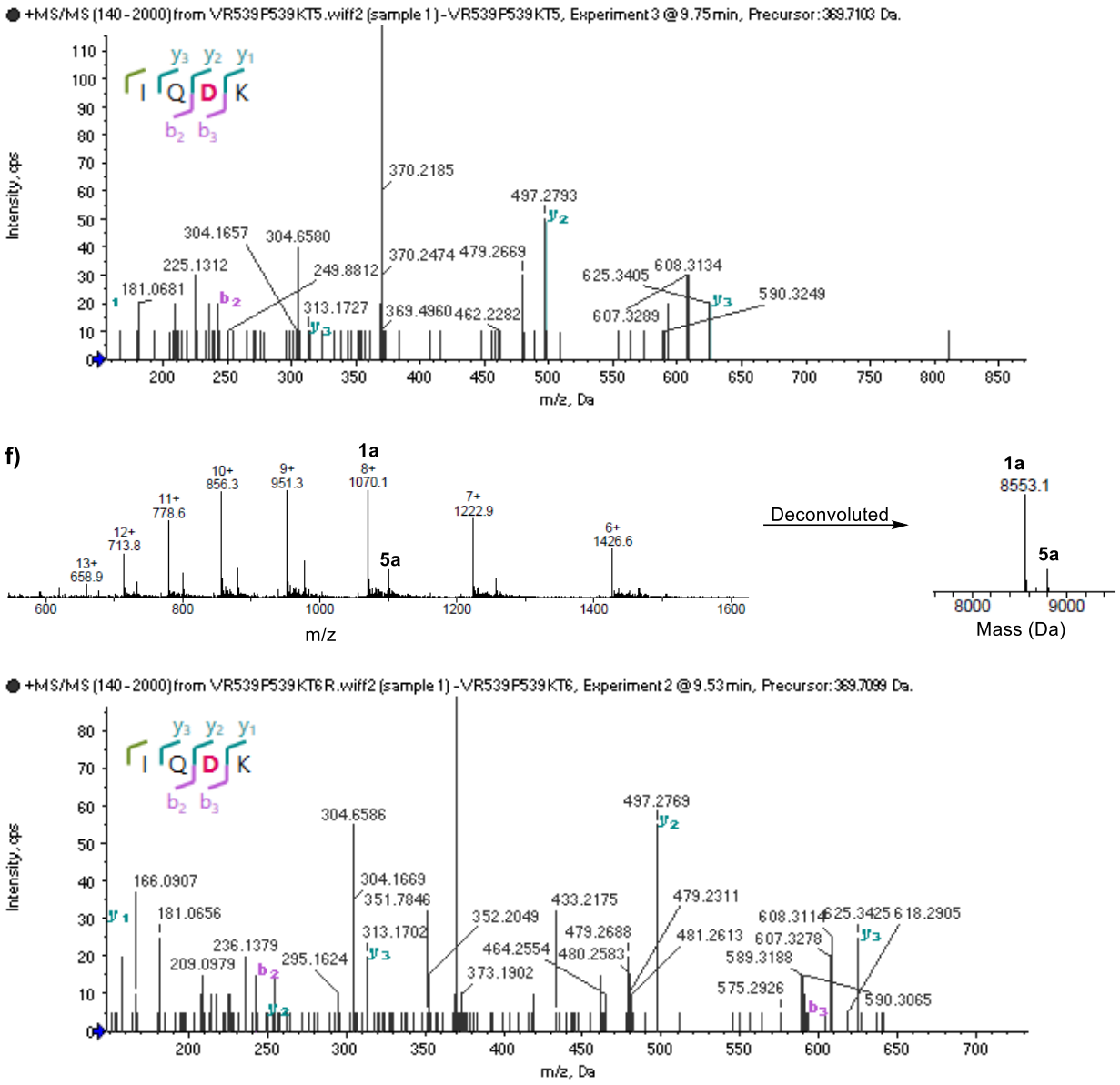

Figure S89. Reaction of ubiquitin with LDM reagent **2c** (a) 25 equivalents; (b) 50 equivalents; (c) 100 equivalents; (d) 250 equivalents; (e) 500 equivalents; (f) 1000 equivalents.

[3] Effect of protein concentration and pH

The concentration has a role to play in the regulation of reactivity and selectivity. The ubiquitin at 5 µM results in 18% D32-labeled bioconjugate (entry 1, Table S6). The increase of concentration to 50 µM (entries 2-4, Table S6) results in increased conversions without compromise in chemoselectivity and site-selectivity. However, a further increase in concentration (75 and 100 µM) shows 4-8% bis-labeling (D58) along with mono-labeling (D32).

Table S6. Effect of protein concentration on bioconjugation.

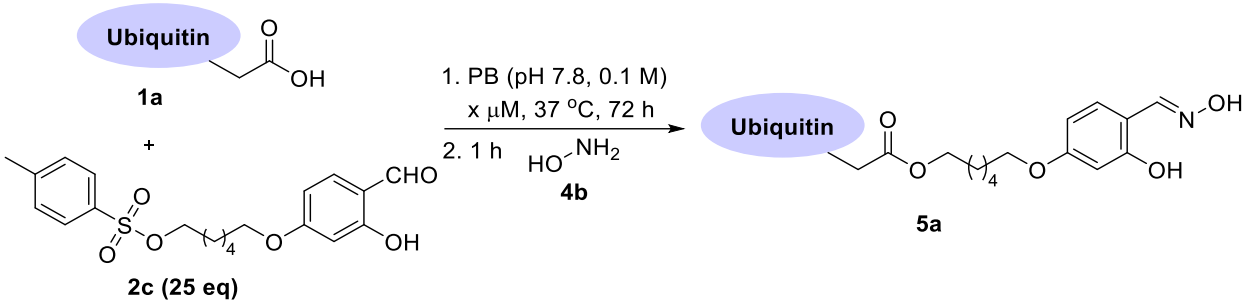

S. No.	Concentration (x μM)	% Conversion[a]		Site(s) of modification
		Mono-labeled	Bis-labeled	
1	5	18	0	D32
2	10	20	0	D32
3	20	28	0	D32
4	50	37[b]	0	D32
5	75	38	8	D32, ***D58***
6	100	30	4	D32, ***D58***

[a] % Conversion was determined by ESI-MS. [b]In another trial, 42% conversion was observed under these conditions.

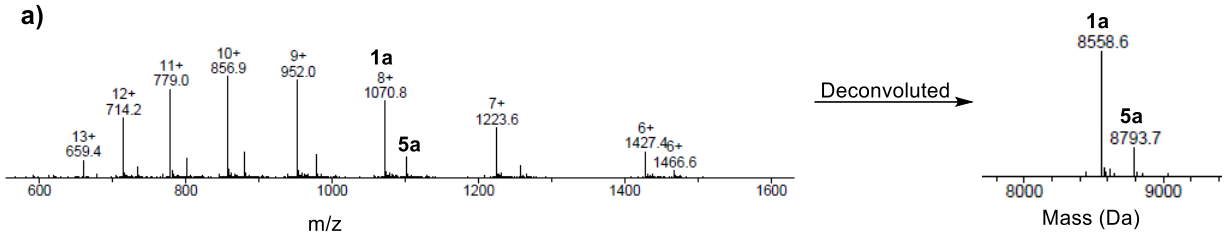

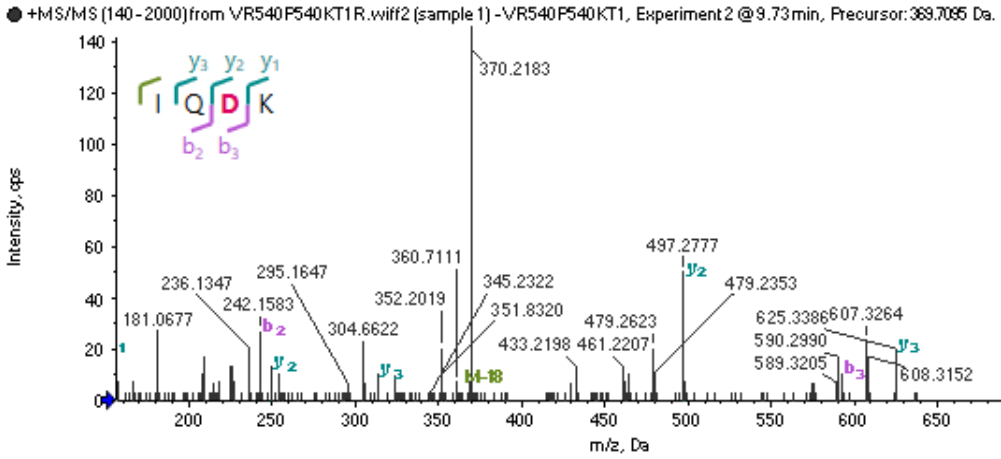

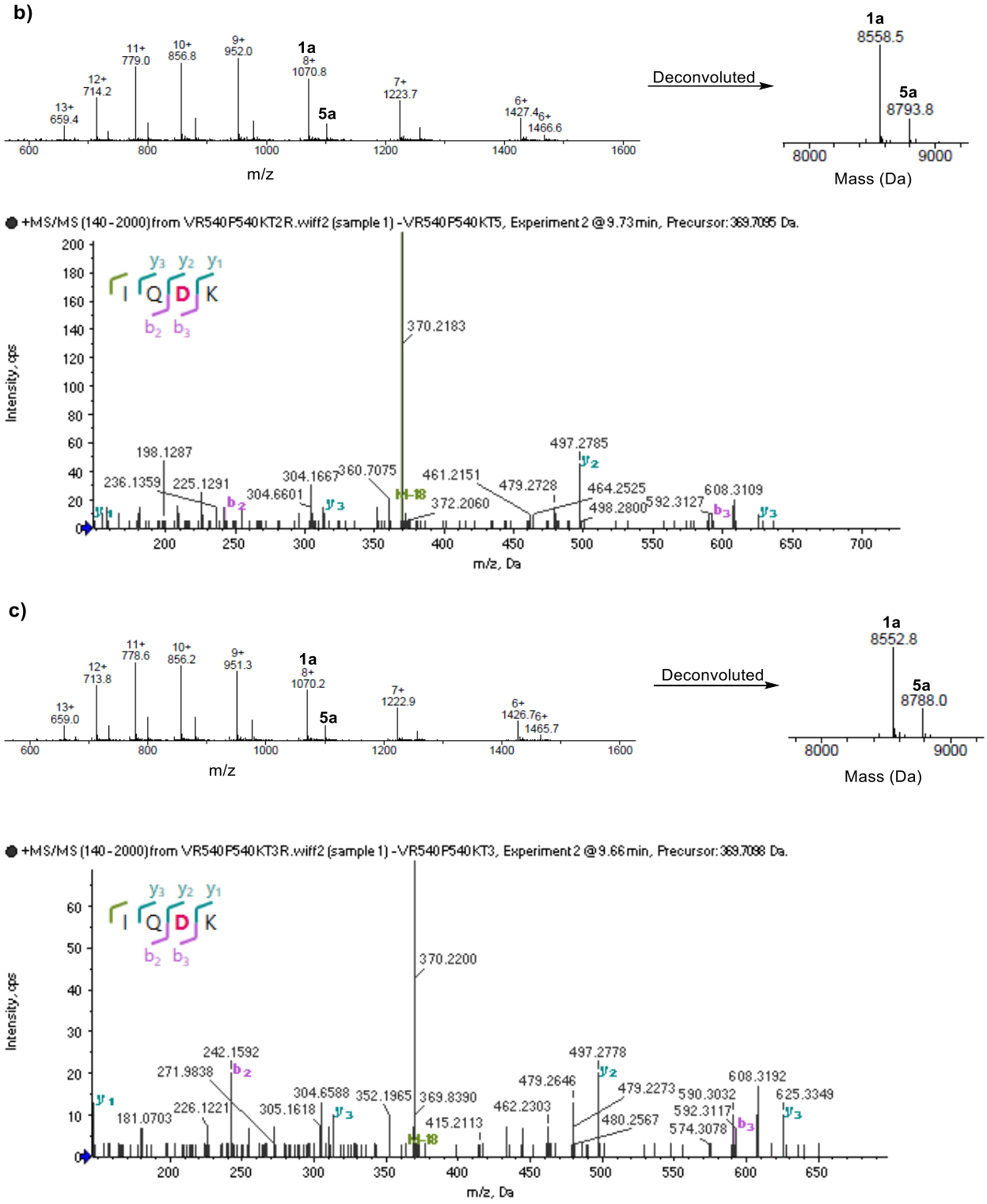
b)
1a
8558.5
5a
8793.8
Deconvoluted
Mass (Da)
m/z
+MS/MS (140 - 2000) from VR540P540KT2R.wiff2 (sample 1) - VR540P540KT5, Experiment 2 @ 9.73 min, Precursor: 369.7085 Da.
Intensity, cps
m/z, Da
c)
1a
8552.8
5a
8788.0
Deconvoluted
Mass (Da)
m/z
+MS/MS (140 - 2000) from VR540P540KT3R.wiff2 (sample 1) - VR540P540KT3, Experiment 2 @ 9.66 min, Precursor: 369.7088 Da.
Intensity, cps
m/z, Da

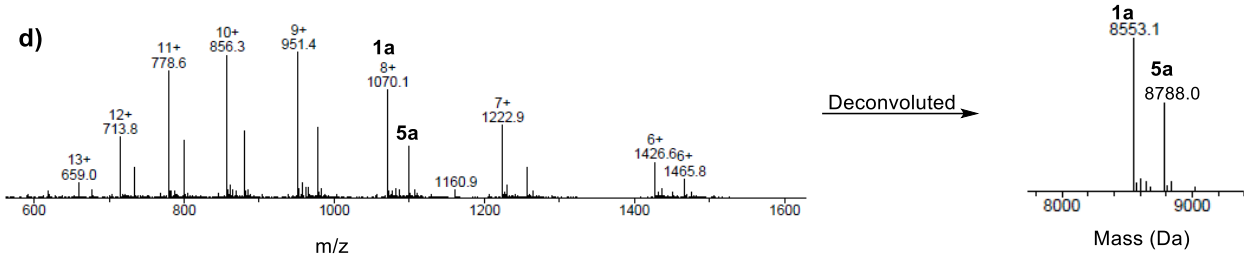
d)
11+
778.6
10+
856.3
9+
951.4
1a
8+
1070.1
12+
713.8
5a
7+
1222.9
13+
659.0
6+
1426.66+
1465.8
1160.9
600
800
1000
1200
1400
1600
m/z
Deconvoluted
1a
8553.1
5a
8788.0
8000
9000
Mass (Da)

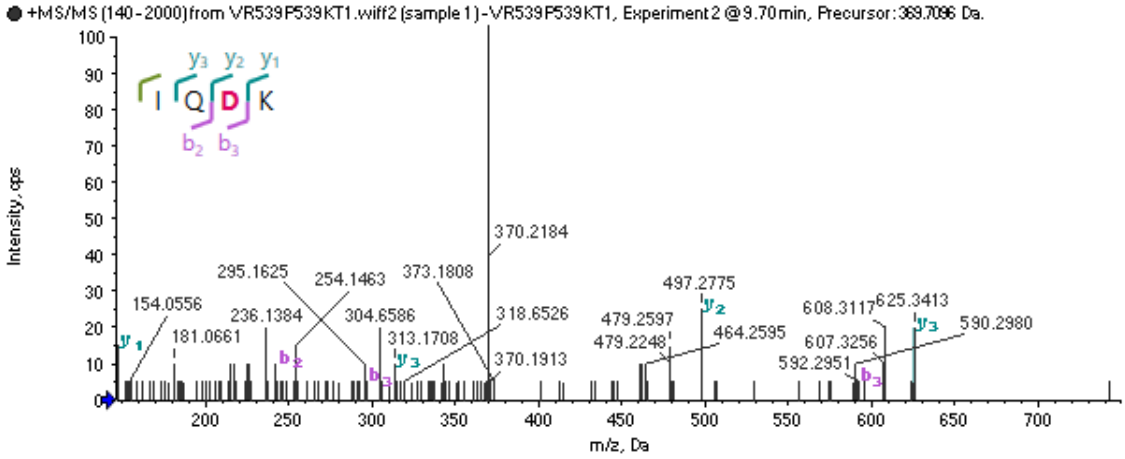
+MS/MS (140 - 2000) from VR539P539KT1.wiff2 (sample 1) - VR539P539KT1, Experiment 2 @ 9.70 min, Precursor: 369.7096 Da.
I Q D K
Intensity, cps
370.2184
295.1625
254.1463
373.1808
497.2775
154.0556
236.1384
304.6586
318.6526
608.3117
625.3413
181.0661
313.1708
479.2597
590.2980
479.2248
464.2595
607.3256
370.1913
592.2951
m/z, Da

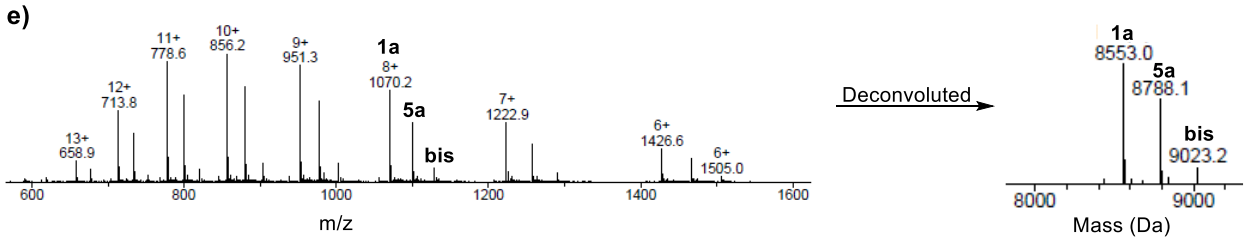
e)
11+
778.6
10+
856.2
9+
951.3
1a
8+
1070.2
12+
713.8
5a
7+
1222.9
13+
658.9
bis
6+
1426.6
6+
1505.0
600
800
1000
1200
1400
1600
m/z
Deconvoluted
1a
8553.0
5a
8788.1
bis
9023.2
8000
9000
Mass (Da)

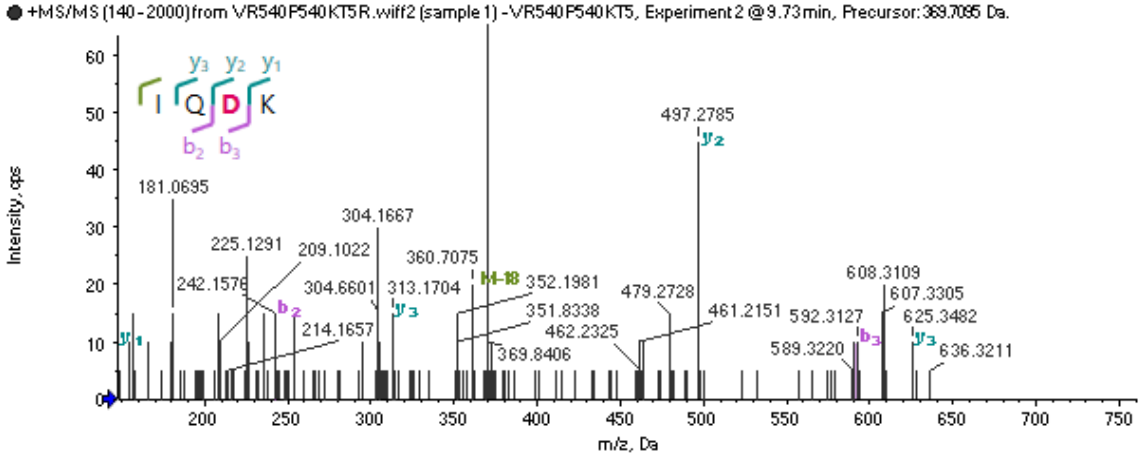
+MS/MS (140 - 2000) from VR540P540KT5R.wiff2 (sample 1) - VR540P540KT5, Experiment 2 @ 9.73 min, Precursor: 369.7095 Da.
I Q D K
Intensity, cps
497.2785
181.0695
304.1667
225.1291
209.1022
360.7075
M-18
352.1981
242.1576
304.6601
313.1704
479.2728
608.3109
607.3305
351.8338
461.2151
592.3127
625.3482
214.1657
462.2325
589.3220
636.3211
369.8406
m/z, Da

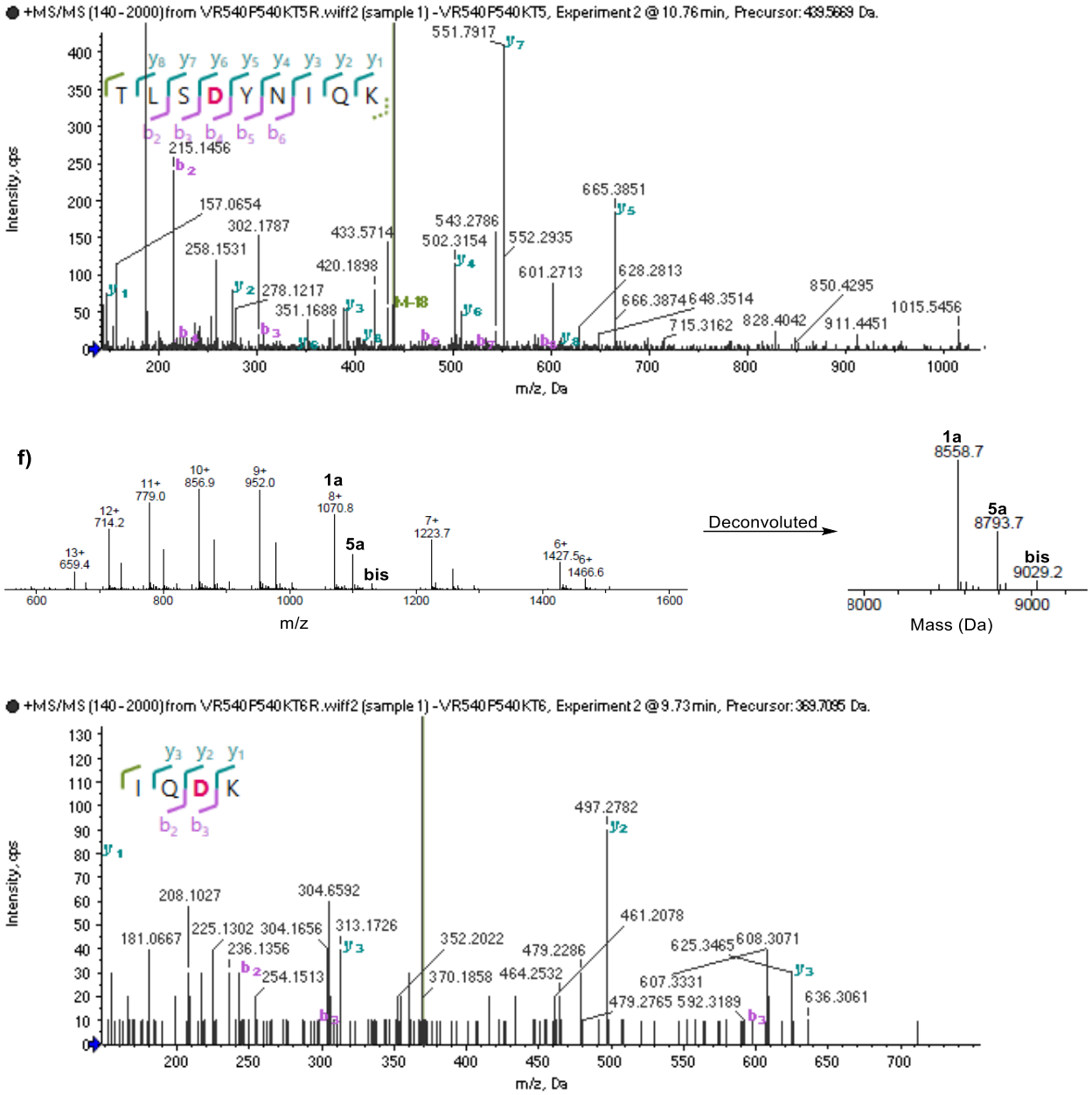

Figure S90. Reaction of ubiquitin with concentration (a) 5 μM; (b) 10 μM; (c) 20 μM; (d) 50 μM; (e) 75 μM; (f) 100 μM.

Next, we investigated the effect of the aqueous buffer's pH (Table S7). While the reaction ceased altogether at pH 6, 10% single-site labeled ubiquitin was observed at pH 7. Further increase of pH to 7.8 allowed the reaction to deliver 37% D32-labeled ubiquitin. Interestingly, the promiscuity of electrophile overpowers at pH 9 and results in the labeling of D32, D58, E64, and H68.

Table S7. Effect of reaction medium's pH on bioconjugation

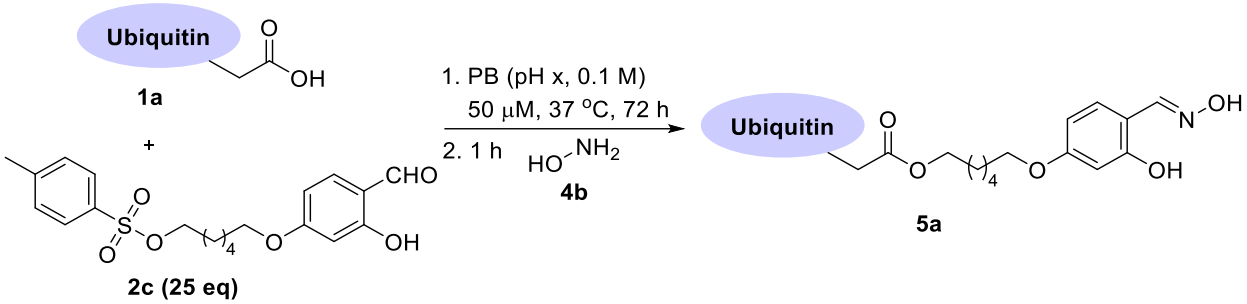

S. No.	pH	% Conversion[a]	Site of modification
1	6.0	0	-
2	7.0	10 mono-labeled	D32
3	7.8	37[b] mono-labeled	D32
4	9.0	39 mono-, 20 bis-, 8 tris-, 5 tetra-labeled	D32, D58, E64, H68

[a] % Conversion was determined by ESI-MS. [b]In another trial; 42% conversion was observed under these conditions.

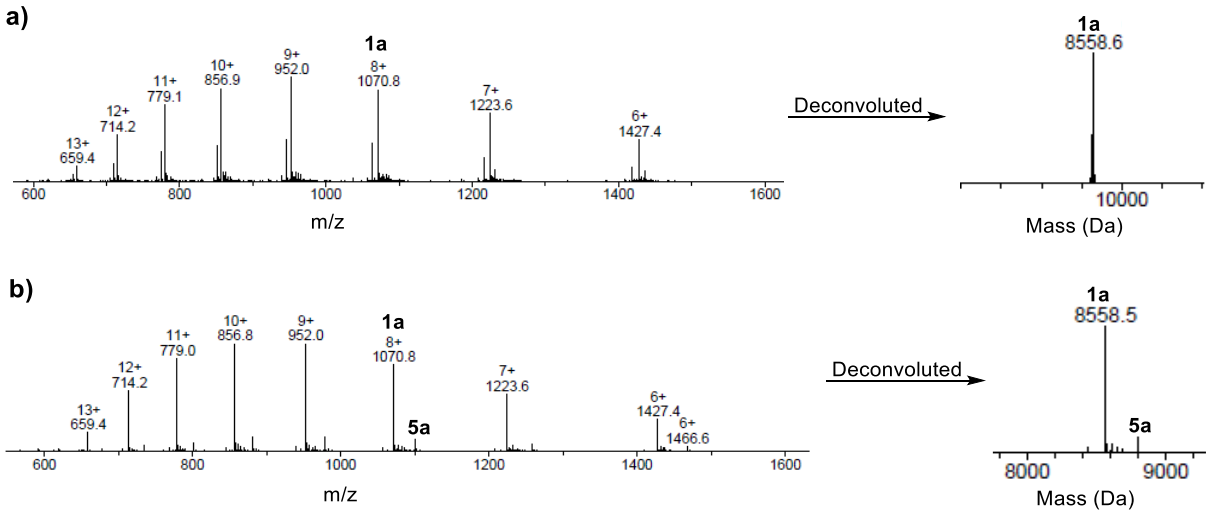

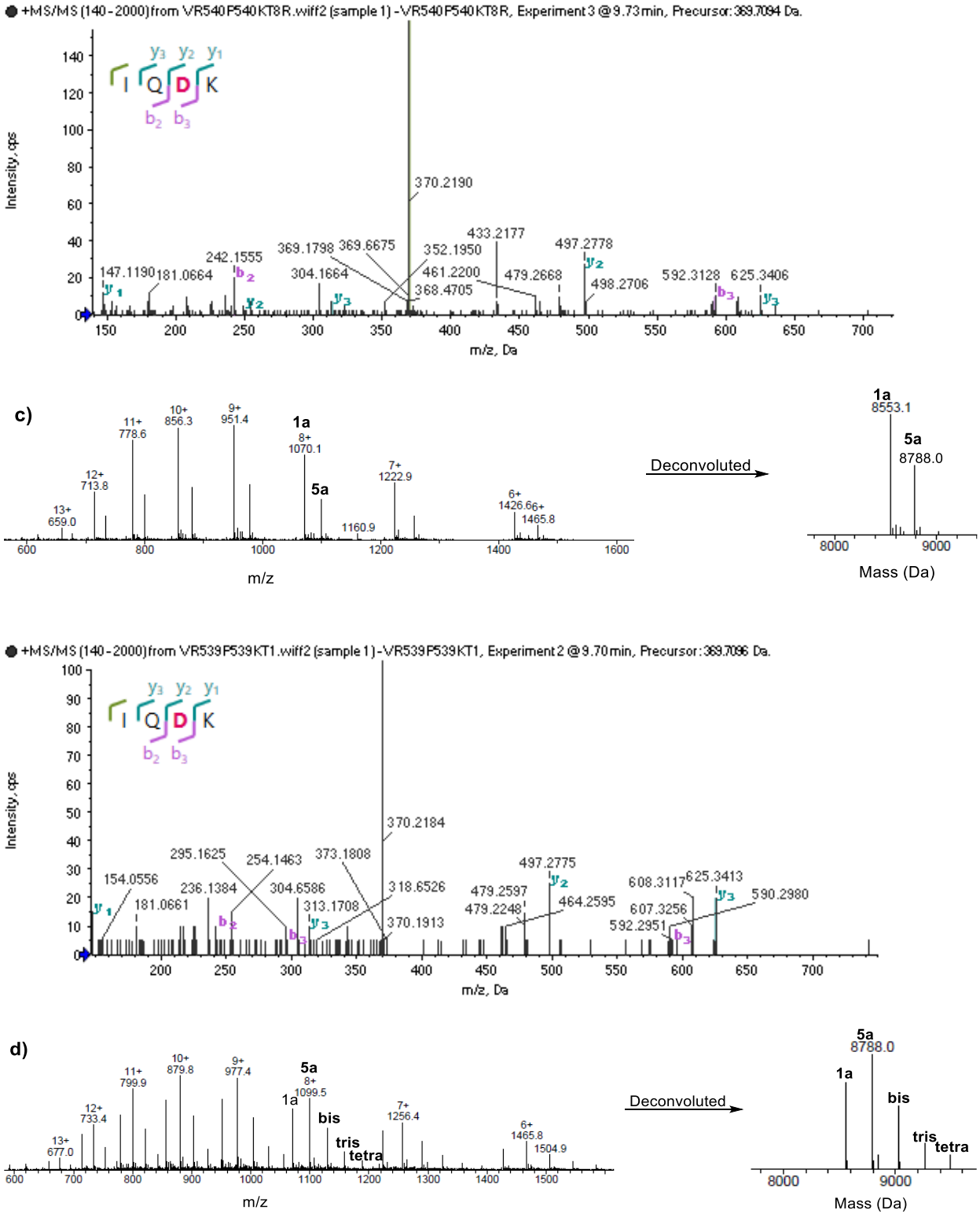
+MS/MS (140 - 2000) from VR540P540KT8R.wiff2 (sample 1) - VR540P540KT8R, Experiment 3 @ 9.73 min, Precursor: 369.7094 Da.
Intensity, cps
m/z, Da
370.2190
433.2177
497.2778
242.1555
369.1798
369.6675
352.1950
147.1190
181.0664
304.1664
461.2200
479.2668
498.2706
592.3128
625.3406
368.4705
c)
m/z
1a
8+
1070.1
5a
11+
778.6
10+
856.3
9+
951.4
12+
713.8
13+
659.0
7+
1222.9
6+
1426.6
1465.8
1160.9
Deconvoluted
1a
8553.1
5a
8788.0
Mass (Da)
+MS/MS (140 - 2000) from VR539P539KT1.wiff2 (sample 1) - VR539P539KT1, Experiment 2 @ 9.70 min, Precursor: 369.7096 Da.
Intensity, cps
m/z, Da
370.2184
295.1625
254.1463
373.1808
497.2775
154.0556
236.1384
304.6586
318.6526
479.2597
608.3117
625.3413
181.0661
313.1708
479.2248
464.2595
607.3256
590.2980
370.1913
592.2951
d)
m/z
5a
8+
1099.5
1a
11+
799.9
10+
879.8
9+
977.4
12+
733.4
13+
677.0
bis
tris
tetra
7+
1256.4
6+
1465.8
1504.9
Deconvoluted
5a
8788.0
1a
bis
tris
tetra
Mass (Da)

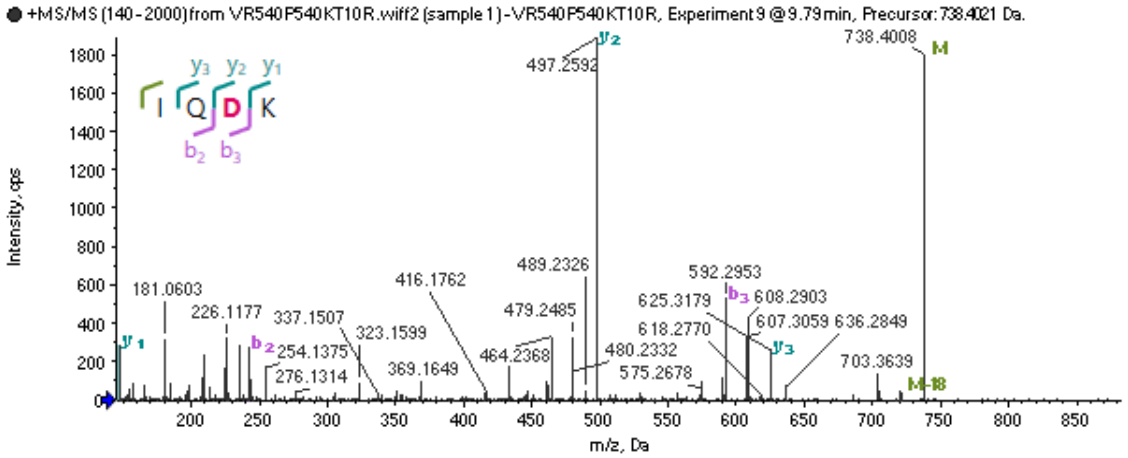
+MS/MS (140 - 2000) from VR540P540KT10R.wiff2 (sample 1) - VR540P540KT10R, Experiment 9 @ 9.79 min, Precursor: 738.4021 Da.
I Q D K
y3 y2 y1
b2 b3
Intensity, cps
m/z, Da
738.4008
M
497.2592
489.2326
592.2953
625.3179
608.2903
607.3059
636.2849
618.2770
703.3639
M-18
480.2332
575.2678
479.2485
464.2368
416.1762
369.1649
337.1507
323.1599
276.1314
254.1375
226.1177
181.0603

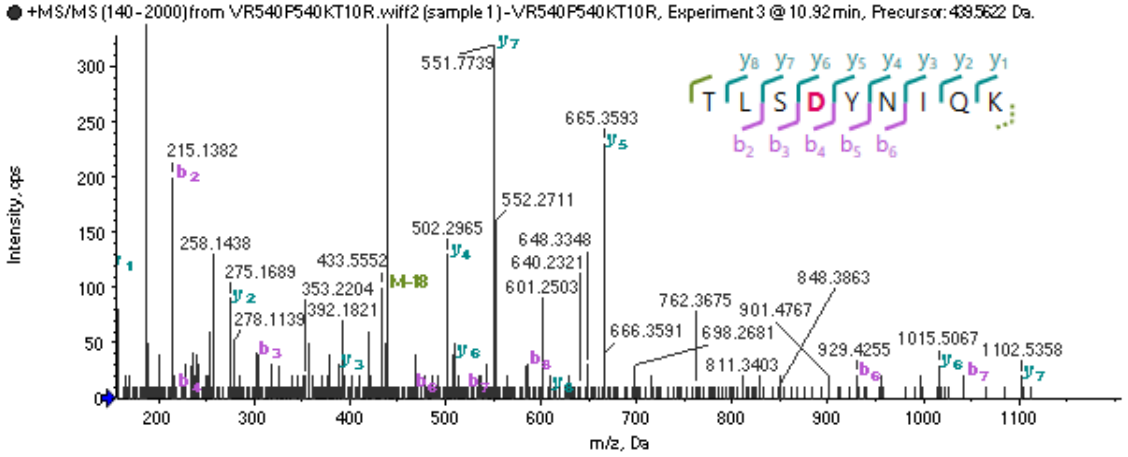
+MS/MS (140 - 2000) from VR540P540KT10R.wiff2 (sample 1) - VR540P540KT10R, Experiment 3 @ 10.92 min, Precursor: 439.5622 Da.
T L S D Y N I Q K
y8 y7 y6 y5 y4 y3 y2 y1
b2 b3 b4 b5 b6
Intensity, cps
m/z, Da
551.7739
665.3593
215.1382
552.2711
502.2965
648.3348
640.2321
601.2503
258.1438
275.1689
433.5552
M-18
353.2204
392.1821
278.1139
762.3675
848.3863
901.4767
666.3591
698.2681
811.3403
929.4255
1015.5067
1102.5358

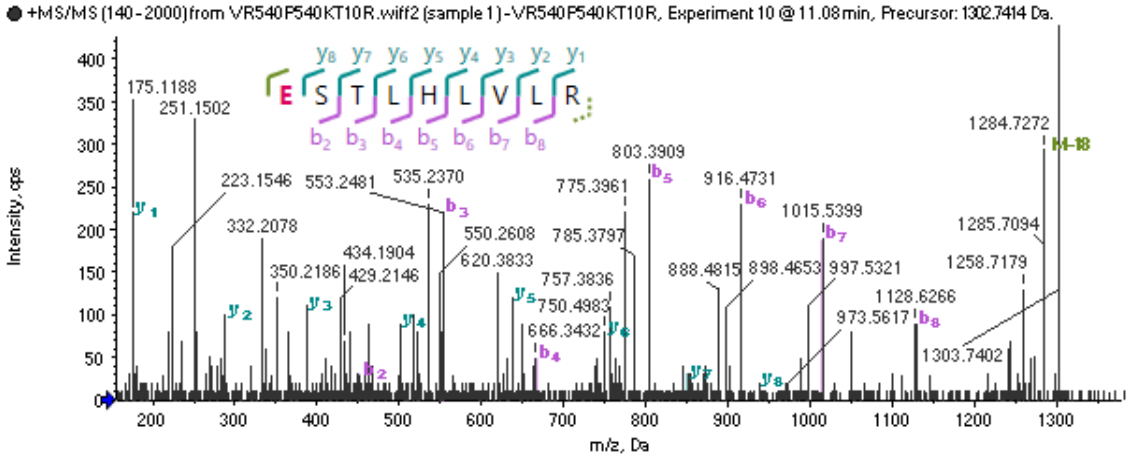
+MS/MS (140 - 2000) from VR540P540KT10R.wiff2 (sample 1) - VR540P540KT10R, Experiment 10 @ 11.08 min, Precursor: 1302.7414 Da.
E S T L H L V L R
y8 y7 y6 y5 y4 y3 y2 y1
b2 b3 b4 b5 b6 b7 b8
Intensity, cps
m/z, Da
175.1188
251.1502
1284.7272
M-18
803.3909
223.1546
553.2481
535.2370
775.3961
916.4731
1015.5399
332.2078
550.2608
785.3797
1285.7094
434.1904
620.3833
888.4815
898.4653
997.5321
1258.7179
350.2186
429.2146
757.3836
1128.6266
750.4983
973.5617
666.3432
1303.7402

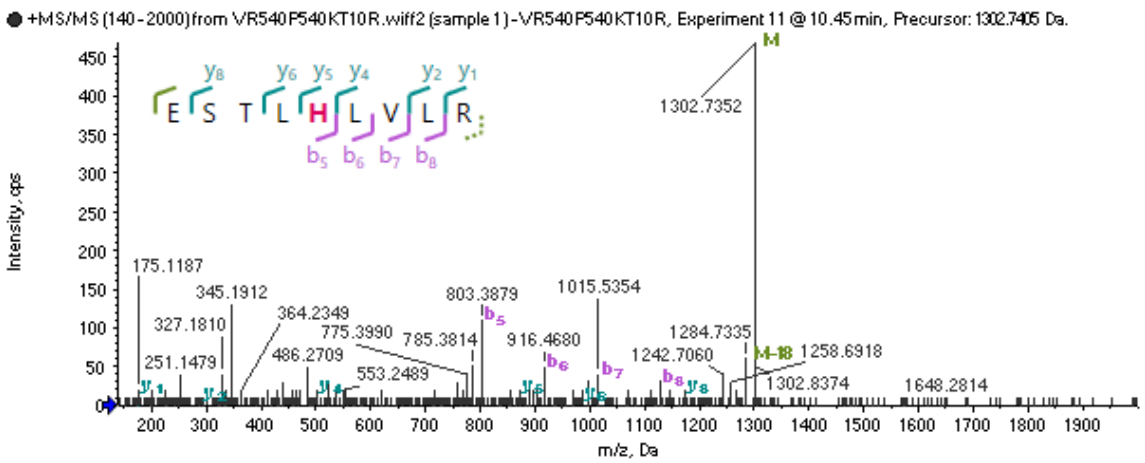

Figure S91. Reaction of ubiquitin with pH (a) 6.0 ; (b) 7.0 ; (c) 7.8 ; (d) 9.0.

[4] Insulin labeling and bioactivity assay

Insulin has three primary amines with discrete placement in space (Figure S92a). The structural evaluation indicates that the N^{α}-NH_2 of N-Phe is suitably positioned (Figure S92b) to guide the alkylating electrophile in the proximity of H10 to enable its irreversible modification.

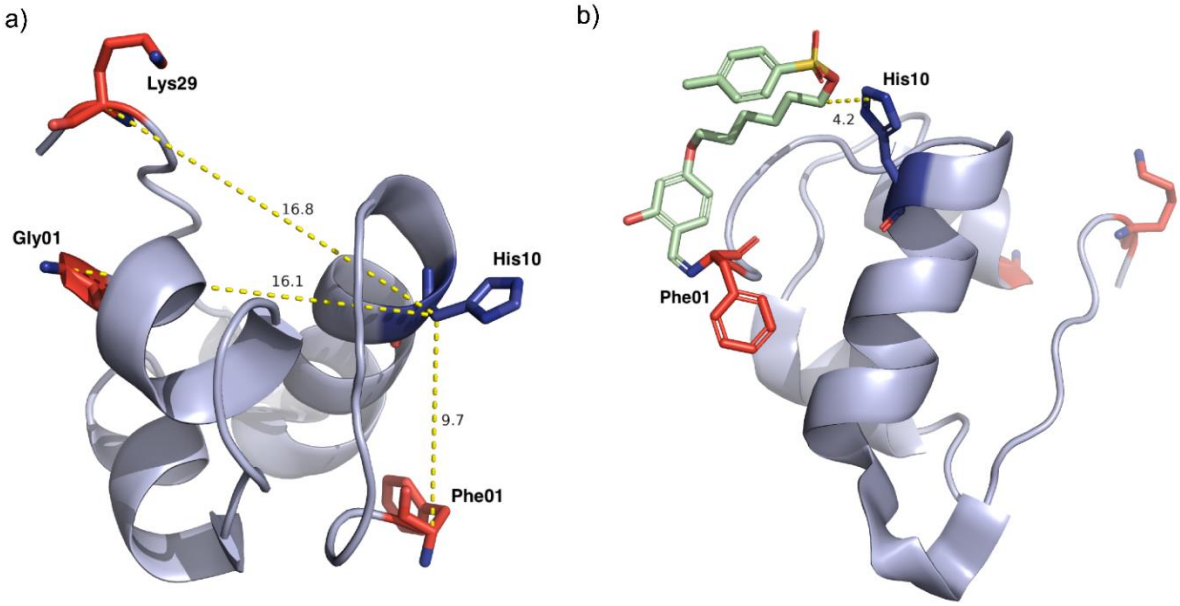

Figure S92. (a) Amine-H10 inter-residue distance (Å) in insulin. (b) N-Phe-derived linchpin places the alkylating electrophile in proximity of H10. (Insulin, PDB ID: 3I40)

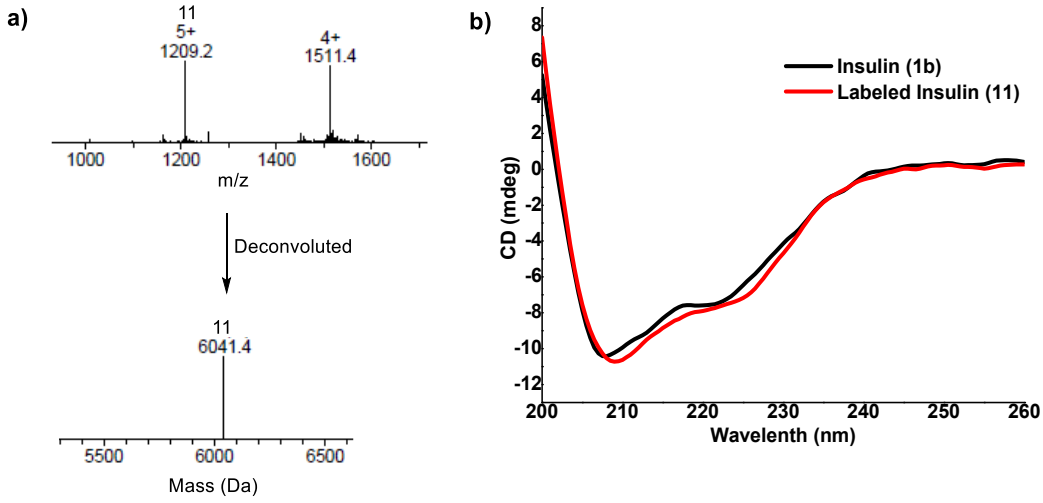

Figure S93. Labeling of insulin with reagent 2c (a) ESI-MS spectra of purified insulin. (b) CD spectra of purified insulin.

The insulin was treated with the LDM reagent to render analytically pure H10-labeled insulin (**11**; Figure S93a). The circular dichroism data confirmed that the labeling and enrichment protocol does not alter the insulin structure (Figure S93b). Next, we took this forward to test the consequences of bioconjugation on its binding to the insulin receptor and its effect on the downstream signalling pathway (Figure 6).

[5] Docking investigations

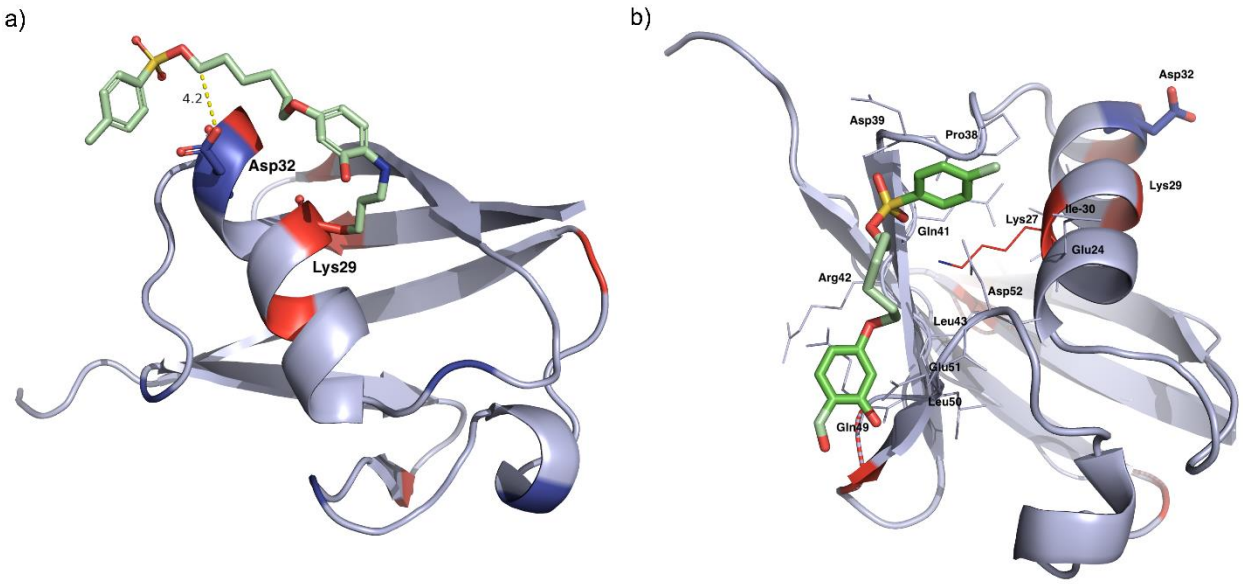

Figure S94. Ubiquitin (PDB ID: 1UBQ) and LDM reagent **2c** (a) Model highlighting K29-derived linchpin directed placement of electrophile near D32. (b) Docking investigations.

The structural model suggests that the imine formation at K29 with reagent **2c** can potentially place the alkylating electrophile in the proximity of D32 residue (Figure S94a). On the other hand, the docking results indicate that the reagent has a binding preference that is not appropriate for the linchpin formation at K29 or irreversible covalent modification of D32 (Figure S94b). Overall, the data indicate that the ligand effect is unlikely to contribute while the linchpin-directed modification regulates the site-of-conjugation.

8. Protein sequence

1. Ubiquitin from bovine erythrocytes
PDB ID: 1UBQ
amino acid sequence:
MQIFVKTLTGKTITLEVEPSDTIENVKAKIQDKEGIPPDQQRLIFAGKQLEDGRTLSDYNIQKESTL
HLVLRLRGG

2. Insulin from human recombinant
PDB ID: 3I40
amino acid sequence:
Chain A: GIVEQCCTSICSLYQLENYCN
Chain B: FVNQHLCGSHLVEALYLVCGERGFFYTPKT

3. α-Lactalbumin from bovine milk
amino acid sequence:[3]
EQLTKCEVFRELKDLKGYGGVSLPEWVCTTFHTSGYDTQAIVQNNDSTEYGLFQINNKIWCKND
QDPHSSNICNISCDKFLNNDLTNNIMCVKKILDKVGINYWLAHKALCSEKLDQWLCEKL

4. Myoglobin from equine skeletal muscle
PDB ID: 1WLA
amino acid sequence:
GLSDGEWQQVLNVWGKVEADIAGHGQEVLIRLFTGHPETLEKFDKFKHLKTEAEMKASEDLKK
HGTVVLTALGGILKKKGHHEAELKPLAQSHATKHKIPIKYLEFISDAIIHVLHSKHPGDFGADAQ
GAMTKALELFRNDIAAKYKELGFQG

9. References

1 M. Kinter and N. E. Sherman, *Wiley Interscience*, **2000**.
2 F. Ito, S. Ando, M. Luchi, T. Ukari, M. Takasaki and K. Yamaguchi, *Tetrahedron* 2011, **67,** 8009-8013.
3 K. Brew, F. J. Castellino, T. C. Vanaman and R. L. Hill, *J. Biol. Chem.* 1970, **245**, 4570-4582.